COMPLETE – Cloud-MicroPhysics-Turbulence-Telemetry funded by the European Commission under the framework programme Horizon 2020

H2020-MSCA-ITN-2015

Grant Agreement Number 675675

Work Package 6: Dissemination and Communication

Deliverable D6.3: 2nd Summer School lecture notes

Editor: Guus Bertens

Date: 15-10-2018

Document status: released - version b

Contents

Report on the first set of lectures of Alain Pumir, ENS Lyon and CNRS

This set of lectures was delivered on Monday, July 9, from 2pm to 6pm, and consisted of 4 lectures, each of approximately 45-50mn.

The first set of lectures of Alain Pumir (ENS Lyon) were devoted to fundamental process of fluid microphysics, leading to the formation of drops via the process known as "collision coalescence", i.e., on the aggregation of small droplets to form much bigger drops. In this process, turbulence plays one of the very important role, which was stressed during the lecture.

The original plan of the lecturer was to present this material in 3 lectures, and to present the second set of lectures on the first days. Overall, the lecture was based on the recent review article by the lecturer in Annual Review of Condensed Matter Physics [1]. The lecturer chose to spend some time deriving some of the most important results on the white board, made available for the lectures. It turned out that the presentation of the material, as well as the derivation of the theoretical results took more time than originally planned by the lecturer, who considered as more important to present in an articulate manner the material, rather than rushing to finish.

The first lecture was devoted to a presentation of the subject in the context of cloud microphysics (discussion of the role of the various processes involved, and of the approximations made in the study presented in the lectures). From a technical side, the first effective treatment of collisions was carried out in the case of a bi-disperse solution of particles, with two different sizes, settling with different terminal velocities. The general formula was derived on the white board. The role of turbulence, which consists of bringing particles together, can be qualitatively understood by focusing on the velocity gradient tensor in the flow, whose properties were briefly presented.

The second lecture was devoted to the general formulation of the collision problem, and to the definition of the collision kernel. With this result, in the case of tracer particles (particles that follow exactly the velocity of the flow), it is relatively simple to establish the seminal result of Saffman and Turner [2]. The derivation of these two results was presented in detailed on the white board.

The third lecture was devoted to a description of the effects of particle inertia. In particular, the effect of preferential concentration, which manifests itself by an inhomogeneous distribution of particles in the flow, can be qualitatively understood by a simple argument, originally due to Maxey and Riley [3], which was presented on the white board. The sling effect, which results from the possibility of two particles in the flow to collide with very different velocities was also discussed.

In the last lecture, the consequence of these processes for the functional dependence of the collision kernel on the various parameters was discussed, and illustrated by numerical results. A brief discussion of the use (and the potential dangers!) of the Smoluchowski approach to study the evolution of the size distribution of the particles.

The hand-written notes of the lecturers, corresponding to the derivations on the white board, as well as the transparencies, were made available to the students.

Among the vast literature, the lecturer suggested the following references to the students for further reading:

[1] A. Pumir and M. Wilkinson, *Ann. Rev. Cond. Matt. Phys.* 7 (2016)
[2] P. G. Saffman and J. S. Turner, J. Fluid Mech. **1**, 16 (1956).
[3] M. R. Maxey and J. J. Riley, Phys. Fluids **26**, 883 (1983)
[4] E. Bodenschatz, S.P. Malinowski, R. A. Shaw and F. Stratmann, Science **327**, 5968 (2010)
[5] G. Falkovich, A. Fouxon and M. Stepanov, Nature, **419**, 151 (2002)
[6] G. Falkovich and A. Pumir, *Phys Fluids* **16** (2004) and *J. Atmos. Sci.* **64** (2007)
[7] T. Gotoh, T. Suheiro and I. Saito, New Journal Physics **18**, 043042 (2016).
[8] T. Gotoh and I. Saito, New Journal Physics, 20, **023001** (2018).
[9] A. Kostinski and R. A. Shaw, BAMS **86**, 235 (2005)
[10] R. A. Shaw, Ann. Rev. Fluid Mech. **35**, 183 (2003)
[11] M. Voßkuhle et al., *Phys. Rev.* E **88** (2013), *J. Fluid Mech.* **749** (2014) and *J. Turbulence* **16** (2015)
[12] L. P. Wang and W. Grabowski, Ann Rev Fluid Mech. **45**, 293 (2013)
[13] M. Wilkinson and B. Mehlig, EPL **71**, 188 (2005).

Report on the second set of lectures of Alain Pumir (ENS Lyon and CNRS)

This set of lectures was delivered on Tuesday, July 10, from 10am to 12am, and consisted of 2 lectures, each of approximately 45mn.

The second set of lectures was a continuation of the investigation of the "collision coalescence" process in the case of mixed-clouds, containing both water droplets, and ice crystals.

The original plan of the lecturer was to present general results on turbulent flows, with a focus on the properties of the velocity gradient tensor. The rationale for presenting this material was to focus on some property of turbulence directly related to one of the aspects already presented, namely the motion and orientation of ice crystals. It would not have made much sense to present this material without discussing first the problem of crystals in clouds. This is why, after discussion with the organizers, the lecturer decided to focus on the properties of collision involving crystals.

Whereas the problem of collisions involving droplets is by now relatively standard, far fewer results are available in the presence of ice crystals. The results presented in this second set of lectures were based on several recent articles by the lecturer and his collaborators [1-3].

The first lecture began by a short reminder of the context of the lectures, in particular in cumulonimbus, and other deep convection clouds. The inherent simplification of the problem of the motion of the crystals, approximated as an ellipsoid, was discussed at length. The equations of the problems were briefly described, as well as the numerical methods used to solve the equations. The problem of orientation of the crystals as they are settling through a turbulent flow was discussed; it shows a strong anisotropy of the distribution of orientation when turbulence is weak.

The second part was devoted to a discussion of numerical results, first in the case of collisions between crystals (favoring the formation of large graupel particles), and then in the case of collisions between crystals and droplets (giving rise to the process known as "riming"). In all cases, the numerical results show that the physical processes have a clear signature on the collision rate, which should be useful for parametrization of the processes.

The following references were pointed out to the students, for further reading:

[1] K. Gustavsson et al., Phys. Rev. Lett. ***119***, *24501* (2017)
[2] J. Jucha et al., Phys Fluids ***3***, *01460* (2018)
[3] A. Naso et al., J. Fluid Mech. 845, (2018)
[4] C. Siewert et al, J. Fluid Mech. ***758**, 686* (2014)
[5] C. Siewert et al., Atmos. Res. ***142**, 45* (2014)

OPTIMAL GUIDANCE OF BUOYANCY-CONTROLLED BALLOONS IN TURBULENT FLOWS USING A NON-QUADRATIC OBJECTIVE AND DISCONTINUOUS ACTUATION

Paolo Luchini[1], Thomas Bewley[2], Gianluca Meneghello[3]
[1] *Università di Salerno – DIIN, 84084 Fisciano (SA), Italy*
[2] *Flow Control Lab, Dept of MAE, UC San Diego, La Jolla CA, USA*
[3] *Dept of Earth, Atmospheric and Planetary Sciences, MIT, Cambridge MA, USA*

Meteorological forecasting of extreme phenomena like hurricanes could strongly benefit from sensor-laden vehicles (typically, balloons) that could be guided to remain in the geographical area of interest for a few days at a time, rather than a dozen minutes or so as is the case with today's free-flying balloons and dropsondes. A promising energy-sparing technology consists of balloons with mechanically-adjustable volume [1] which can reversibly provide increased or decreased buoyancy and move to an altitude where the prevailing wind blows in the desired direction. In previous work we have shown that a) guidance of balloons in specified orbits, and even in orderly formations, can numerically be achieved in realistic hurricane simulations [2], and b) a control objective proportional to the absolute value of the inflation rate, more representative of required electric power than its square, leads to the choice of a discontinuous control law where the balloon is left most of the time at a constant volume and only inflated or deflated for abrupt short periods (ideally, in a discontinuous way) [3, 4].

Whereas the optimal control of a linear system, disturbed by white noise, towards a quadratic objective can be mathematically proved to require a linear feedback control and to lead to gaussian statistical distributions of all the quantities involved, a non-quadratic objective removes all these nice mathematical properties, and in particular the optimal controller can no longer be assumed to be linear even when the system to be controlled is linear. In this context, result (b) mentioned above was achieved by extremely simplifying the dynamics, to the point that the entire turbulent flow was replaced by a white noise with its spectral amplitude as the only tunable parameter. A more realistic approximation must at least involve a spectrum that more closely resembles a turbulent flow. It is an almost forgotten result that the lagrangian correspondent of the Kolmogorov $k^{-5/3}$ spatial spectrum of turbulent energy is a temporal spectrum proportional to ω^{-2} [5]. An ω^{-2} power spectrum implies an ω^{-1} amplitude spectrum, and is quite easy to achieve in a lumped numerical simulation by passing white noise through an integrator.

The simplest abstract model of the motion of a balloon in a hurricane is then a two-degree-of-freedom mechanical system disturbed by once-integrated white noise. The power spent to inflate and deflate the balloon is proportional to the absolute value of vertical velocity, and its integral is the energy to be minimized. This nonquadratic objective makes even such a simplified system nontrivial to analyze; its optimization implies solving a partial differential Fokker-Planck equation for the statistical distribution function of position and velocity, a mathematical technique often referred to as dynamic programming. The numerical solution of this problem and the resulting discontinuous, stepwise optimal control strategies will be discussed at the conference.

References

[1] G. Meneghello, T.R. Bewley, M. de Jong, and C. Briggs. A coordinated balloon observation system for sustained in-situ measurements of hurricanes. *IEEE Aerospace Conference*, Big Sky. 2017
[2] T.R. Bewley and G. Meneghello. Efficient coordination of swarms of sensor-laden balloons for persistent, in situ, real-time measurement of hurricane development, *Phys. Rev. Fluids* 1, 060507, 2016.
[3] G. Meneghello, P. Luchini, and T.R. Bewley On the control of buoyancy-driven devices in stratified, uncertain flowfields, *International Symposium on Stratified Flows (ISSF)*, San Diego. 2016.
[4] G. Meneghello, P. Luchini, and T.R. Bewley. A Probabilistic Framework for the Control of Systems with Discrete States and Stochastic Excitation, *Automatica*, to appear. 2017.
[5] H. Tennekes. Eulerian and Lagrangian time microscales in isotropic turbulence. *J. Fluid Mech.* 67(3):561–567, 1975.

Ten lectures on tropical cloud dynamics

Juan Pedro Mellado, Ann Kristin Naumann and Julia Windmiller

1 General Aim

The aim of these 10 lectures is to use examples from on-going research to illustrate how clouds actively shape climate-relevant tropospheric dynamics, how clouds are polymorphous paradigms of multi-physics, multi-scale problems, compounding fluid dynamics, micro-physics and radiative transfer from millimeter to hundreds of kilometers, and how clouds remain a key uncertainty for understanding our warming climate. For conciseness and because of its relevance, the lectures focus on tropical and subtropical cloud regimes.

2 Introductory lectures

The first two lectures introduce the course.

The first lecture explains the relevance of clouds in the climate system, and the large uncertainty associated with them in the analysis of the consequence of the current warming. The lecture emphasizes the relevance of moist convection in the tropics and subtropics because this region constitutes more than half of Earth's surface and is a paradigm to study clouds, circulation and climate sensitivity: as we move from the subtropics towards the equator following the trade winds, we find stratocumulus, shallow cumulus and deep convection regimes. The lectures have been organized around specific aspects of these three regimes. This first lecture also describes the three challenges of moist convection: it is multi-scale, multi-physics, and polymorphous.

The second lecture summarizes the governing equations commonly used in the study of tropical convection. Starting from first principles, we derive typical approximations to the governing equations in differential and integral forms, typical moist variables, and discuss various formulations of the condensate phase: Lagrangian, statistical, and bulk formulations. The lecture also emphasizes the importance of the various lapse rates, namely, the environmental lapse rate, the dry adiabatic lapse rate, and the moist adiabatic lapse rate, introducing the concept of convective instability.

Recommended references:

- on moist convection Stevens (2005).
- on climate relevance of clouds: Stevens and Bony (2013a), Stevens and Bony (2013b), Bony and coauthors (2015).
- on the formulation of cloud droplets: Shaw (2003), Grabowski and Wang (2013), Khain et al. (2015), Seifer and Beheng (2006).
- on microphysics: Rogers and Yau (1989), Pruppacher and Klett (1997)

3 Stratocumulus Clouds

The first lecture on stratocumulus clouds introduce their relevance, the stratocumulus-topped boundary layer, the various processes controlling their dynamics, and various modeling approaches.

The relevance of stratocumulus in the climate system stems from their large area coverage and net cooling effect (low level and high albedo), which makes them crucial for Earth's energy budget. Early estimates showed that increasing the area coverage by 4% could offset about 2 K of climate warming. There is some consensus that low-level clouds contribute to a positive global cloud feedback, but its quantification remains a challenge.

Stratocumulus are intricately coupled to the planetary boundary layer that contains them. We refer to it as stratocumulus-topped boundary layer (STBL). The lecture describes the vertical and horizontal structure of the STBL, and the transition towards shallow cumulus through the decoupling between the sub-cloud and clouds layers.

Turbulence generation by cloud-top cooling distinguishes stratocumulus from other cloud types. Radiative cooling is the main process, as a source of turbulence generation by convective instability and by maintaining a sharp interface. It is induced by the cloud-top divergence of net upward long-wave radiative flux. Other processes, however, strongly modulate it. Cloud-top entrainment causes warming and drying of the cloud. Turbulence in the STBL interior brings water from near the surface towards the cloud. Surface latent heat flux maintains the moist conditions necessary to form the cloud. Latent heat effects, namely, evaporative cooling at the top, and condensational warming in the updrafts, promote turbulence and mixing. Microphysical properties (the droplet size distribution) determines sedimentation and drizzle, and finite rate effects of phase change. The delicate compensating effects of these various processes is a challenge for quantification of the sensitivity of stratocumulus to a warming climate.

Regarding the modeling approaches, the lecture introduces and compares three of them, from more parameterized to less parameterized: mixed layer models, large eddy simulations and direct numerical simulations. All of them have advantages and disadvantages and complement each other. Last, the concept of Reynolds number similarity is reviewed, explaining the relevance of the Ozmidov scale at the top of the STBL to understand entrainment and cloud-top properties, which are crucial for stratocumulus because they are predominantly controlled by cloud-top cooling.

Recommended references: Stevens (2002), Stevens et al. (2005), Wood (2012), Mellado et al. (2018).

4 Entrainment in Stratocumulus Clouds

This second and last lecture on stratocumulus focuses on cloud-top entrainment. It explains that the cloud-top region has a complex structure where interfacial layers of various properties, such as liquid water content, turbulence and buoyancy, coexist but not necessarily coincide, and therefore inferring properties from one property to another is difficult. The lecture also shows how one of the most important variables in the study of entrainment, the mean entrainment velocity, can be analytically related to well-defined and quantifiable terms associated with various phenomena: mixing, radiative cooling, evaporative cooling, and droplet sedimentation.

The lecture considers two examples to illustrate the interaction and local analysis of some of those processes. The first example considers the role of shear and evaporation. This pair of phenomena is interesting because, separately, each of them do not play a key role in the cloud dynamics. However, together they can, showing a clear example of two phenomena that do not add linearly. The second example considers the entrainment reduction by droplet sedimentation (or gravitational settling of droplets). Comparing results from simulations with 2.5-5.0 m resolution and with 20-40 cm resolution, we observe that the relevance of settling can become 2 to 3 times more important in the highly resolved case. The likely reason is that turbulence models mix too much when the grid spacing is larger than the Ozmidov scale. This example shows the relevance of having high resolution in measurements and simulations. Besides, this second example shows the need to better characterize the droplet size distribution in the cloud-top region.

Recommended references: Stevens (2002), Malinowski et al. (2013), de Lozar and Mellado (2017), Mellado (2017).

References

S. Bony and coauthors. Clouds, circulation and climate sensitivity. *Nature Geosci.*, 8:261–268, 2015.

A. de Lozar and J. P. Mellado. Reduction of the entrainment velocity by cloud-droplet sedimentation in stratocumulus. *J. Atmos. Sci.*, 74:751–765, 2017.

W. W. Grabowski and L.-P. Wang. Growth of cloud droplets in a turbulent environment. *Annu. Rev. Fluid Mech.*, 45:293–324, 2013.

A. Khain, K. D. Beheng, A. Heymsfield, A. Korolev, S. O. Krichak, Z. Levin, M. Pinsky, V. Phillips, T. Prabhakaran, A. Teller, S. C. van den Heever, and J.-I. Yano. Representation of microphysical processes in cloud-resolving models: Spectral (bin) microphysics versus bulk parameterization. *Rev. Geophys.*, 53:247–322, 2015.

S. P. Malinowski, H. Gerber, I. Jen-La Plante, M. K. Kopec, W. Kumala, K. Nurowska, P. Y. Chuang, D. Khelif, and K. E. Haman. Physics of Stratocumulus Top (POST): turbulent mixing across capping inversion. *Atmos. Chem. Phys.*, 13:15234–15269, 2013.

J. P. Mellado. Cloud-top entrainment in stratocumulus clouds. *Annu. Rev. Fluid Mech.*, 41: 145–169, 2017.

J. P. Mellado, C. S. Bretherton, B. Stevens, and M. C. Wyant. DNS and LES of stratocumulus: Better together. *J. Adv. Model. Earth Syst.*, 2018.

H. R. Pruppacher and J. D. Klett. *Microphysics of clouds and precipitation.* Kluwer Academic Publishers, 1997.

R. R. Rogers and M. K. Yau. *A Short Course in Cloud Physics.* Butterworth-Heinemann, third edition, 1989.

A. Seifer and K. D. Beheng. A two-moment cloud microphysics parameterization for mixed-phase clouds. Part 1: Model description. *Meteorol. Atmos. Phys.*, 92:45–66, 2006.

R. A. Shaw. Particle-turbulence interactions in atmospheric clouds. *Annu. Rev. Fluid Mech.*, 35:183–227, 2003.

B. Stevens. Entrainment in stratocumulus-topped mixed layers. *Q. J. Roy. Meteorol. Soc.*, 128: 2663–2690, 2002.

B. Stevens. Atmospheric moist convection. *Annu. Rev. Earth Planet. Sci.*, 33:605–643, 2005.

B. Stevens and S. Bony. What are climate models missing? *Science*, 340:1053–1054, 2013a.

B. Stevens and S. Bony. Water in the atmosphere. *Phys. Today*, 66:29–34, 2013b.

B. Stevens, C.-H. Moeng, A. S. Ackerman, C. S. Bretherton, A. Chlond, S. de Roode, J. Edwards, J.-C. Golaz, H. Jiang, M. Khairoutdinov, M. P. Kirkpatrick, D. C. Lewellen, A. Lock, F. Müller, D. E. Stevens, E. Whelan, and P. Zhu. Evaluation of large-eddy simulations via observations of nocturnal marine stratocumulus. *Mon. Wea. Rev.*, 133:1443–1462, 2005.

R. Wood. Stratocumulus clouds. *Mon. Wea. Rev.*, 140:2373–2423, 2012.

Lecture notes UFS summer school - Shallow cumulus - Ann Kristin Naumann

Three lectures on shallow cumulus convection are given. The first one is supposed to give an overview of general concepts of shallow cumulus clouds, while the second and the third lecture are intended to reflect two particular aspects of shallow cumulus, which are still areas of active research.

Lecture 1: Introduction to shallow cumulus convection

The introductory lecture gives an overview of the climatology of shallow clouds, the boundary layer structure in the shallow cumulus regime, and the role of mixing and turbulence for the shallow cumulus lifecycle and their moisture transport. The following aspects are emphasized:

- Shallow cumulus undergo a distinct lifecycle, which is moderated by mixing with the environment.
- Shallow cumulus are imbedded in the large-scale circulation in the tropics. By transporting moisture towards the ITCZ, shallow cumulus fuel the large-scale circulation.
- The representation of shallow cumulus in large-scale models remains a challenge.

<u>Recommended reading:</u>
Stevens, 2005: Atmospheric moist convection. Ann. Rev. Earth Plant. Sci. 33: 605-634.

Siebesma, 1998: Shallow convection. In Buoyant Convection in Geophysical Flows, ed. EJ Plate, EE Fedorovich, DX Viegas, JC Wyngaard, 513:441–86. Dordrecht, The Neth.: Kluwer Acad. 491 pp.

Lecture 2: How do shallow cumulus rain?

Although precipitation from shallow cumulus is often neglected, shallow cumulus are found to rain about 30 % of the time. This lecture introduces the size gap (or the collision-coalescence bottleneck), the role of turbulence for warm rain microphysical processes and the super-droplet method to study recirculation of raindrops in shallow cumulus. The following aspects are emphasized:

- Shallow cumulus clouds produce rain through warm microphysical processes.
- Turbulent enhancement of collision rates and recirculation of raindrops contribute to rapid rain formation.
- The Lagrangian super-droplet method is too expensive for large-scale models but can be used for process studies on small domains.

<u>Recommended reading:</u>
Size gap:
Curry and Webster, 1999: Cloud characteristics and processes. In Thermodynamics of Atmospheres and Oceans, ed. J. Holton, 65: 209-220. International geophysics series, Academic press. (Here, in particular Section 8.2: Precipitation processes)

Lagrangian super-droplet method:
Shima et al., 2009: The super-droplet method for the numerical simulation of clouds and precipitation: A particle-based and probabilistic microphysics model coupled with a non-hydrostatic model. Q. J. R. Meteorol. Soc. 135: 1307–1320.

Naumann, A. K., and A. Seifert (2016), Recirculation and growth of raindrops in simulated shallow cumulus, J. Adv. Model. Earth Syst., 08, doi:10.1002/ 2016MS000631.

Lecture 3: How do shallow cumulus organize?

Organization of shallow cumulus has been noted at least since early field studies in the 50s and 60s. This lecture introduces different form of mesoscale organisation of shallow cumulus. The following aspects are emphasized:

- Organization of shallow cumulus is ubiquitous in the trades. This organisation occurs in a variety of different forms, which reflects the mechanism of their formation:
    - Cold pools occur due to evaporative cooling and organize shallow cumulus into arcs and lines.
    - Radiatively driven shallow circulations are able to suppress convection in colder areas and enhance convection in warmer areas.
- Shallow circulations are not well captured in coarse resolution models but might influence cloud feedbacks for global warming.

<u>Recommended reading:</u>
Organisation by cold pools:
Seifert and Heus, 2013: Large-eddy simulation of organized precipitating trade wind cumulus clouds. Atmos. Chem. Phys., 13:5631-5645.

Organisation by shallow circulation:
Bretherton and Blossey, 2017: Understanding Mesoscale Aggregation of Shallow Cumulus Convection Using Large-Eddy Simulation, J. Adv. Mod. Earth Syst., 9:2798–2821.

Naumann et al.: A conceptual model for the BL structure and radiatively driven shallow circulations in the trades. In preparation.

Lecture notes UFS summer school - Deep convection - Julia Windmiller

The three lectures on deep convection were centered around three key questions. First, what drives deep convection (with a particular focus on what determines the amount of precipitation)? Second, what determines the distribution of deep convection, in particular why are updrafts narrow and have a life-cycle? Finally, lecture three addressed the question of how deep convection is represented in climate models and some common problems of parameterizing convection.

Lecture 1 - What drives deep convection?

Deep convection, as stratocumulus and shallow cumulus clouds, is a type of atmospheric moist convection. In contrast to the two other types of atmospheric convection, deep convection rises up to the tropopause, where the ozone layer absorbs most of the incoming UV radiation.

Deep convection is driven by the sun warming the surface more strongly than the atmosphere, as the atmosphere is almost transparent to the incoming solar radiation which is therefore mostly absorbed at the surface. The importance of deep convection for the mean state of the atmosphere can easily be seen when comparing observed temperature profiles in the atmosphere with the radiative equilibrium profile, the temperature profile calculated from only the radiative forcing. This radiative equilibrium state is characterized by higher than observed temperatures at the surface and lower temperatures in the free troposphere. This temperature profile is unstable to convection. The effect of the resulting convection is to render the atmosphere closer to a profile neutral to further convection. As the convective timescale is shorter than the radiative timescale, the mean state of the atmosphere is close to the profile neutral to moist convection, i.e. moist adiabatic. The difference between the observed and the radiative equilibrium temperature profile highlights the importance of deep convection for the mean state of the tropical atmosphere and also constraints the average precipitation rate.

<u>Recommended Reading</u>

General introduction:

Stevens, B. (2005). Atmospheric Moist Convection. Annual Review of Earth and Planetary Sciences, 33:605–643.

Radiative equilibrium:

Wallace, J. M. and Hobbs, P. V. (2006). Radiative Transfer. *Atmospheric Science : an Introductory Survey* (pp. 113-145). Academic Press, Cambridge, Massachusetts, 2. edition.

Radiative-convective equilibrium:

Emanuel, K. A. (1994). Deep Convective Regimes. *Atmospheric convection* (pp. 463-487). Oxford University Press.

Lecture 2 - What determines the spatial distribution of deep convection?

While the previous lecture focussed on the average amount of precipitation, the topic of the second lecture was to understand how precipitation is distributed. In particular addressing the questions of why deep convective updrafts (which account for most of the precipitation in the tropics) are narrow compared to the subsiding regions and why deep convective clouds have a life-cycle. To understand these properties it was first noted that the typical state of the tropical atmosphere is conditional instability, which requires the temperature lapse rate of the atmosphere to be larger than the dry adiabatic lapse rate and smaller than the moist adiabatic lapse rate.

Using this condition, one can argue that fast and narrow updrafts and slow subsiding downdrafts are the most unstable as this type of updraft, within the time of their ascent, induce the least warming of the surrounding atmosphere. That single updrafts do not prevail for a long time but typically end within one hour is explained by so called cold pools, downdrafts induced by precipitation, which act as a self-destruct mechanism in typical thunderstorms. Aside from cutting off the ascending air and thus ending the convective life-cycle, cold pools can trigger new convection in the surrounding of the previous updraft.

Recommended Reading

Narrow updrafts:

Randall, D. A. (2012). How turbulence and cumulus clouds carry energy upward. Atmosphere, clouds, and climate (pp. 55-96). Princeton University Press.

Bjerknes, J. (1938). Saturated-adiabatic ascent of air through dry-adiabatically descending environment. Quart. J. Roy. Meteor. Soc., 64: 325-330.

Deep convective lifecycle and cold pools:

Wallace, J. M. and Hobbs, P. V. (2006). Deep Convection. *Atmospheric Science : an Introductory Survey* (pp. 344-366). Academic Press, Cambridge, Massachusetts, 2. edition.

Nakajima, K. and Matsuno, T. (1988). Numerical Experiments Concerning the Origin of Cloud Clusters in the Tropical Atmosphere. Journal of the Meteorological Society of Japan. Ser. II, 66(2): 309–329.

Rotunno, R., Klemp, J. B., and Weisman, M. L. (1988). A Theory for Strong, Long-Lived Squall Lines. Journal of the Atmospheric Sciences, 45(3):463–485.

Lecture 3 - Representation of convective organization—Challenges for climate models

Resolution of current climate models is too coarse to represent deep convective updrafts explicitly and thus their effect has to be parameterized. The goal of the parameterization is to determine the impact of convection on the mean state, in particular temperature and humidity. To this end, one possibility is to try to estimate the number and properties of the convective updrafts expected in each grid cell and then estimate their impact.

The parameterization of deep convection is an important source of uncertainty. One problem of the above mentioned approach is that it usually makes the amount of convection a function of the large-scale atmospheric state only and thus cannot represent any triggering of deep convection by previous deep convection. This deficiency might explain why climate models have problems in reproducing propagating systems, such as squall lines over Africa. Ongoing work suggests that one way to address this problem is by coupling the convective activity of neighboring grid-cells.

Recommended Reading

Challenges for climate models:

Bony, S., Stevens, B., Frierson, D. M. W., Jakob, C., Kageyama, M., Pincus, R., Shepherd, T. G., Sherwood, S. C., Siebesma, A. P., Sobel, A. H.,Watanabe, M., and Webb, M. J. (2015). Clouds, circulation and climate sensitivity. Nature Geoscience, 8:261–268.

Convection parameterization:

Emanuel, K. A. (1994). Cumulus representation in numerical models. Atmospheric convection (pp. 524-558). Oxford University Press.

Arakawa, A. and Schubert, W. H. (1974). Interaction of a cumulus cloud ensemble with the large scale environment, Part I. Journal of the atmospheric sciences, 31:674–701.

Experimental Techniques

E. Bodenschatz

Max Planck Institute for Dynamics and Self-Organization
University of Göttingen
Cornell University

Warm clouds; plinian volcanic eruption

$$\frac{\partial \vec{u}}{\partial t} + (\vec{u} \cdot \vec{\nabla})\, \vec{u} = -\frac{1}{\rho} \vec{\nabla} p + \frac{1}{Re} \Delta \vec{u}$$

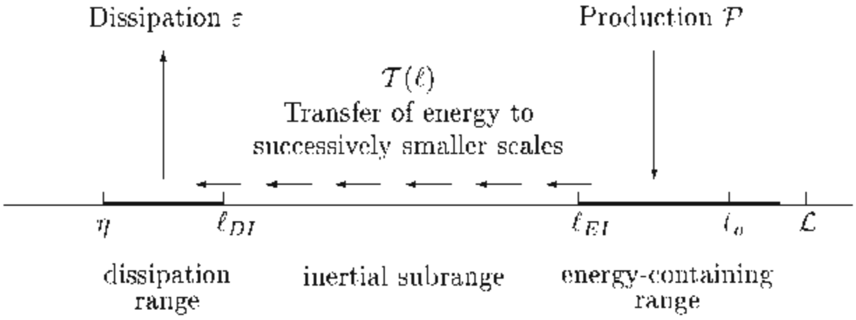

$$\frac{\partial \vec{u}}{\partial t} + (\vec{u} \cdot \vec{\nabla})\, \vec{u} = -\frac{1}{\rho} \vec{\nabla} p + \frac{1}{Re} \Delta \vec{u}$$

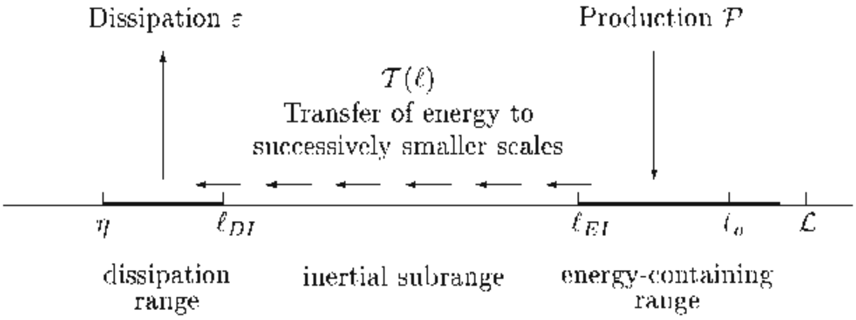

Kolmogorov length:

$$\eta \equiv \left(\frac{\nu^3}{\varepsilon}\right)^{1/4}$$

Kolmogorov time:

$$\tau_\eta \equiv \left(\frac{\nu}{\varepsilon}\right)^{1/2}$$

$$\boxed{Re \sim \left(\frac{l}{\eta}\right)^{4/3}}$$

Microscale Reynolds number: R_λ

$$R_\lambda = \frac{\langle u_i \rangle \lambda}{\nu} = \sqrt{15\,\mathrm{Re}}$$

$$R_\lambda = \sqrt{15}\left(\frac{L}{\eta}\right)^{2/3} = \sqrt{15}\frac{T_L}{\tau_\eta} = \sqrt{15}\left(\frac{T_L}{t_0}\right)\left(\frac{\Delta_0}{\eta}\right)^{2/3}$$

$$\underset{100}{\uparrow} \qquad \underset{60}{\uparrow}$$

$$\longrightarrow R_\lambda \sim 6000$$

E. Bodenschatz et al., Science 327, 970-971 (2010)

Science AAAS

E. Bodenschatz et al., Science 327, 970-971 (2010)

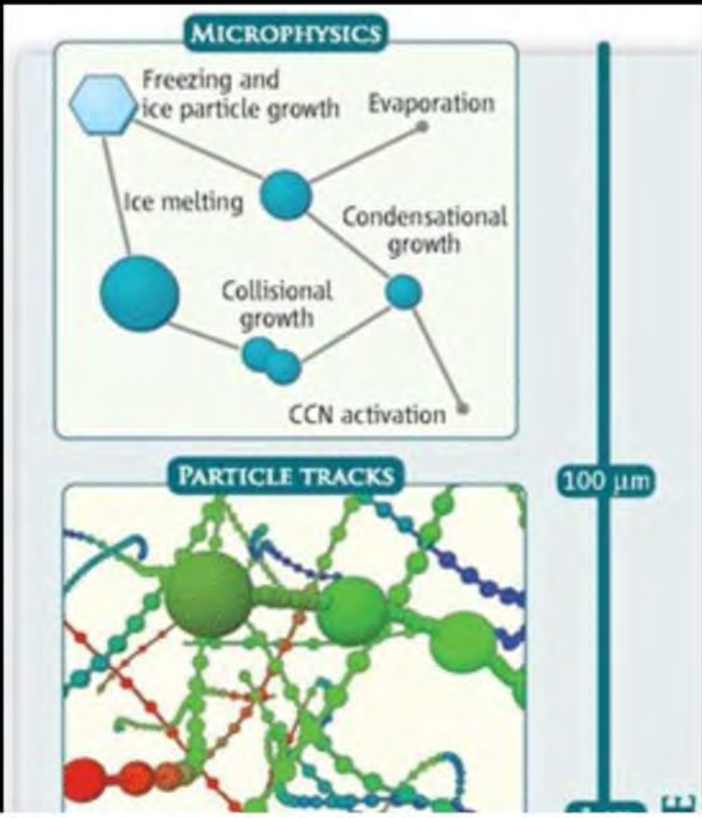

E. Bodenschatz et al., Science 327, 970-971 (2010)

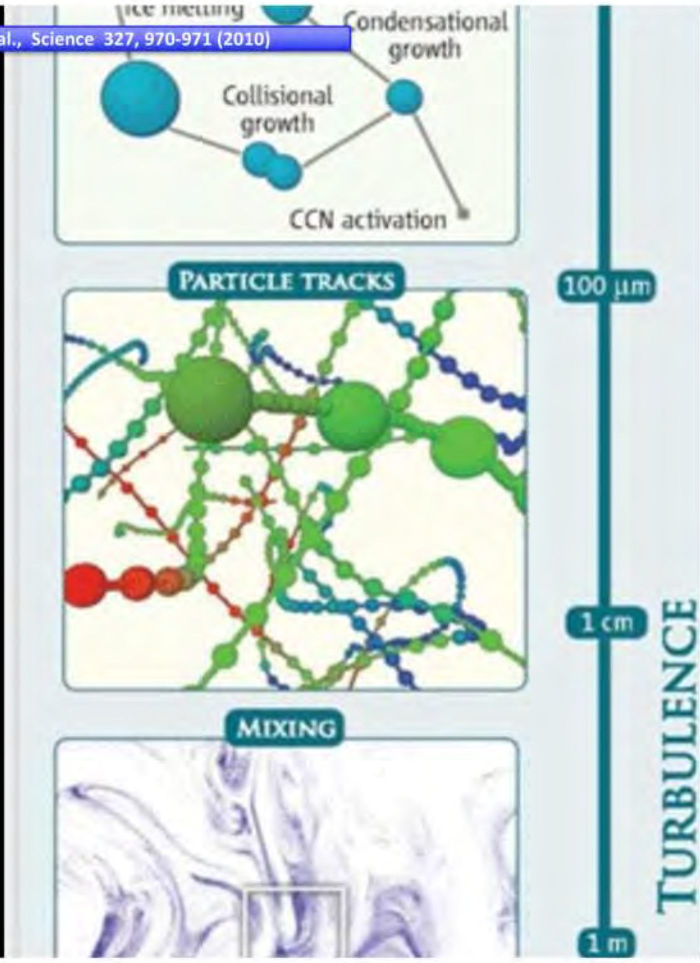

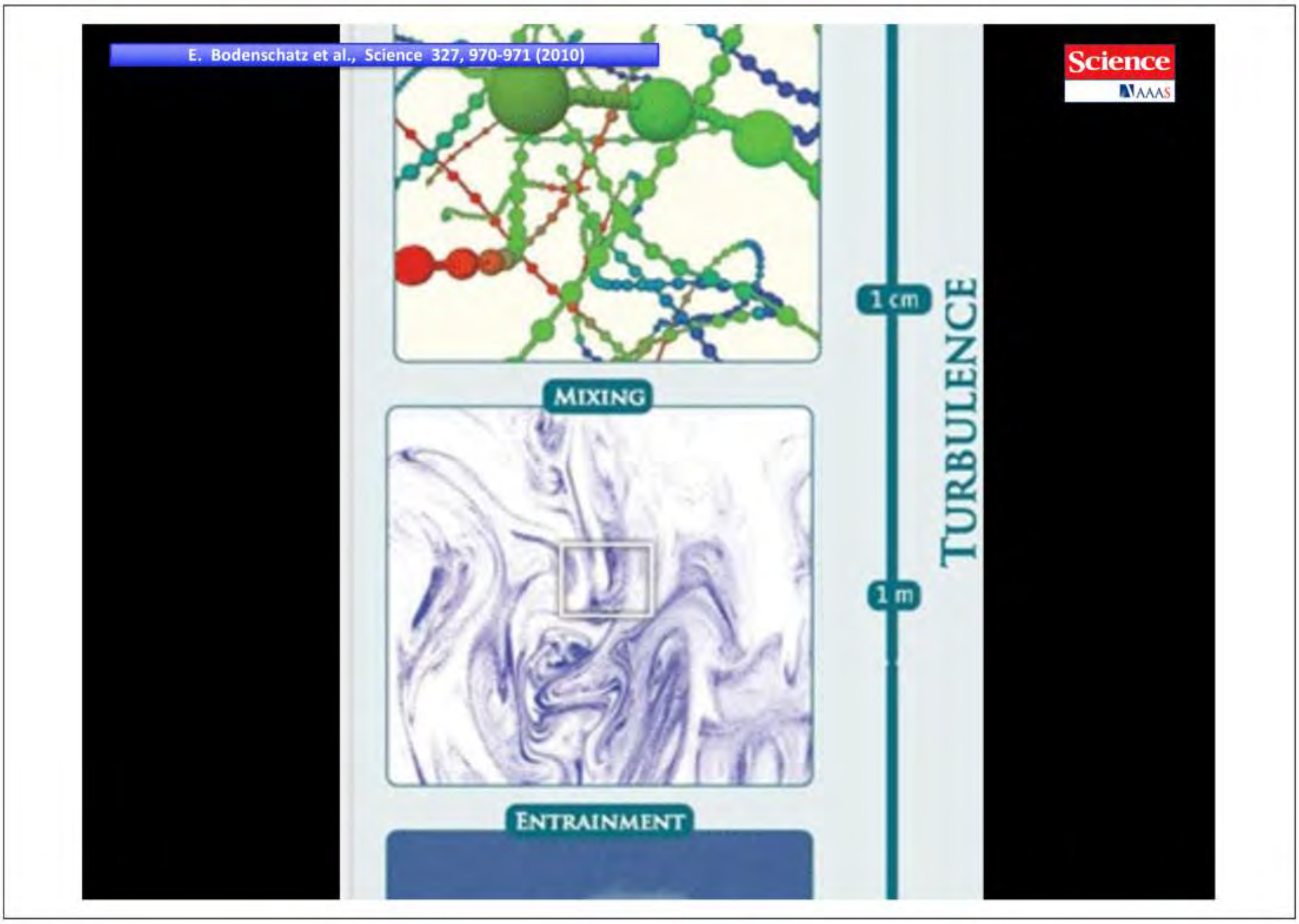
E. Bodenschatz et al., Science 327, 970-971 (2010)
Science
AAAS
1 cm
TURBULENCE
MIXING
1 m
ENTRAINMENT

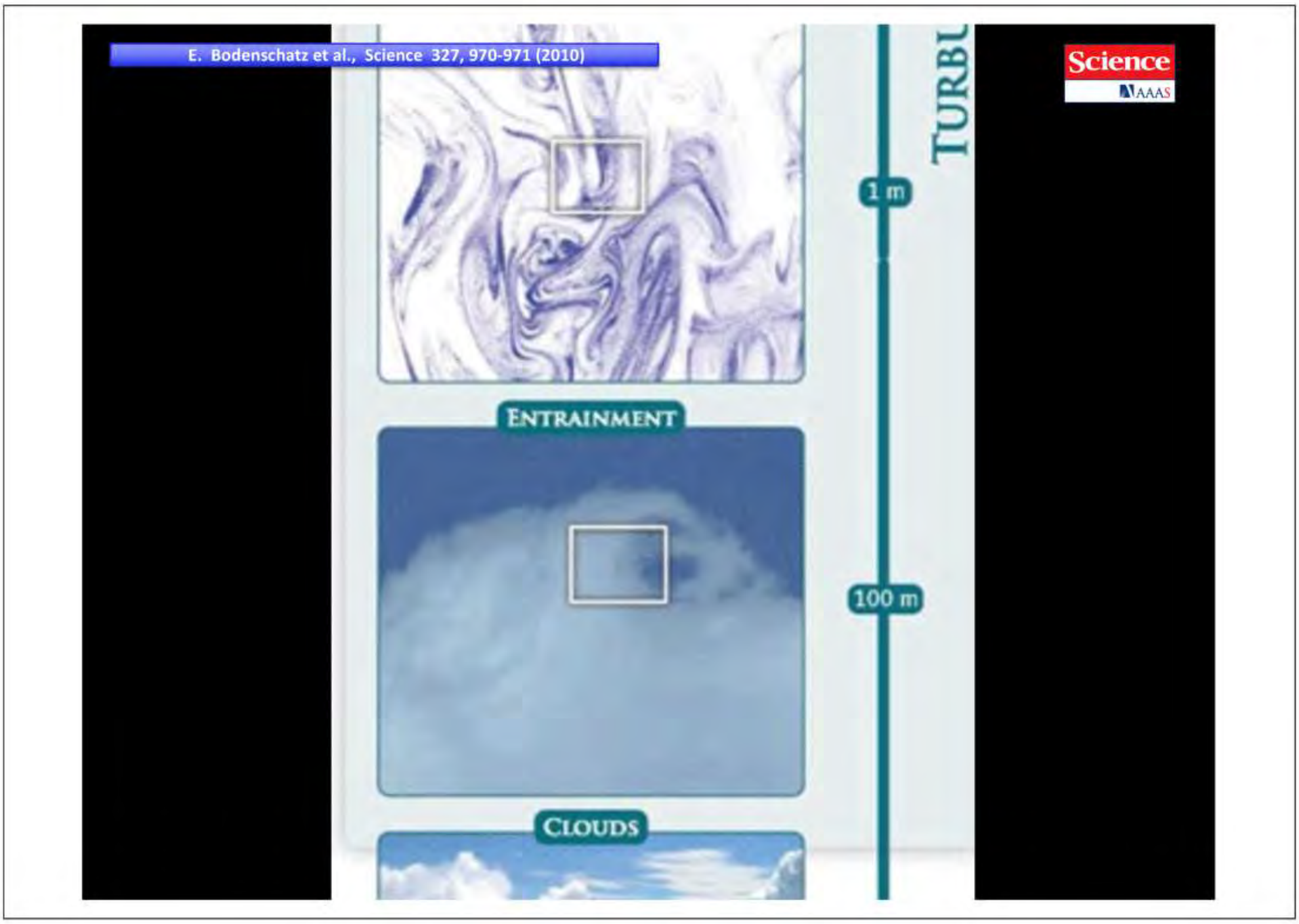
E. Bodenschatz et al., Science 327, 970-971 (2010)
Science
AAAS
1 m
ENTRAINMENT
100 m
CLOUDS

E. Bodenschatz et al., Science 327, 970-971 (2010)

Science AAAS

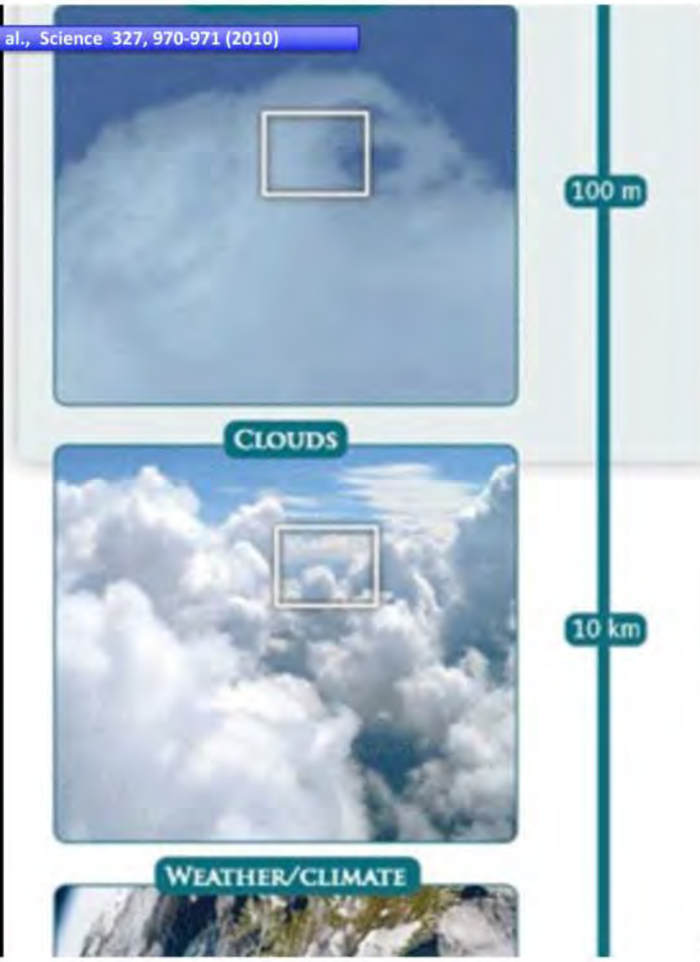

E. Bodenschatz et al., Science 327, 970-971 (2010)

Science AAAS

Leibniz-Institute for Tropospheric Research

German Dutch Windtunnel:
LLF: $Re < 6x10^6$; < 150 m/s ; < 13 MW

Göttingen (2009) Turbulence tunnel
$Re < 7x10^6$; < 5 m/s ; < 200 kW

To generate High Reynolds number turbulence:

$$Re = \frac{\rho U L}{\mu}$$

under controllable conditions:

homogeneity,
isotropy,
turbulence intensity,
integral length scale,
shear,
...

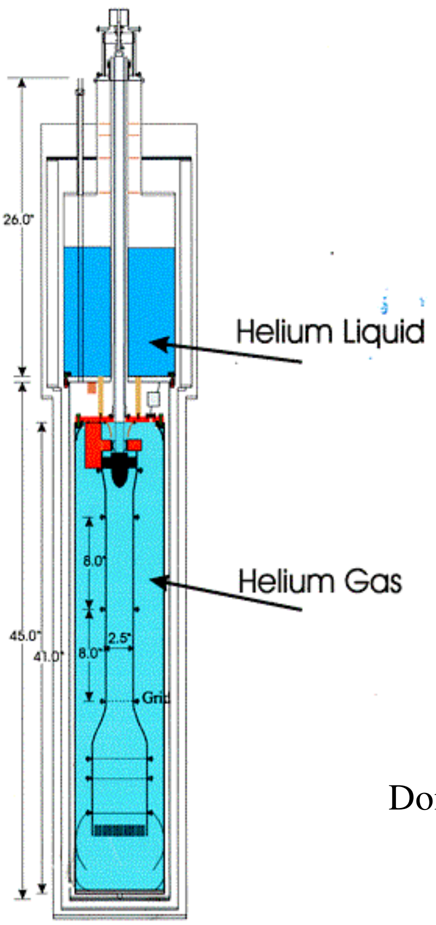

Donnelly, Oregon


, Corrsin windtunnel with active grid; Johns Hopkins
HIFI
NORMAL

The Uboot

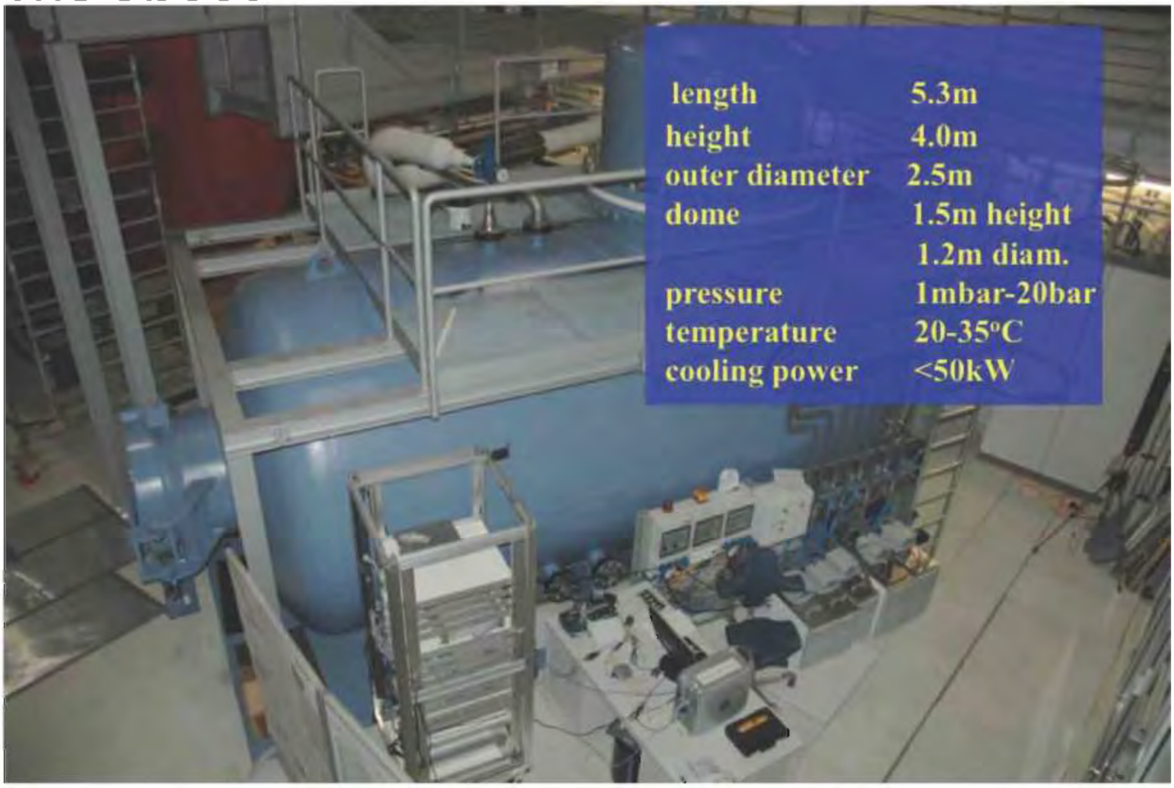

The convection cell in the Uboot

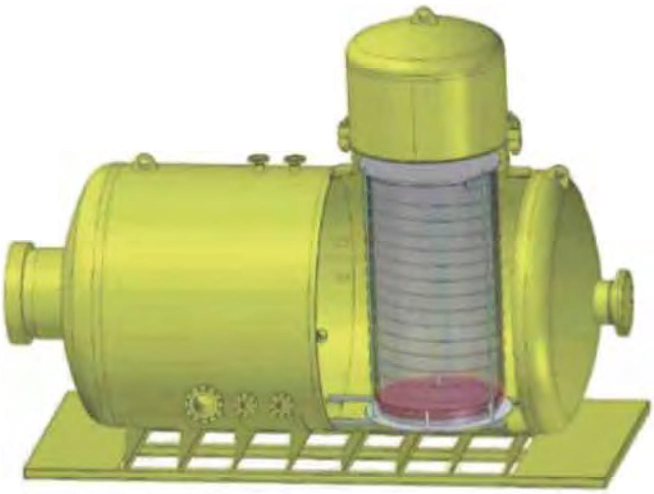

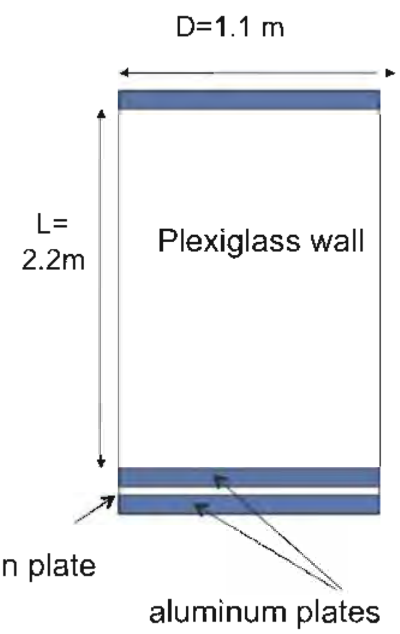

$Pr = 0.8$ and $10^{11} \leq Ra \leq 10^{15}$

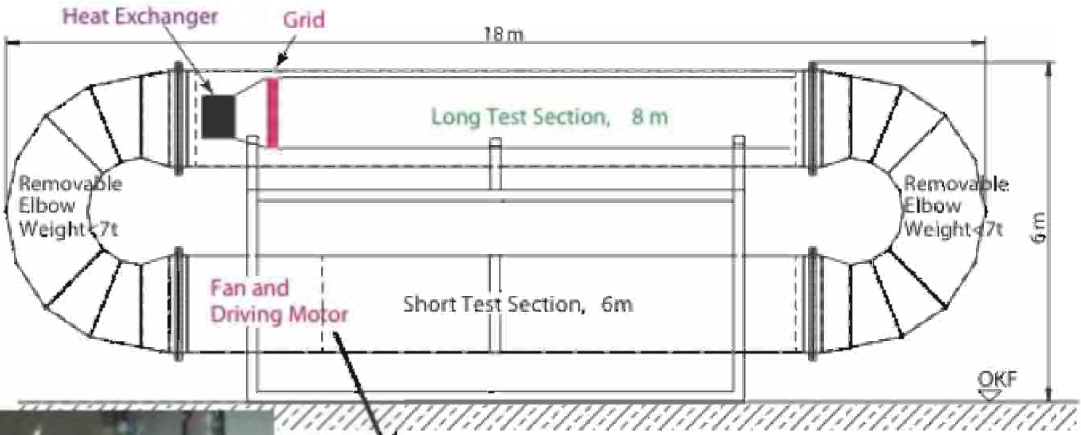

Gas storage

Passive grid turbulence

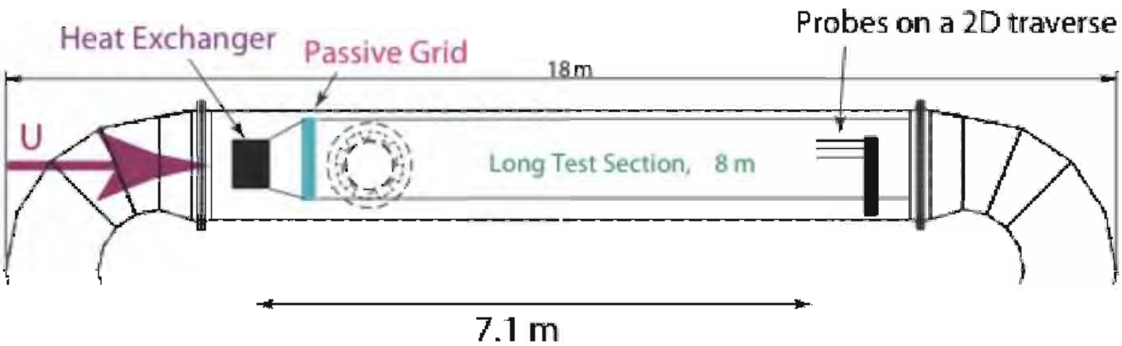

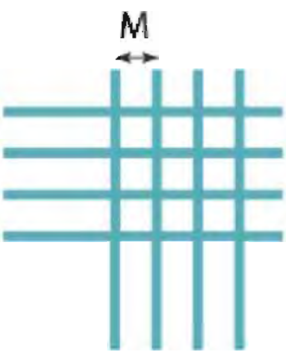

Passive Grid:

biplanar mesh of square bars with 35% solidity

mesh spacing, M = 107 mm

probes are x/M = 67 meshes downstream

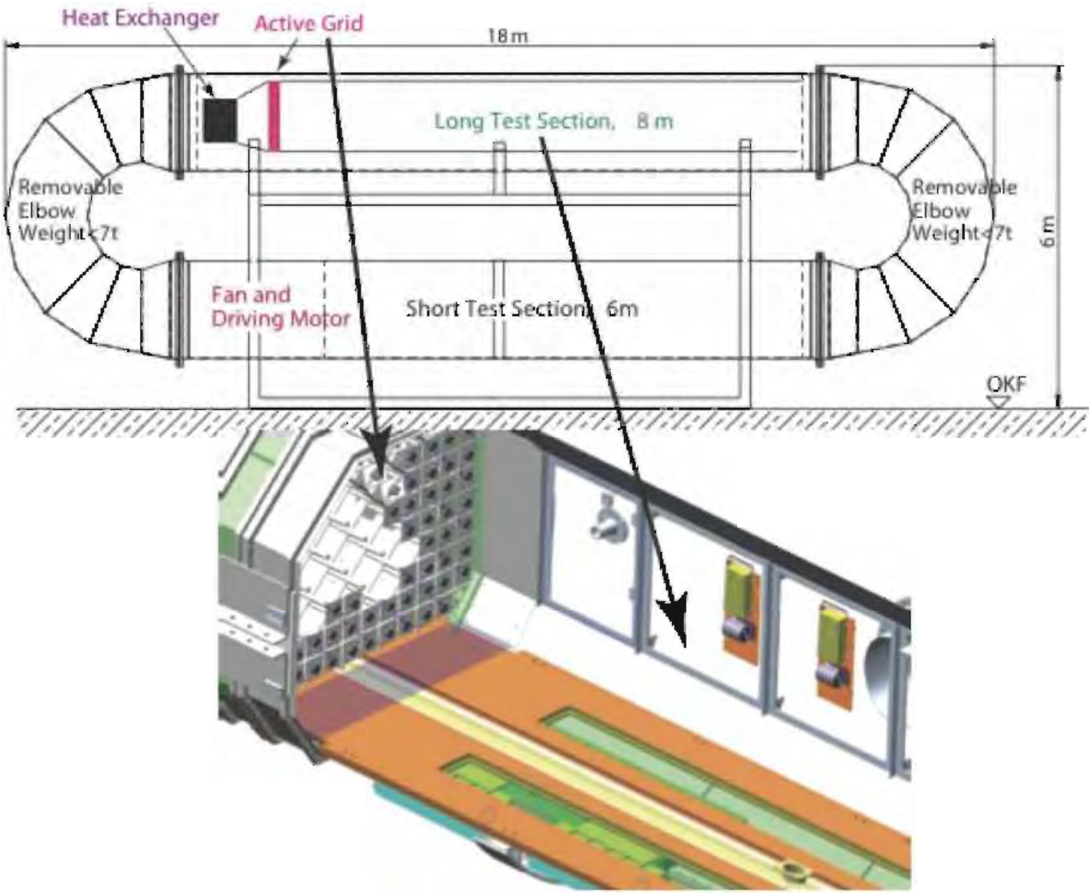

The active grid

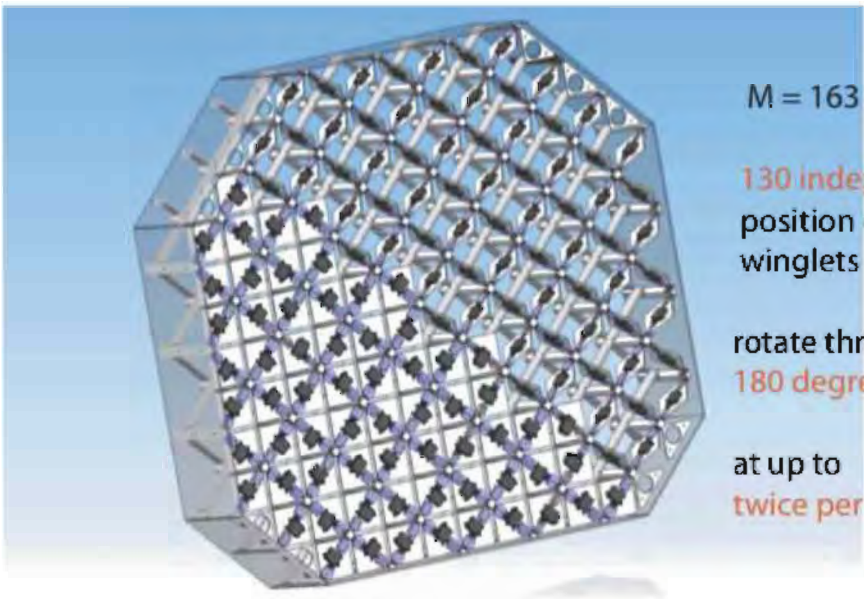

M = 163 mm

130 independent position controlled winglets

rotate through 180 degrees

at up to twice per second.

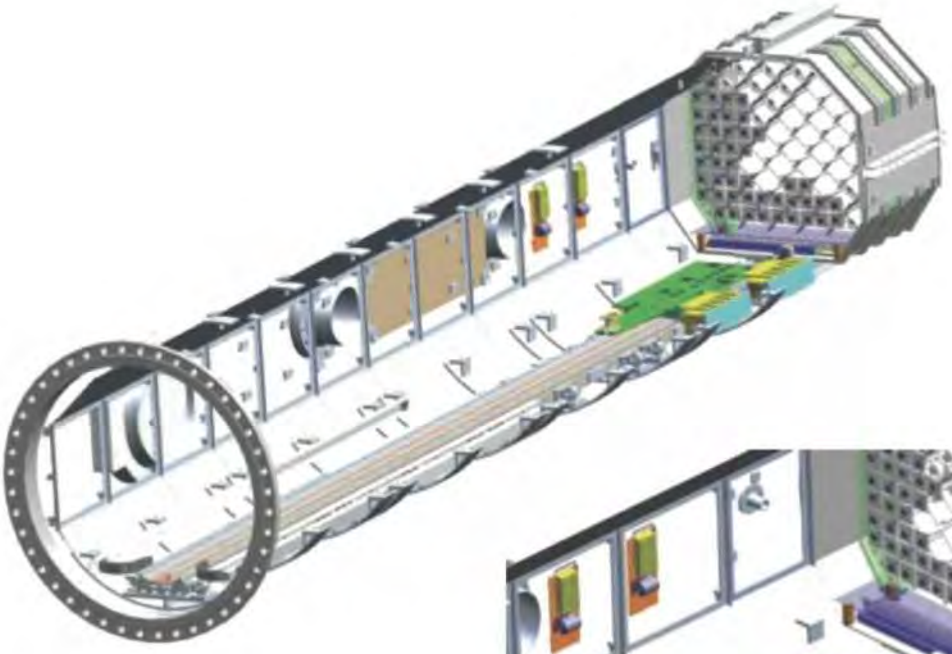

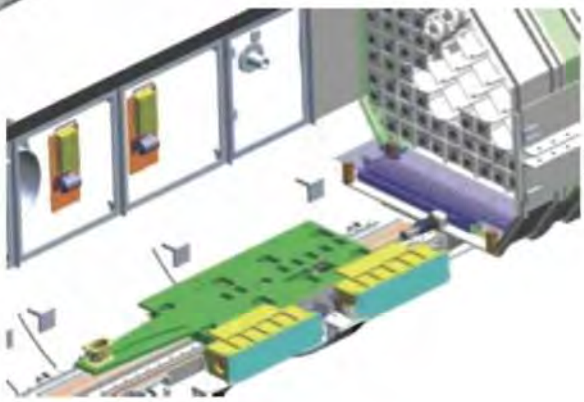

Cornell Windtunnel

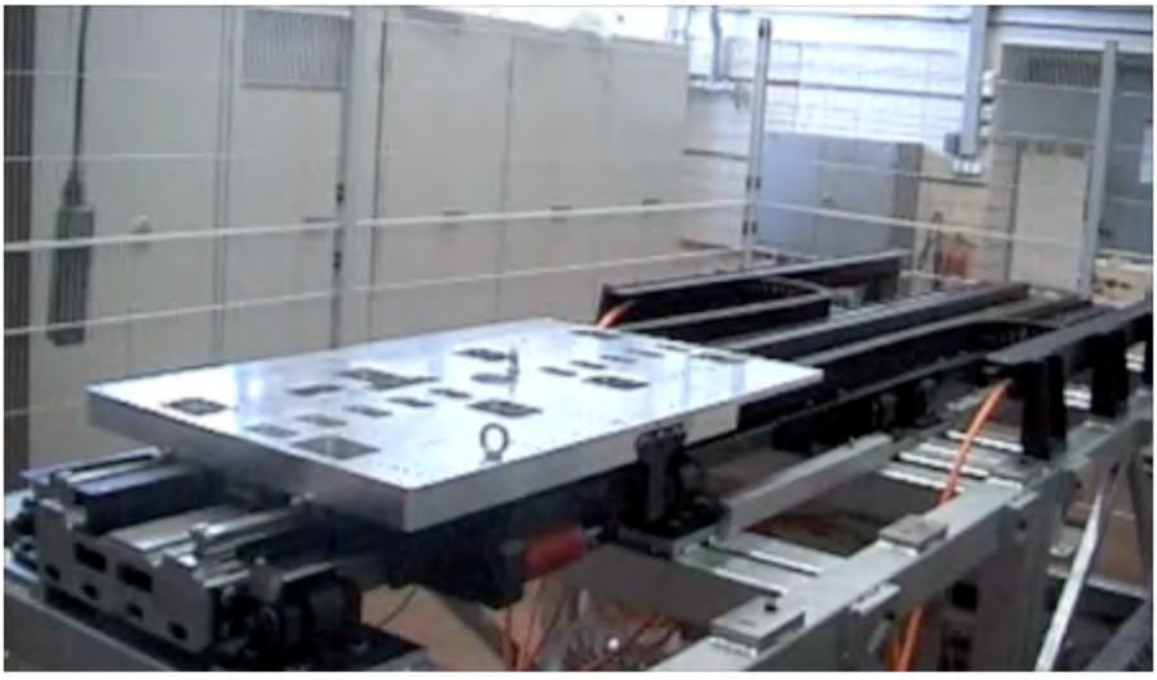

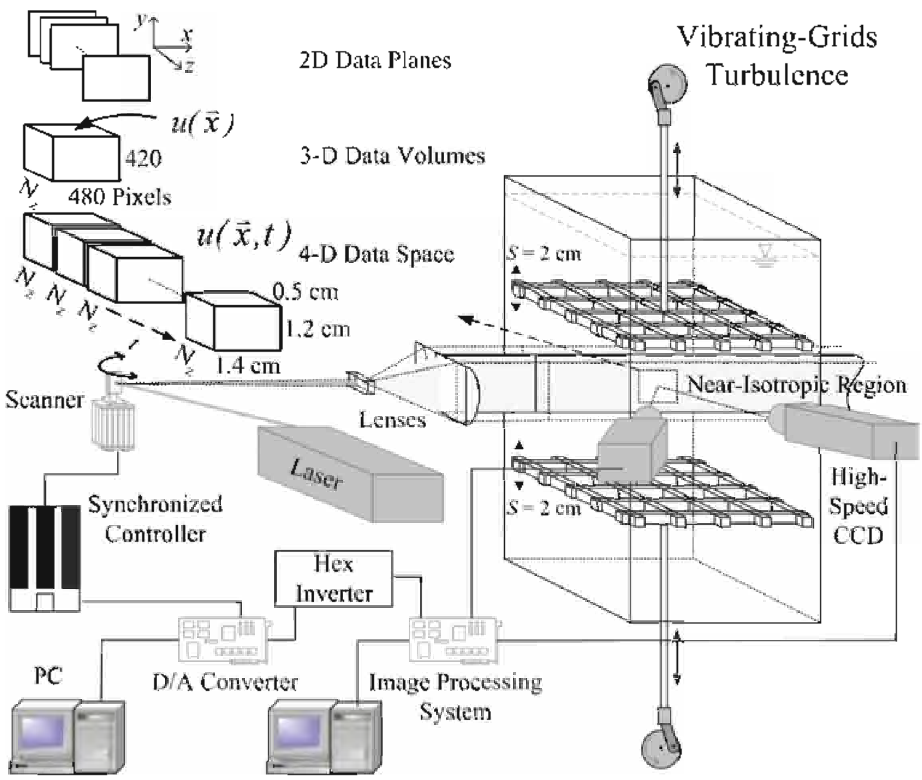

ON DISSIPATIVE STRUCTURES OF STIRRING-GRIDS TURBULENCE

L. J. Jiang, S. S. Shy, and T. H. Yuan
Department of Mechanical Engineering, National Central University, Chung-Li 32054, Taiwan

Random-jet-stirred turbulence tank

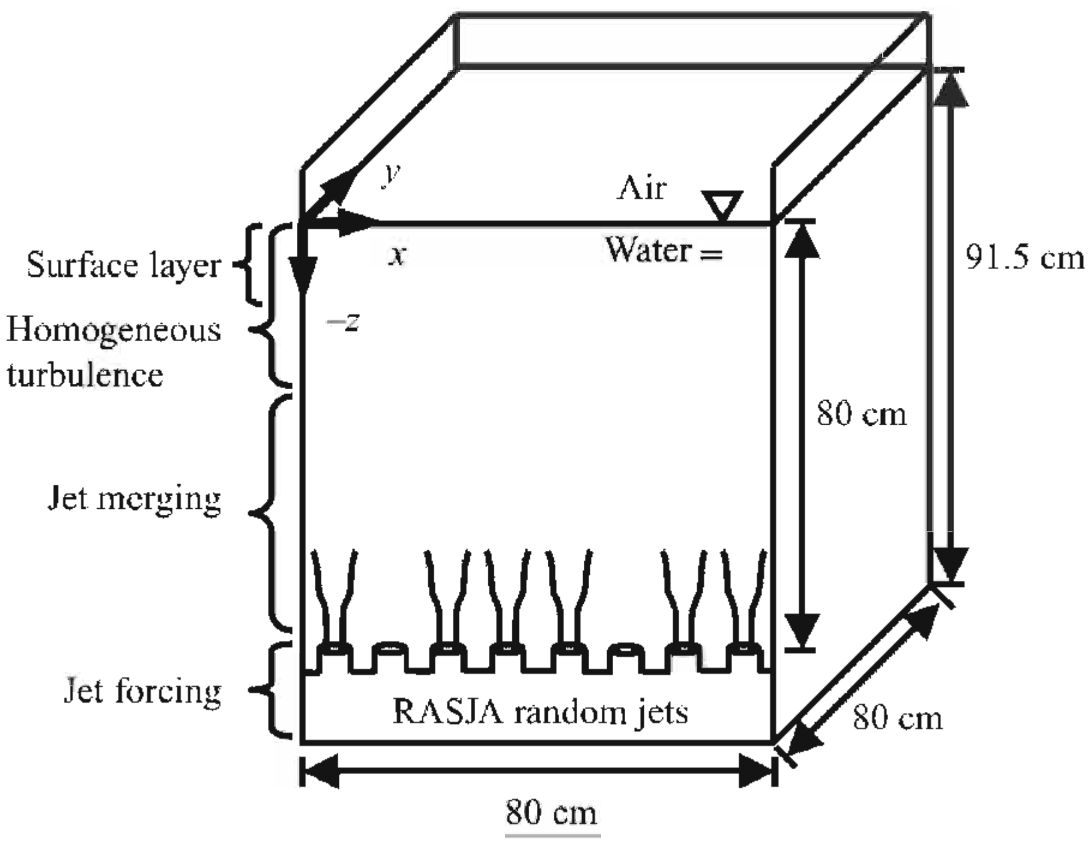

A Random-jet-stirred Turbulence Tank,

E. A. Variano and E. A. Cowen

Horizontal von Karman mixer

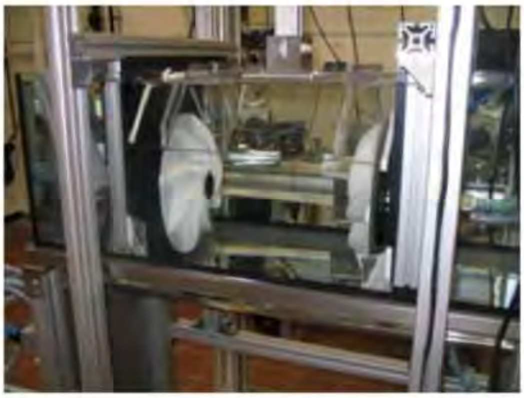

40 cm length, 38 cm width
28 cm propellers

R_λ = ~200 - ~1000
η = ~200μm - ~20 μm
τ_η = ~40ms - 0.4ms
spacial resolution > 11μm
particle size > 30 μm
frame rate < 40 kHz

Heavy particles stay in the flow.

Inertial effects on two-particle relative dispersion in turbulent flows

Mathieu Gibert[1,4 (a)], Haitao Xu[1,4 (b)] and Eberhard Bodenschatz[1,2,3,4 (c)]

The Flow

- closed container
- no meanflow in middle
- driven by 1kW DC motors
- temperature controlled to 50mK
- water filtered to 0.3 microns

$Re_\lambda = 1000$
($Re = 70.000$)

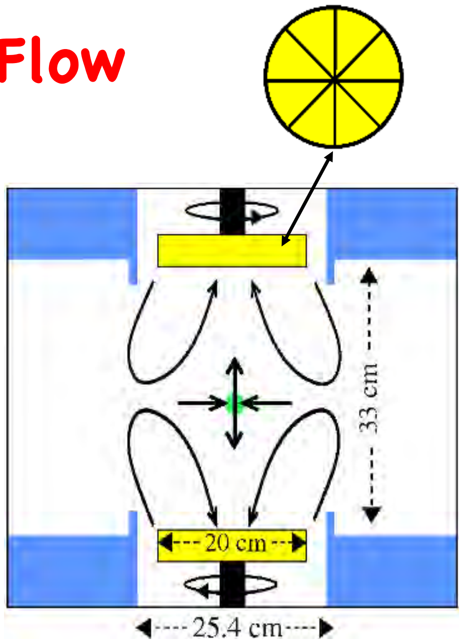

- closed container
- no meanflow in middle
- driven by 1kW DC motors
- temperature controlled to 50mK
- water filtered to 0.3 microns

$Re_\lambda = 1000$
($Re = 70.000$)

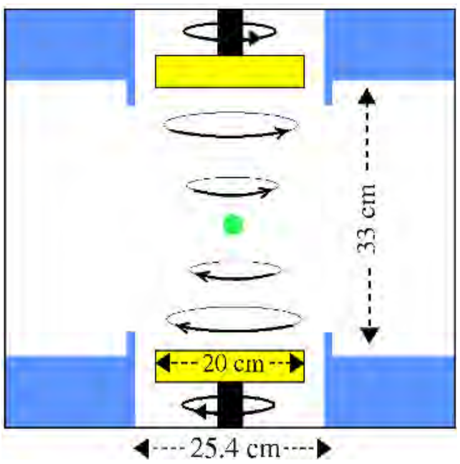

LIMNOLOGY
and
OCEANOGRAPHY: METHODS

Limnol. Oceanogr.: Methods 2, 2004, 1–12

A novel laboratory apparatus for simulating isotropic oceanic turbulence at low Reynolds number

Donald R. Webster[1], *Aisha Brathwaite*[1], *and Jeannette Yen*[2]
[1]School of Civil & Environmental Engineering, Georgia Institute of Technology, Atlanta, GA, USA 30332
[2]School of Biology, Georgia Institute of Technology, Atlanta, GA, USA 30332

Fig. 2. Photograph of the turbulence chamber and actuators

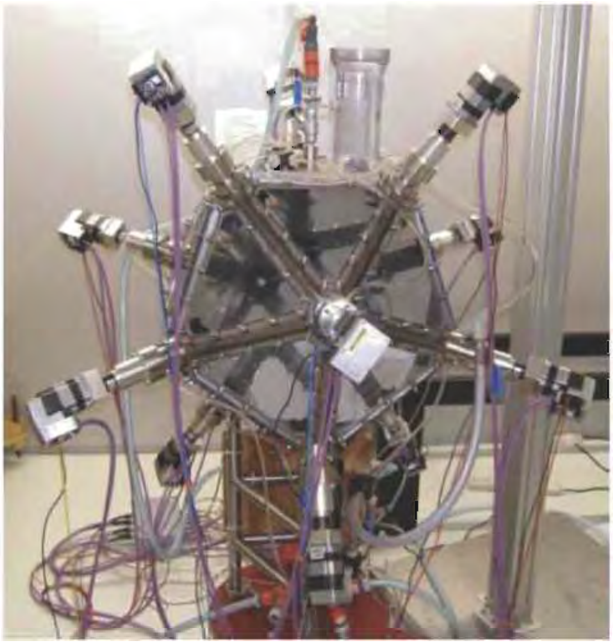

Lateral size: 40 cm

12 independently controlled propellers

20 windows allow simultaneous operation of multiple instruments to obtain both Eulerian (such as LDV, PIV, etc.) and Lagrangian (e.g. particle tracking) measurements.

R_λ : 100 - 900

The Lagrangian Exploration Module: An Apparatus for the Study of Statistically Homogeneous and Isotropic Turbulence

Robert Zimmermann* †,[1,2] Haitao Xu‡,[1,2] Yoann Gasteuil,[1,3] Mickaël Bourgoin,[1,4] Romain Volk,[1,5] Jean-François Pinton,[1,3] and Eberhard Bodenschatz[1,2]
[1]*International Collaboration for Turbulence Research*
[2]*Max Planck Institute for Dynamics and Self-Organization, Göttingen, D-37077 Germany*
[3]*Laboratoire de Physique, CNRS &Ecole Normale Supérieure de Lyon, UMR 5672, Lyon, F-69007 France*
[4]*Laboratoire des Ecoulements Geophysiques et Industriels, CNRS UJF INPG, UMR5519, F-38041 Grenoble, France*
[5]*Laboratoire de Physique, Ecole Normale Supérieure de Lyon, Lyon, F-69007 France*

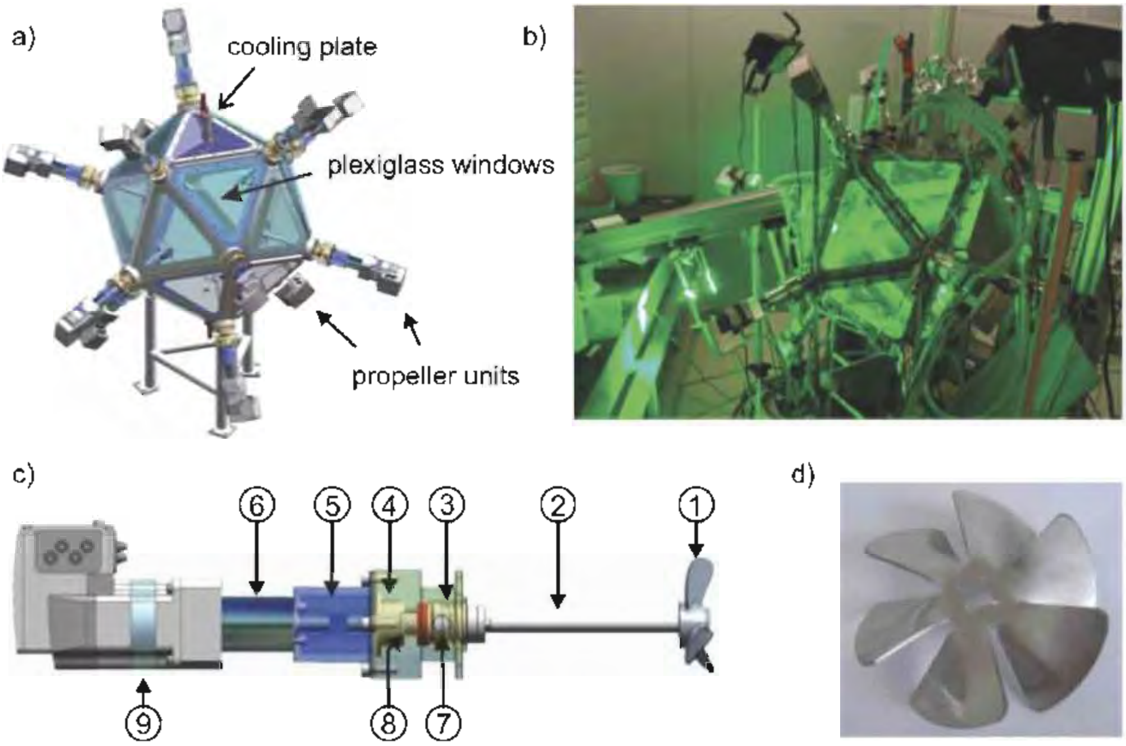

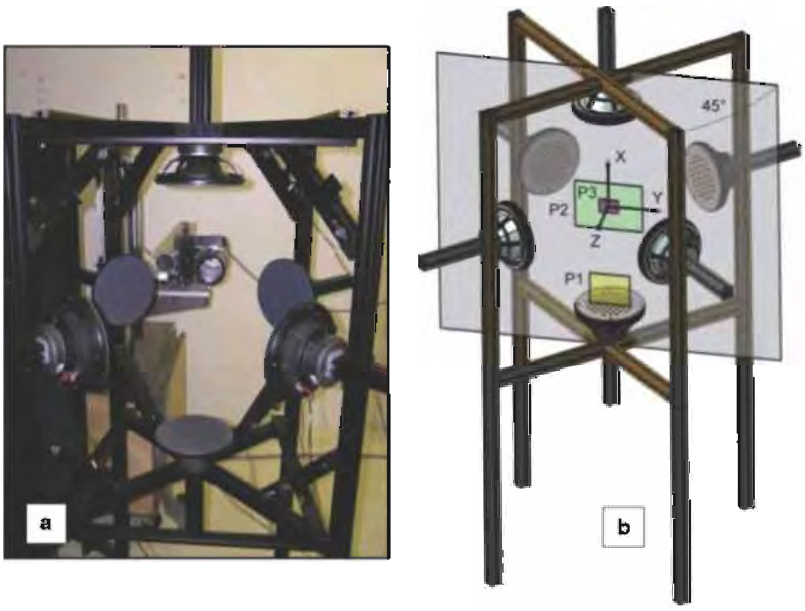

Fig. 1 a Experimental facility, b sketch of the facility. *P1* 130 mm × 103 mm, *P2* 162 mm × 219 mm, *P3* 62 mm × 46 mm

Exp Fluids (2010) 48:809–822
DOI 10.1007/s00348-009-0768-5

RESEARCH ARTICLE

Characterization of a system generating a homogeneous isotropic turbulence field by free synthetic jets

Charles Goepfert · Jean-Louis Marié ·
Delphine Charreyron · Michel Lance

The Soccer Ball

← 1 m →

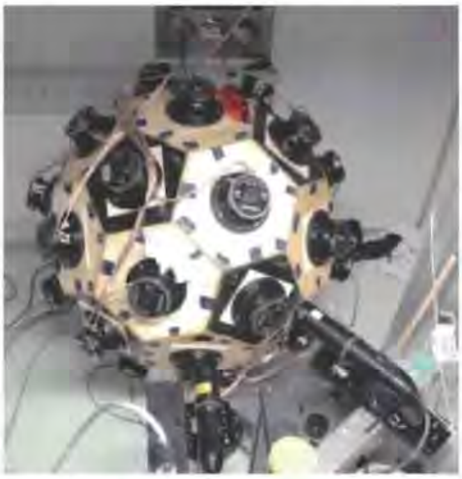

-Flow driven by 32 independently modulated, loud-speaker driven air jets.

-Turbulence is homogeneous and isotropic within 5 cm of the center of the ball.

-Droplets tracked using 20 W pulsed YAG laser illumination, 3 CMOS cameras that image 128x128 pixels each at 20,000 frames per second.

$u \sim 1$ m/s
$\varepsilon \sim 5\ m^2/s^3$
$\eta \sim 150\ \mu m$
$R_\lambda \sim 450$

Manipulating the anisotropy of turbulence

KELKEN CHANG, GREGORY P. BEWLEY AND EBERHARD BODENSCHATZ

Scales

Apparatus	P (bar)	ν (m^2/s)	u' (m/s)	ϵ (m^2/s^3)	ℓ (m)	λ (μm)	η (μm)	τ_η (ms)	R_λ
SF_6 tunnel	15	1.5×10^{-7}	1.0	1.2	0.45	1400	7.3	0.36	9600
air tunnel	1	1.5×10^{-5}	1.2	3.9	0.4	9100	172	2.0	730
SF_6 tank	15	1.5×10^{-7}	1.0	5.5	0.094	648	5.0	0.17	4360
water tank	1	8×10^{-7}	2.2	59	0.094	1000	9.7	0.12	2800

Clouds: 0.01 100 >50 >10 >10000

Lagrangian stochastic models (Langevin-model -- Pope, Sawford)

$$d\mathbf{v} = -A(v)dt + B(v)d\mathbf{W}$$

$$d\mathbf{v} = -\frac{v}{T_L}dt + \sqrt{C_0\epsilon}\,d\mathbf{W}$$

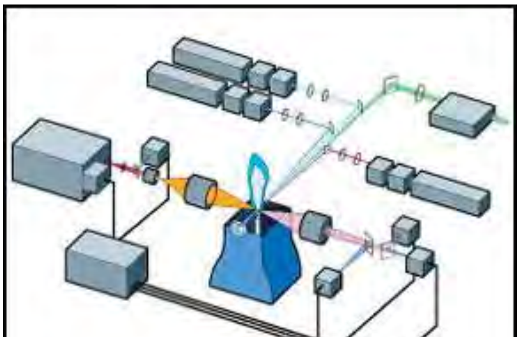

R. Barlow (Sandia Nat. Lab.)

Spatial Properties (Eulerian)

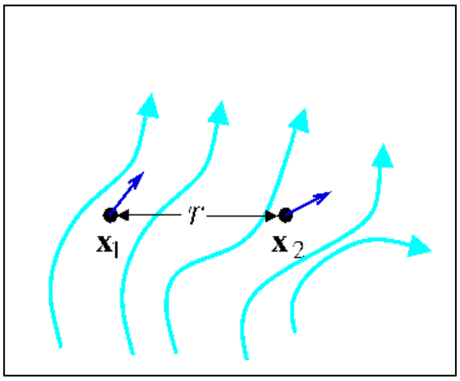

Point measurements

$$\Delta u_i = u_i(\vec{x} + \hat{e}_i r) - u_i(\vec{x})$$

Inertial scale:

$$\langle (\Delta_r u_i)^p \rangle \sim (\epsilon r)^{p/3}$$

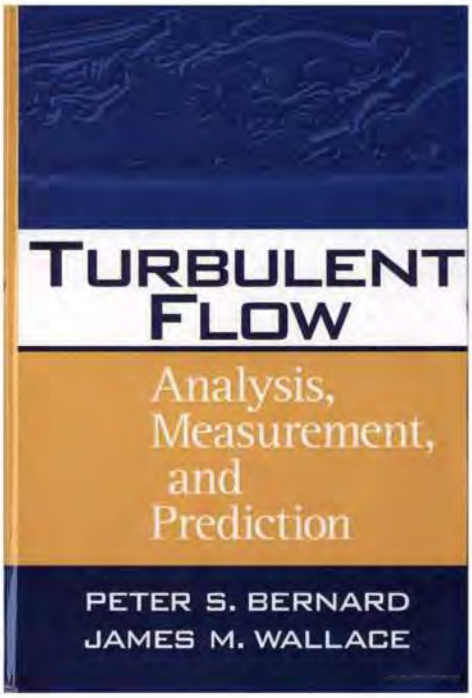

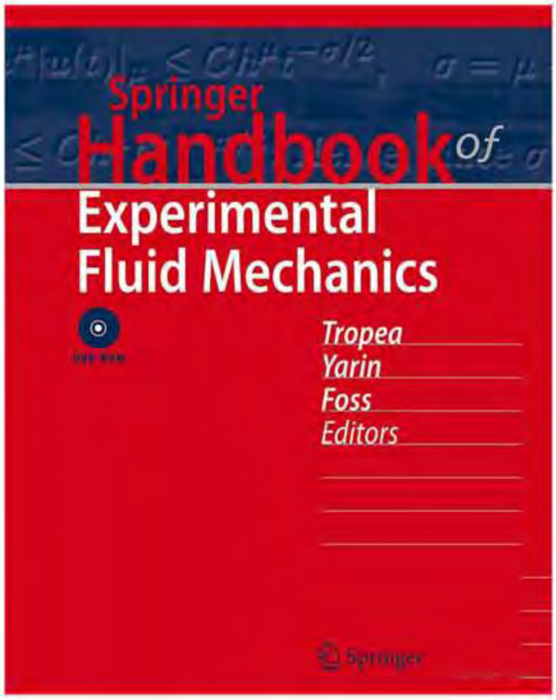

http://www.aoe.vt.edu/~simpson/aoe4154/hotwirelab.pdf

Hot Wire Anemometry

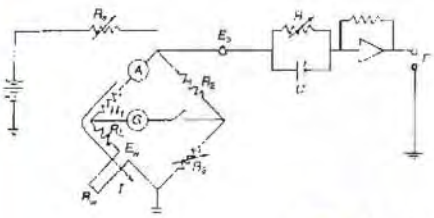

DANTEC

- Measures velocity by heat transfer from a wire
- Allows high temporal resolution and has very high signal to noise ratio.
- Taylor's Hypothesis: Large mean velocity allows a time sequence to be converted into a spatial cut across the flow.

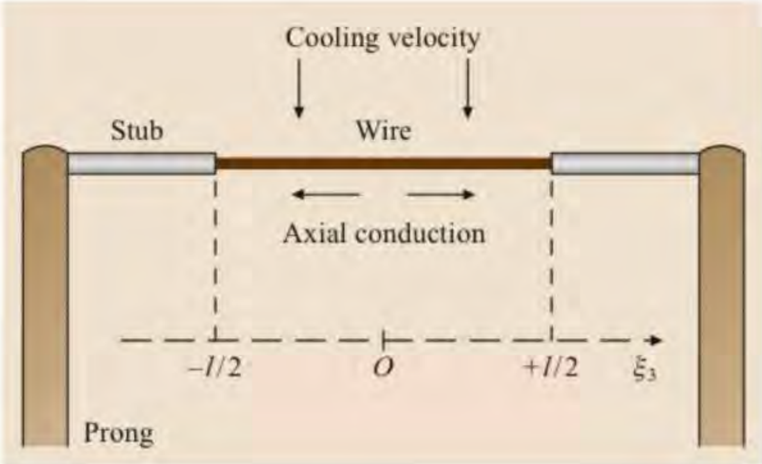

CCA constant current anemometer
CTA constant temperature anemometer
CVA constant voltage anemometer

Table 5.1 Physical properties of sensor materials at 293 K (approximate values for MEMS polysilicons doping, P is phosphor and B boron)

Material	Resistivity (Ωm)	Temperature coefficient of resistivity χ (K^{-1})	Density ρ (kg/m^3)	Specific heat c ($J\,kg^{-1}K^{-1}$)	Thermal conductivity k ($W\,m^{-1}K^{-1}$)	Ref.
Copper	1.6×10^{-8}	$+4.0\times10^{-3}$	8900	385	400	[5.57]
Nickel	7.0×10^{-8}	$+6.0\times10^{-3}$	8900	438	90	
Platinum	1.1×10^{-7}	$+3.9\times10^{-3}$	21500	130	70	[5.58]
Pt/10% Rh	1.9×10^{-7}	$+1.7\times10^{-3}$	19900	150	40	[5.59]
Silver	1.6×10^{-8}	$+3.8\times10^{-3}$	10500	235	428	[5.57]
Tungsten	6.0×10^{-8}	$+4.5\times10^{-3}$	19300	140	170	[5.58]
Silicon	2.3×10^{3}	-7.5×10^{-2}	2330	705	148	[5.60]
Polysilicon						
High P doping	5×10^{-5}	$+1.0\times10^{-3}$			50	[5.61]
Low P doping	5×10^{-5}	-2.5×10^{-3}				
B doping	2×10^{-5}	$+8.5\times10^{-4}$			60	[5.61, 62]
B doping 2×10^{16} /cm^2	5×10^{-5}	$+8.0\times10^{-4}$				[5.63, 64]

Part B, 5.2 Springer Hand Book.

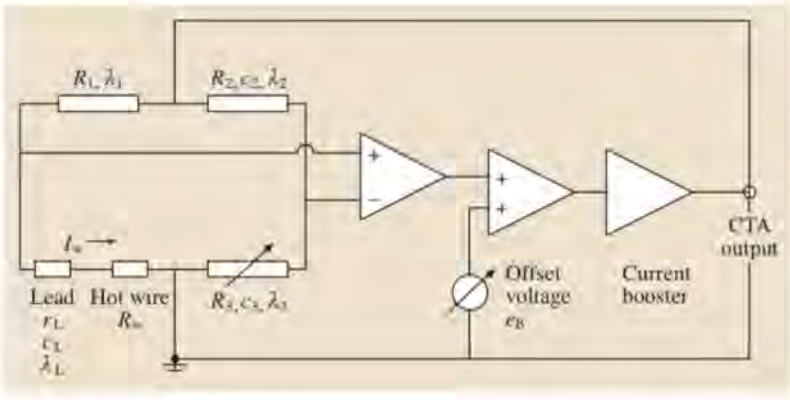

Fig. 5.31 Block diagram of a constant-temperature anemometer (CTA). The wire overheat is adjusted by modifying resistance R_3. The adjustable capacities and inductances placed in arms 2 and 3 of the bridge, c_2, λ_2, c_3, λ_3, and the offset voltage e_B, make the CTA stable

More details see book…

Tracer based techniques:

Molecular Tagging Velocimetry

Particle based:

Laser Doppler Velocimetry

Particle Image Velocimetry

Lagrangian Particle Tracking

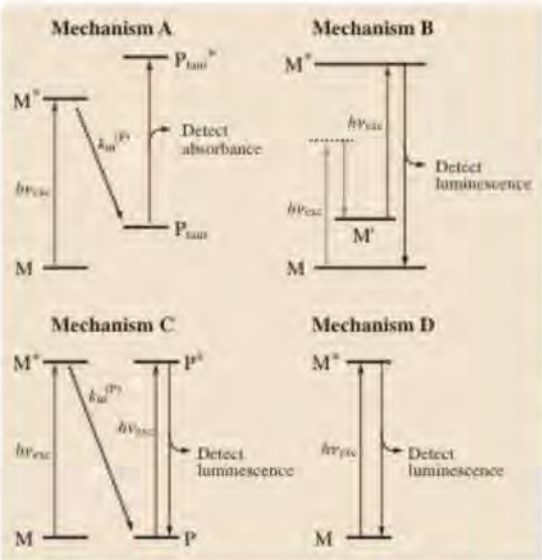

Fig. 5.151 The different mechanisms of MTV. M and M* designate a molecule in its ground and electronic excited state, respectively, and P indicates the formation of a new molecule. Consistent with Fig. 5.150, *solid arrows* describe radiative transitions and *wavy arrows* indicate nonradiative transitions. The excitation lines are color-coded to emphasize the number of different frequencies typically needed for each experiment. The different diagrams summarize the photochemistry and photophysics that give rise to the various MTV techniques under the various acronyms of LIPA based on photochromism (type A), RELIEF (type B), PHANTOMM, OTV, HTV (type C), and direct luminescence (type D)

MTV

LIPA:
laser-induced photochemical anemometry

RELIEF: Raman excitation plus laser-induced electronic fluorescence

PHANTOMM:
photoactivated non-intrusive tracing of molecular motion
OTV: oxygen tagging velocimetry
HTV: hydroxyl tagging velocimetry
NO: photorelease of NO.

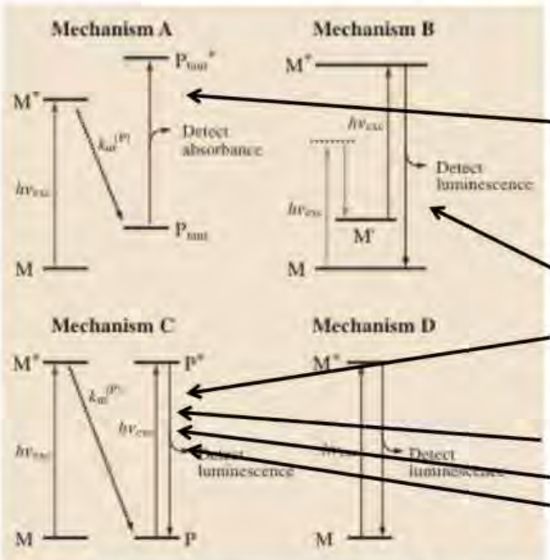
Fig. 5.151 The different mechanisms of MTV. M and M* designate a molecule in its ground and electronic excited state, respectively, and P indicates the formation of a new molecule. Consistent with Fig. 5.150, *solid arrows* describe radiative transitions and *wavy arrows* indicate nonradiative transitions. The excitation lines are color-coded to emphasize the number of different frequencies typically needed for each experiment. The different diagrams summarize the photochemistry and photophysics that give rise to the various MTV techniques under the various acronyms of LIPA based on photochromism (type A), RELIEF (type B), PHANTOMM, OTV, HTV (type C), and direct luminescence (type D)

MTV

LIPA:
laser-induced photochemical anemometry

RELIEF: Raman excitation plus laser-induced electronic fluorescence

PHANTOMM:
photoactivated non-intrusive tracing of molecular motion
OTV: oxygen tagging velocimetry
HTV: hydroxyl tagging velocimetry
NO: photorelease of NO.

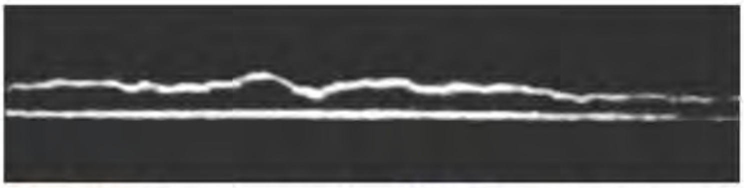

Fig. 5.158 Typical single-line RELIEF image pair taken in a turbulent free air jet with 0 μs (*lower line*), and 7 μs (*upper line*) time delay. The *line* is approximately 1.2 cm long (after [5.590], with permission of Cambridge Univ. Press)

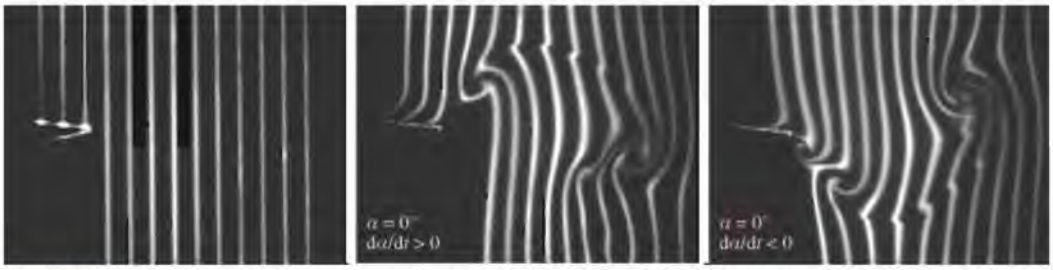

Fig. 5.160 Multiline tagging in the trailing region of a NACA-0012 airfoil pitching sinusoidally with an amplitude of 2° [5.659]. The tagging pattern (*left image*) right after the laser pulse is a series of parallel lines with a spacing of 3 mm (about 0.025 chord length). The displaced lines are shown at zero angle of attach during pitch-up (*middle image*) and pitch-down (*right image*)

Particle based:

Laser Doppler Velocimetry
Particle Image Velocimetry
Lagrangian Particle Tracking

Fluid	Material	Diameter (μm)	Density (kg/m³)
Air	DEHS	1–3	10^3
–	Glycol–water solution	1–3	10^3
–	Vegetable oil	1–3	10^3
–	TiO_2	0.2–0.5	$1–4 \times 10^3$
Water	Latex	5–50	10^3
–	Sphericell	10–100	$0.95–1.05 \times 10^3$
–	Silver-coated hollow glass spheres	30–100	$> 10^3$

Example: Particles in turbulent water flow

	ρ_p/ρ_f	d_p (μm)	d_p/η	St
Polystyrene	1.06	74 ± 10	0.98	0.09
Glass	4	75 ± 8	1.04	0.27
Steel	7.8	75 ± 15	1.04	0.50

Table 1: Characteristics of the different particles used in the experiments. The Stokes number is defined as $St \equiv \frac{1}{12\beta}(d_p/\eta)^2$, where d_p is the particle diameter, $\beta \equiv 3\rho_f/(2\rho_p + \rho_f)$ is the modified density ratio with ρ_p and ρ_f being, respectively, the particle and the fluid densities, and η is the Kolmogorov length scale of the turbulence.

From: **Inertial effects on two-particle relative dispersion in turbulent flows**

MATHIEU GIBERT[1,4] (a), HAITAO XU[1,4] (b) and EBERHARD BODENSCHATZ[1,2,3,4] (c)

diameter > wavelength: Mie sacttering

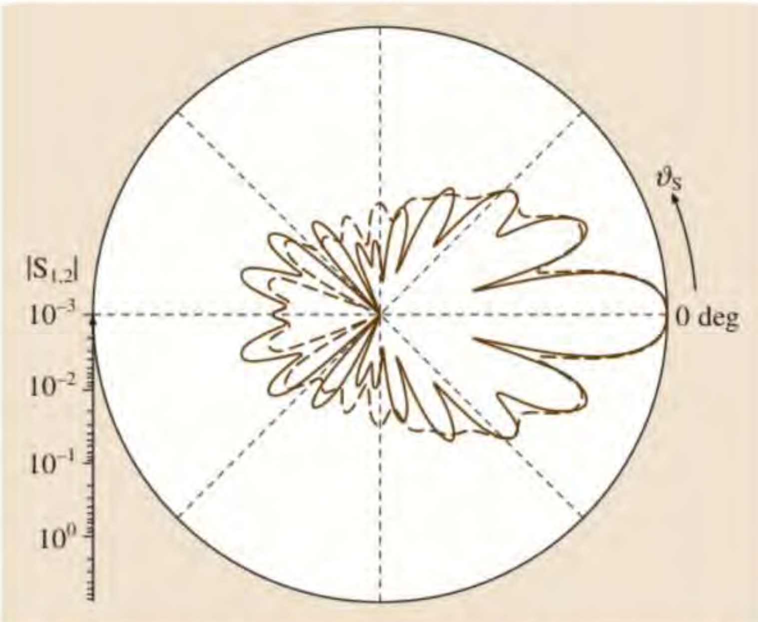

Fig. 5.61 Scattering function for a Mie parameter value of 10 computed for a water droplet in air ($m = 1.334$); *solid line*: perpendicular polarization, *dashed line*: parallel polarization (after *Albrecht* et al. [5.356])

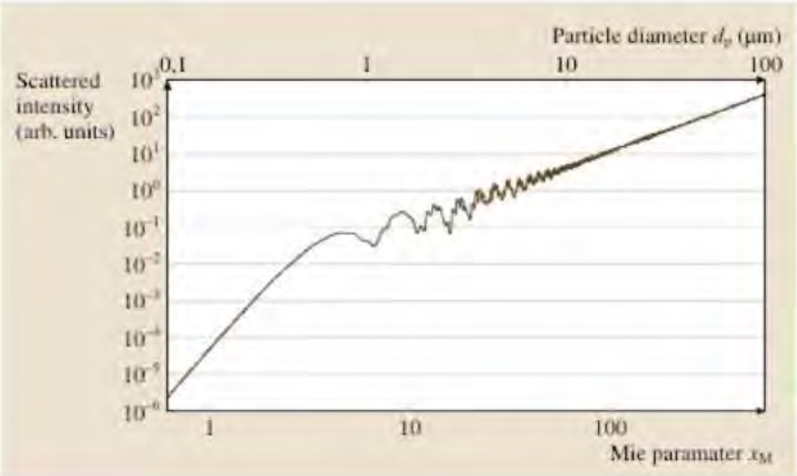

Fig. 5.62 Scattering intensity as a function of the Mie parameter x_M computed for a water droplet in air ($m = 1.333$, $\lambda_w = 514.5$ nm) at a scattering angle of $\vartheta_s = 30°$ and a circular receiver aperture of radius 10 mm (after *Albrecht* et al. [5.356])

Particle generation:

Atomizer – also solid particles

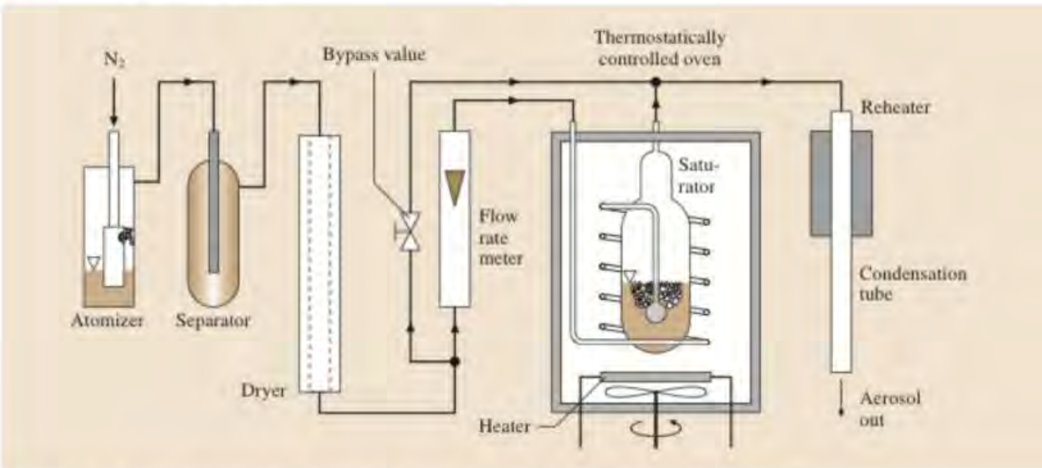

Fig. 5.63 Modified Sinclair–La Mer aerosol generator (after *Helsper* and *Mölter* [5.359])

Laser Doppler Velocimetry

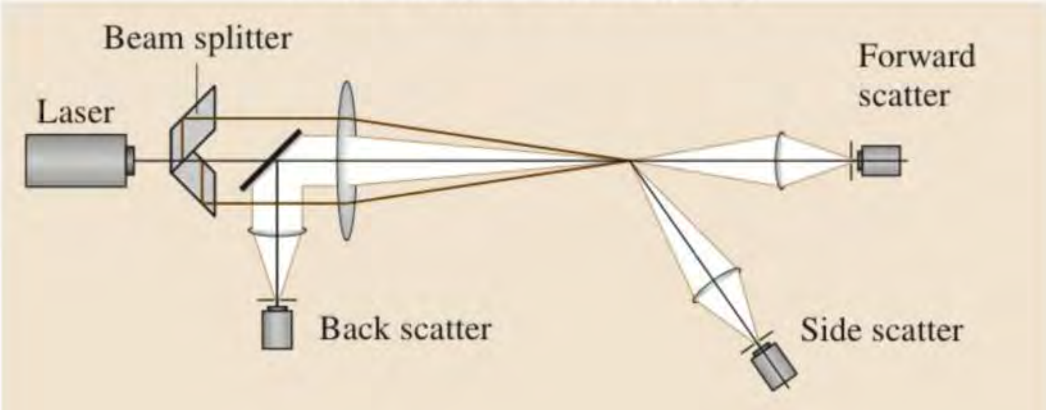

Fig. 5.73 Possible optical configurations of a laser Doppler system

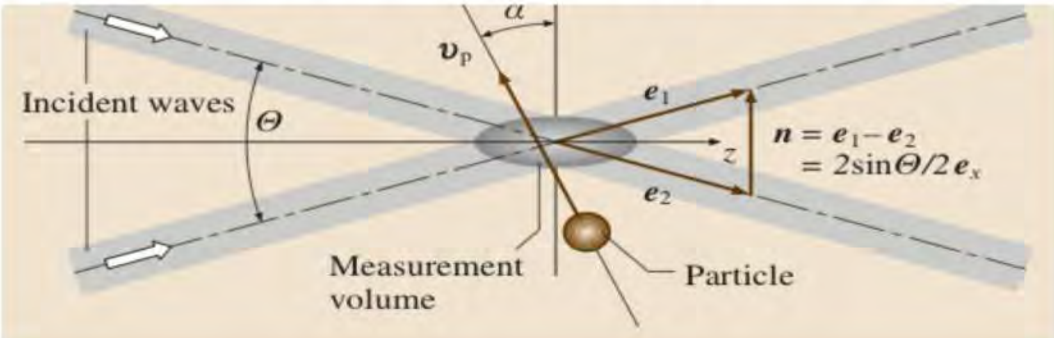

b)

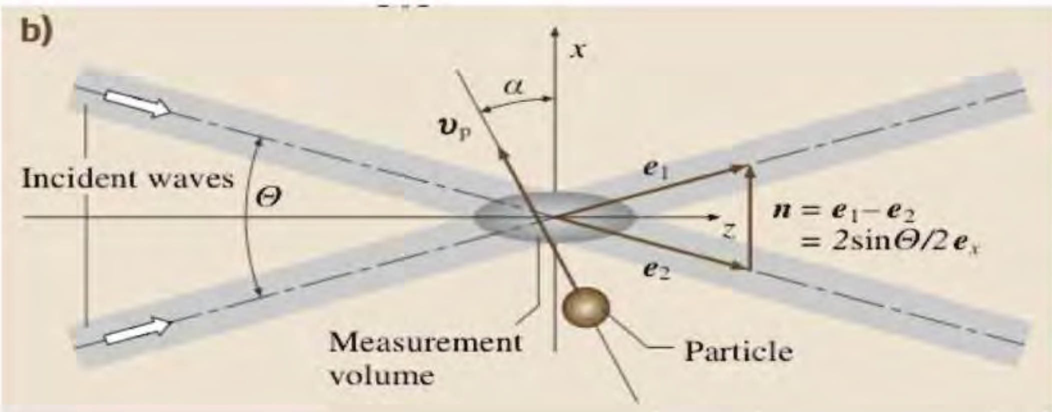

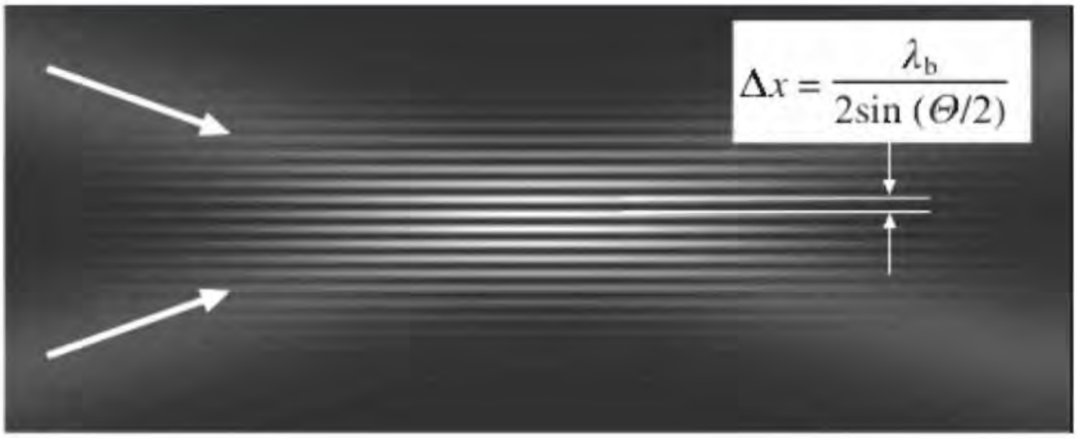

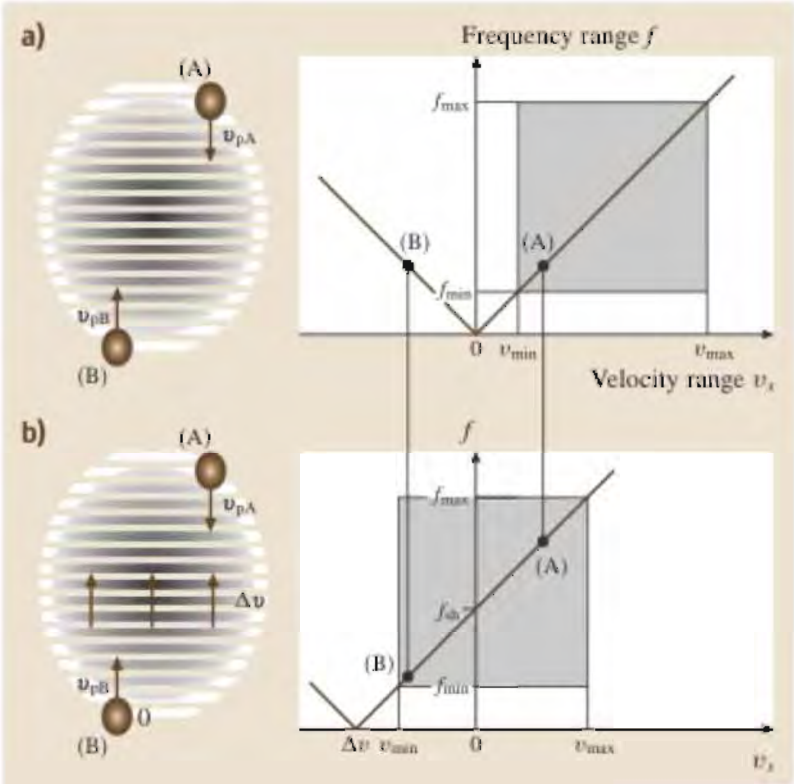

Fig. 5.72a,b Measured frequencies for particles crossing the measurement volume in positive (A) and negative (B) x directions: (**a**) without frequency shift; and (**b**) with frequency shift

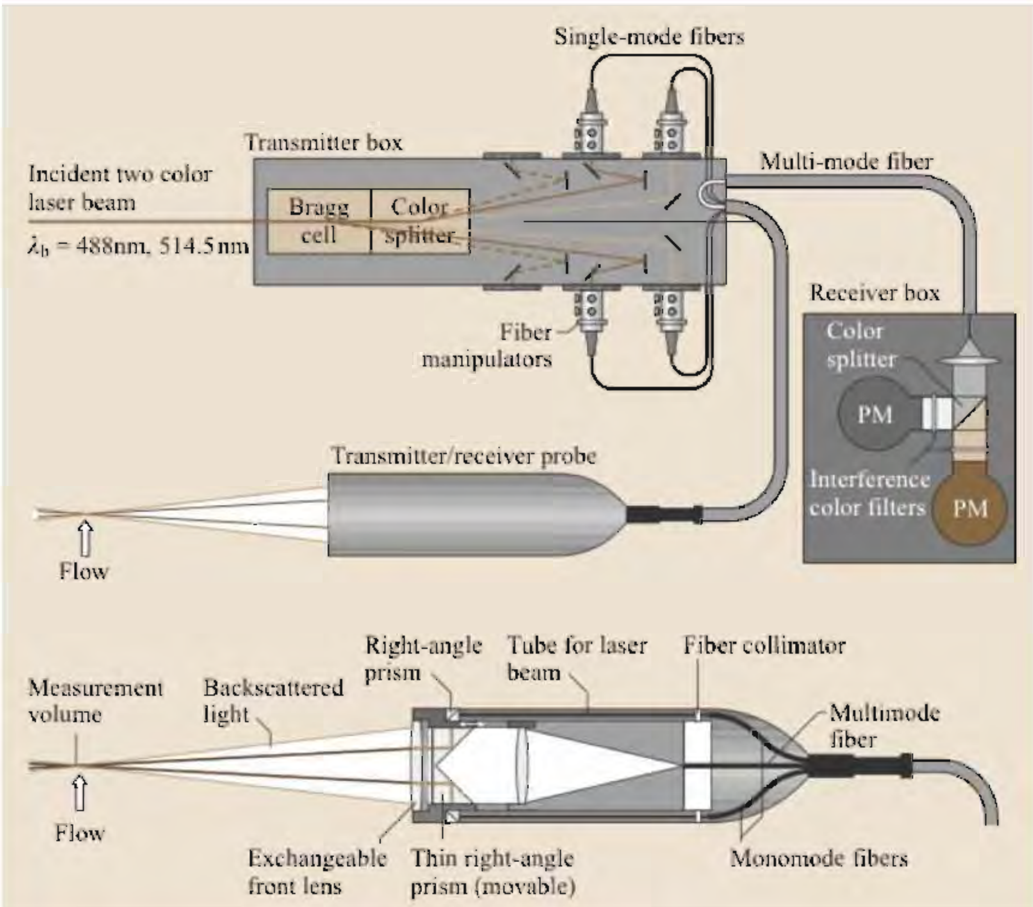

Particle Image Velocimetry

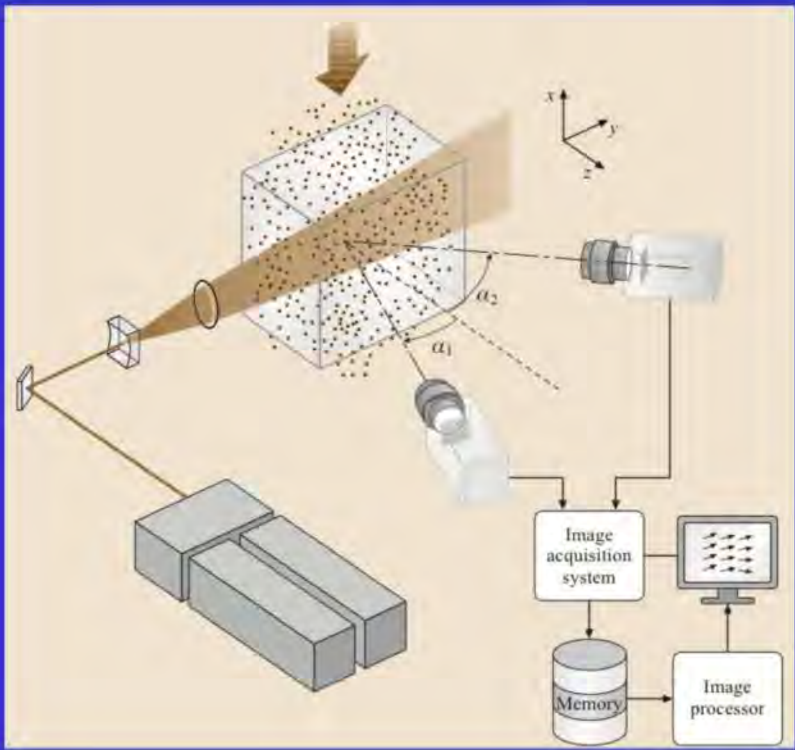

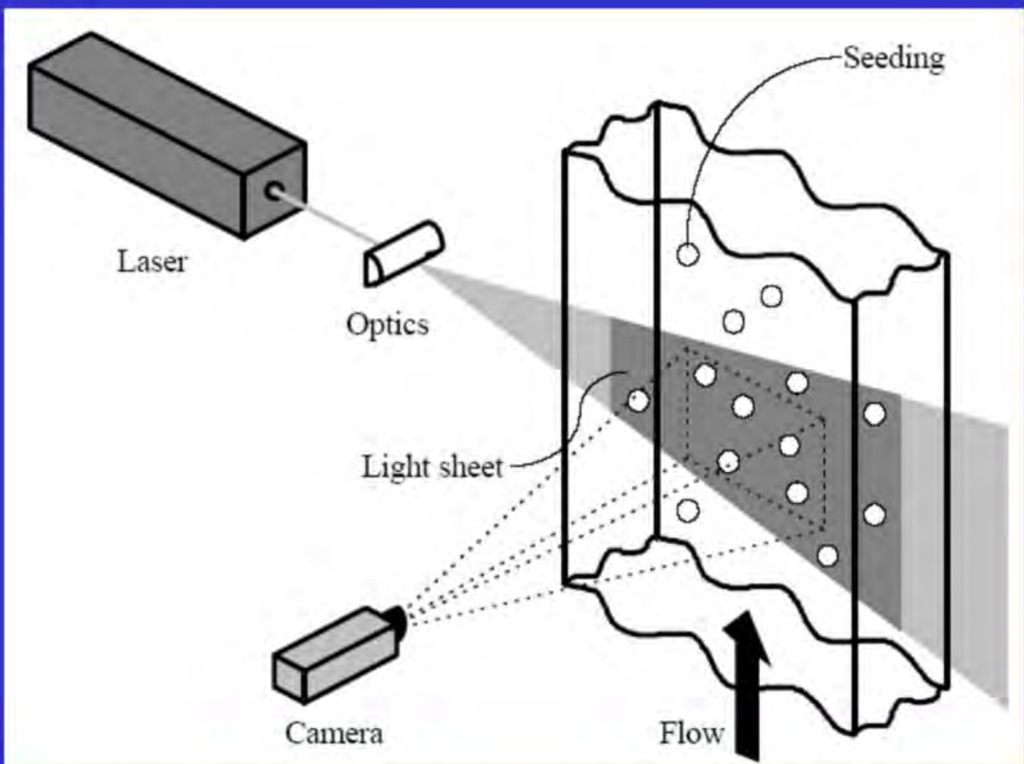

[Dantec Dynamics A/S]

Image 1:

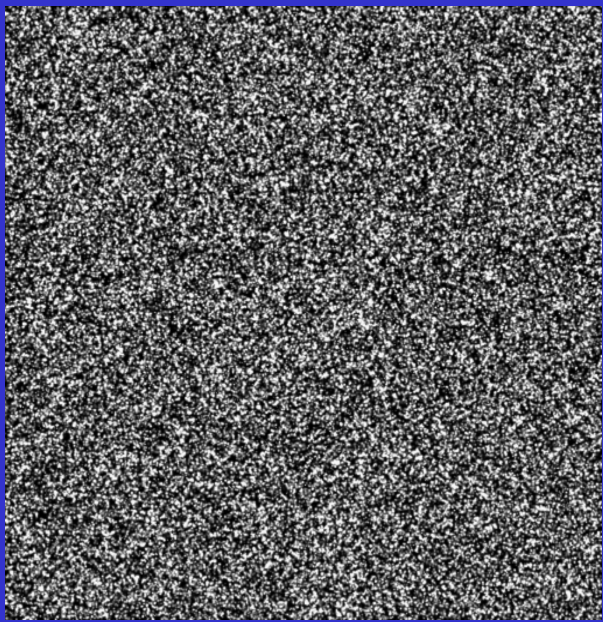

Image 2:

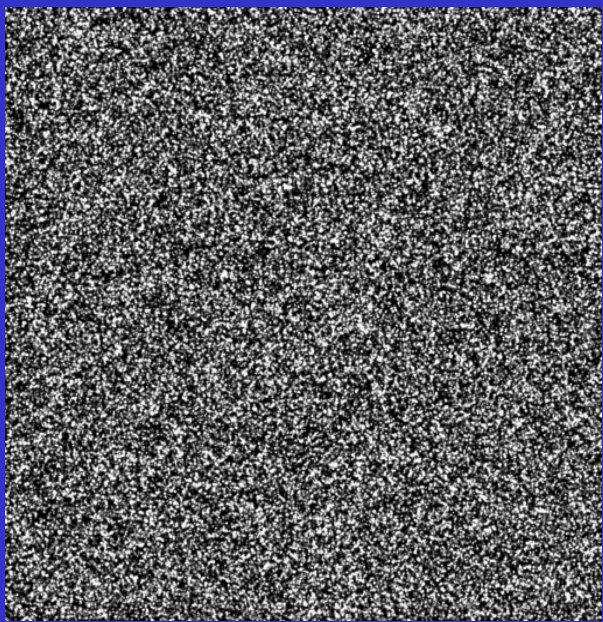

Interrogation Areas (16×16, 32×32):

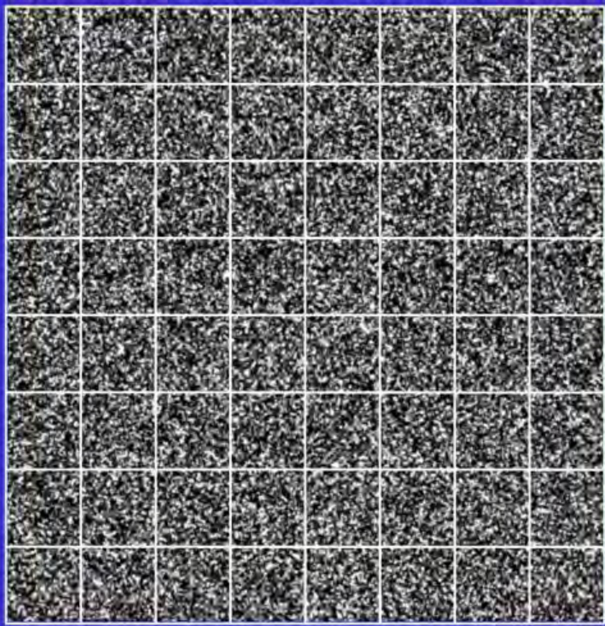

Two-dimensional cross-correlation:

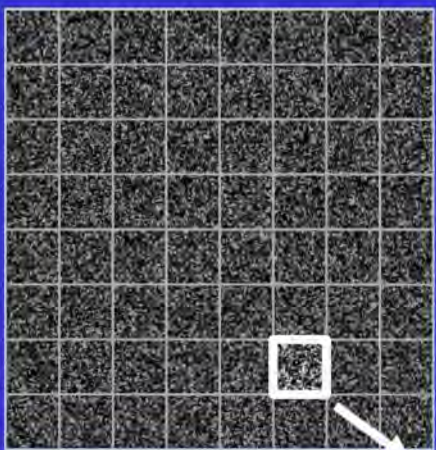

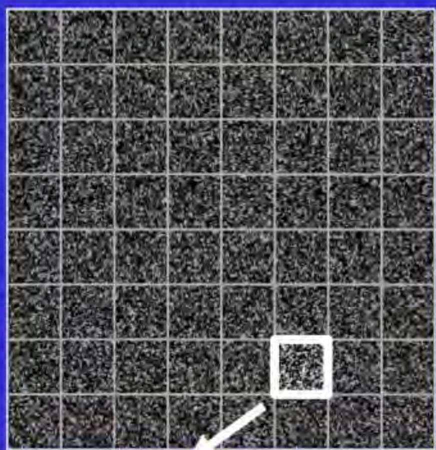

$$R(k,l)=\frac{1}{MN}\sum_i\sum_j z_1(i,j)\,z_2(i+k,j+l)$$

$z_1(i,j) \rightarrow$ FFT

$\overset{*}{\odot} \rightarrow$ IFFT $\rightarrow R(k,l)$

$z_2(i,j) \rightarrow$ FFT

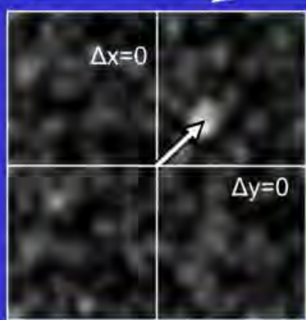

Two-dimensional cross-correlation:

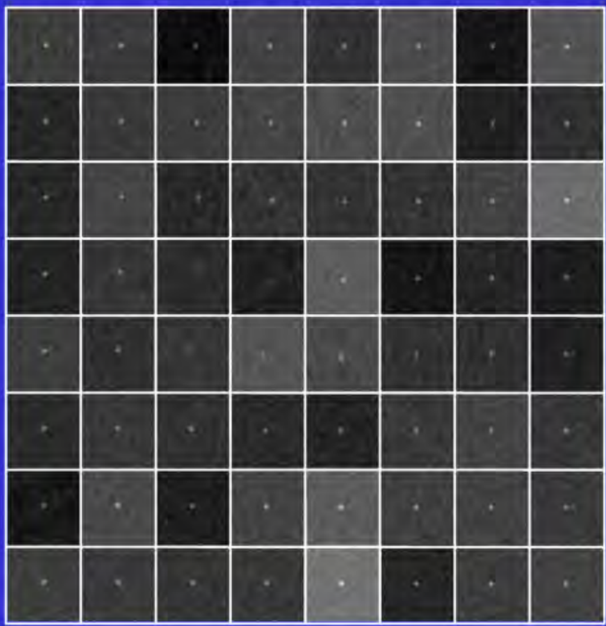

Velocities:

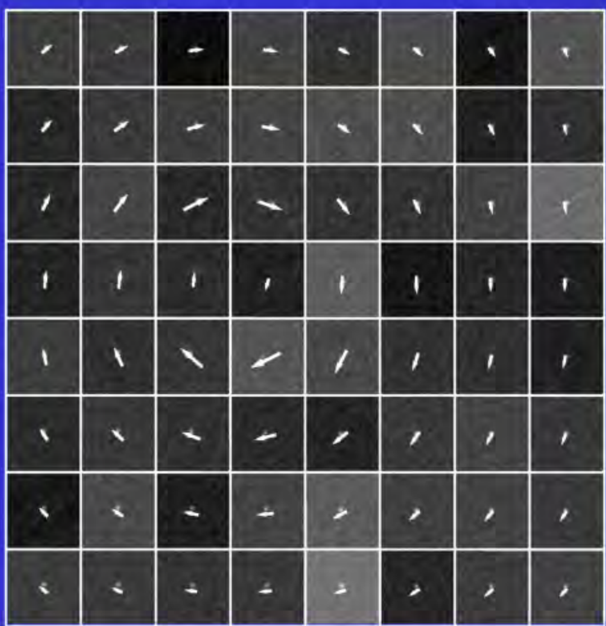

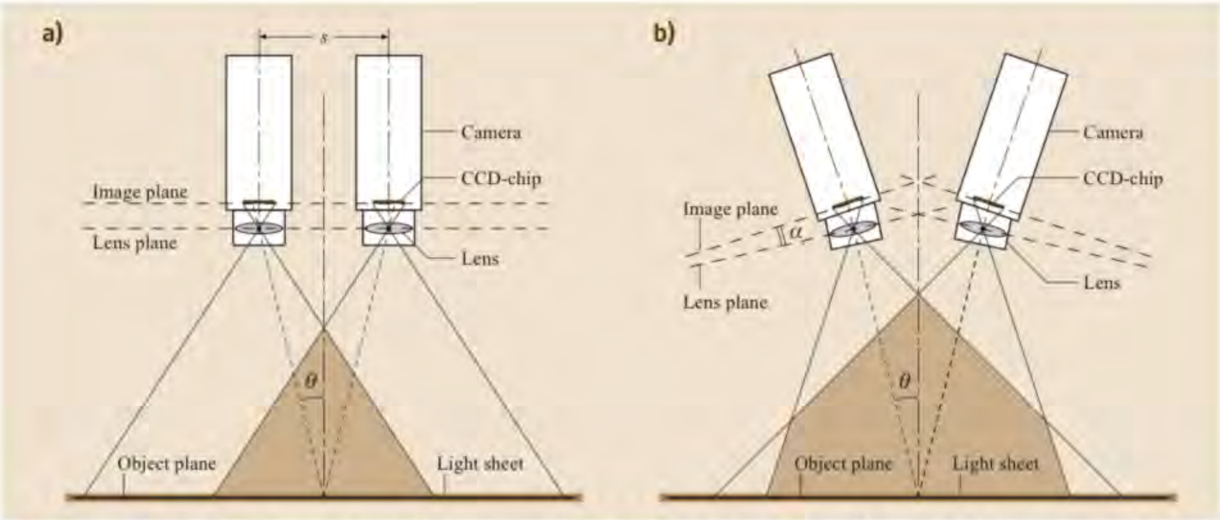

Fig. 5.92a,b Optical configurations for stereoscopic imaging: the translation method (**a**) and angular displacement method (**b**)

Scheimpflug configuration

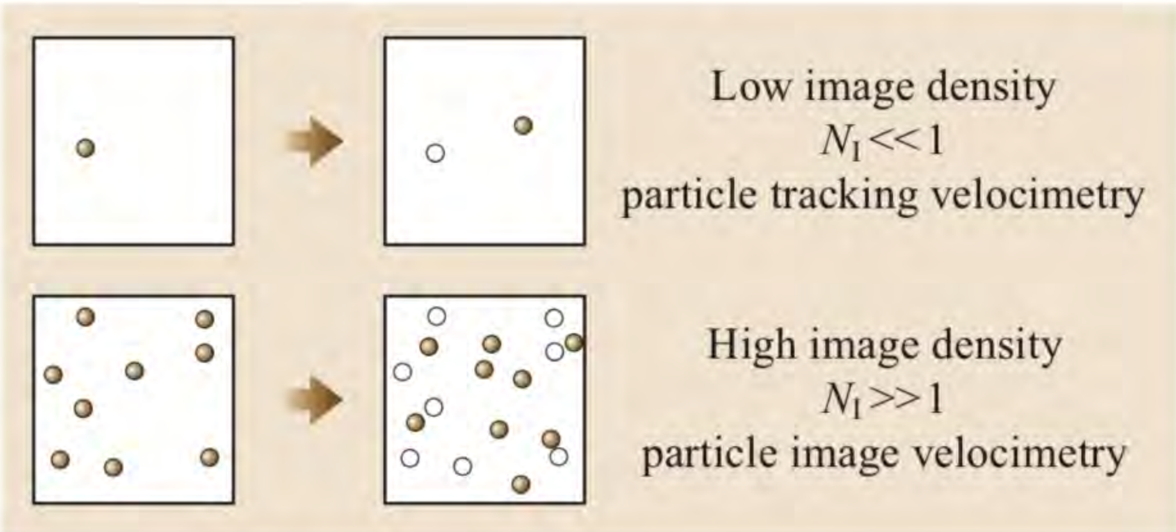

Additional info see Springer handbook

Temporal Properties (Lagrangian)

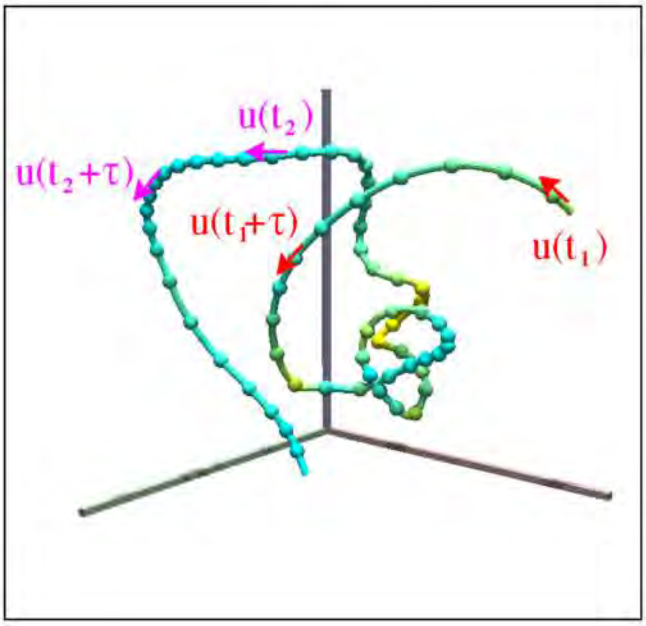

Temporal Properties (Lagrangian)

Inertial scales:

$$\langle (\Delta_t u_i)^p \rangle \sim (\epsilon \tau)^{p/2}$$

velocity structure function

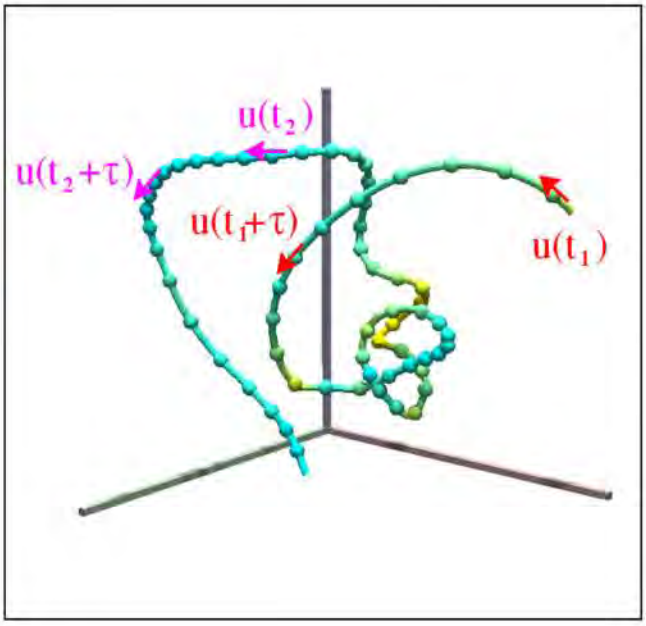

Fluid particle acceleration a

$$\underbrace{\frac{\partial}{\partial t}\mathbf{u} + \mathbf{u}\cdot\vec{\nabla}\mathbf{u}}_{\mathbf{a}} = \underbrace{-\frac{1}{\rho}\vec{\nabla}p}_{\text{large}} + \underbrace{\nu\nabla^2\mathbf{u}}_{\text{small}}$$

scaling:

$$\boxed{\langle a_i^2 \rangle = a_0 \frac{\epsilon^{3/2}}{\nu^{1/2}}}$$

Two particle dispersion

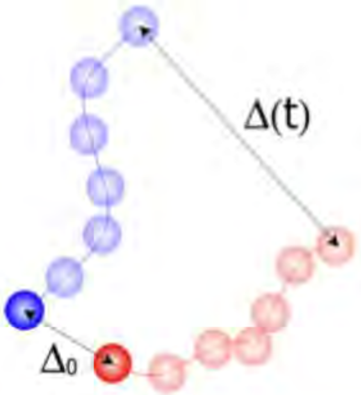

- Inertial range scaling theory
- Δ(t) = separation between two fluid particles

$$\langle [\Delta_i(t) - \Delta_{0i}]^2 \rangle = \begin{cases} \frac{11}{3} C_2 \left(\epsilon \Delta_0\right)^{2/3} t^2 & t < t_0 = \left(\frac{\Delta_0^2}{\epsilon}\right)^{1/3} \\ g \epsilon t^3 & t_0 < t < T_L \end{cases}$$

Lagrangian Particle Tracking

1. *Imaging and camera model (Xu)*
2. *2-d particle centre localization*
3. *3-d particle localization*
4. *tracking algorithm*
5. *drop out correction - segment connection*
6. *example.*

CMOS cameras:

2000 x 2000	pixels	6,000 fps
256 x 256	pixels	70,000 fps

typical in 3d:

2000 x 2000	20000 particles
1000 x 1000	5000 particles
256 x 256	300 particles

+ real time compression (Voth et al., Liberzon & Luethi, us)

- follow many particles in space and time
- high repetition rates
- direct imaging

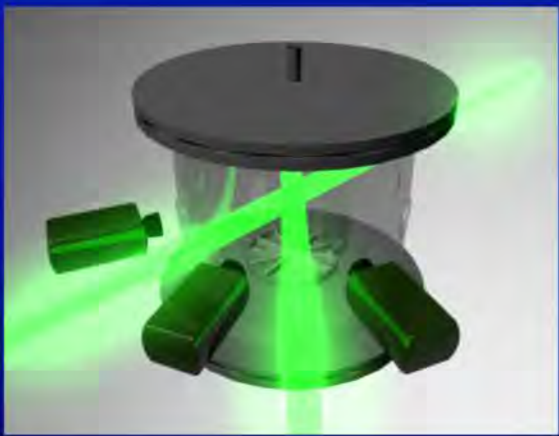

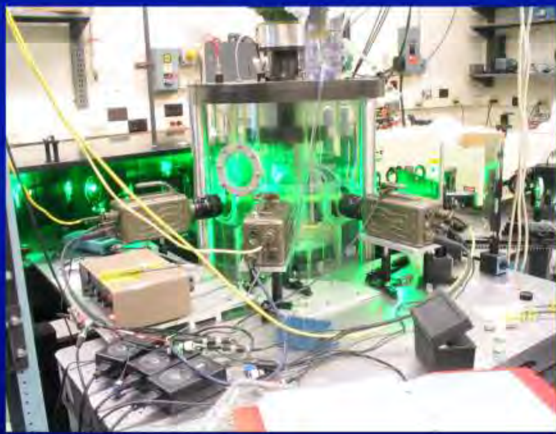

Pinhole camera model

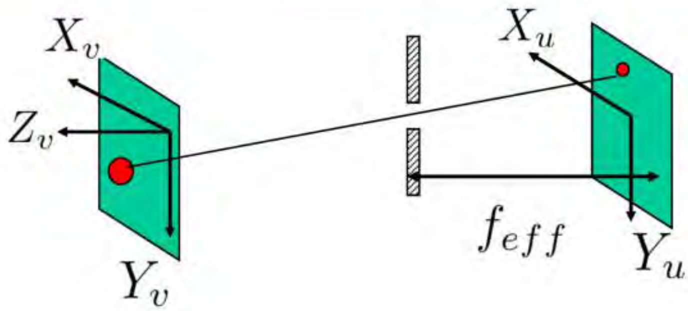

$$\begin{pmatrix} X_u \\ Y_u \end{pmatrix} = \frac{f_{eff}}{Z_v} \begin{pmatrix} X_v \\ Y_v \end{pmatrix}$$

Distortion

Radial distortion

Barrel   Pin-cushion   Tangential distortion

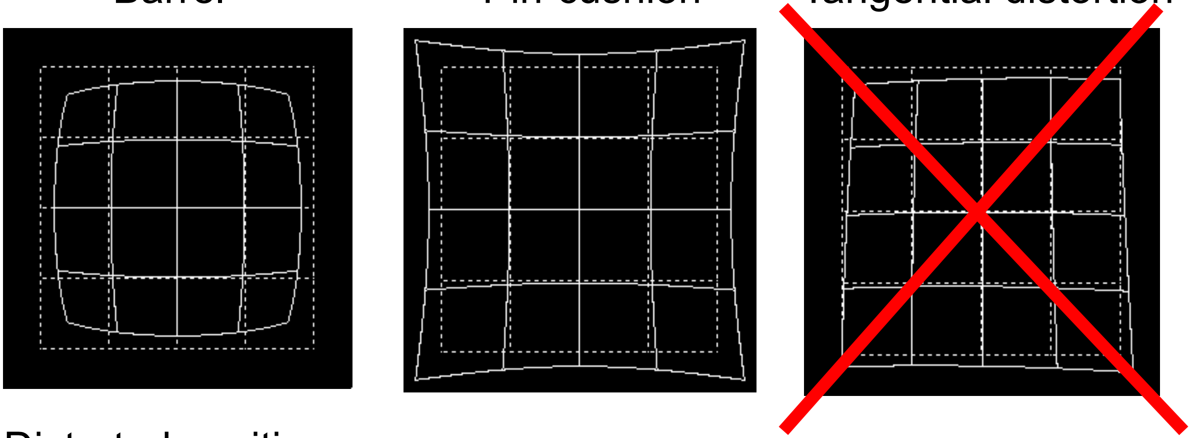

Distorted position:

$$\begin{pmatrix} X_d \\ Y_d \end{pmatrix} = (1 + kr^2) \begin{pmatrix} X_u \\ Y_u \end{pmatrix}$$

Camera Position

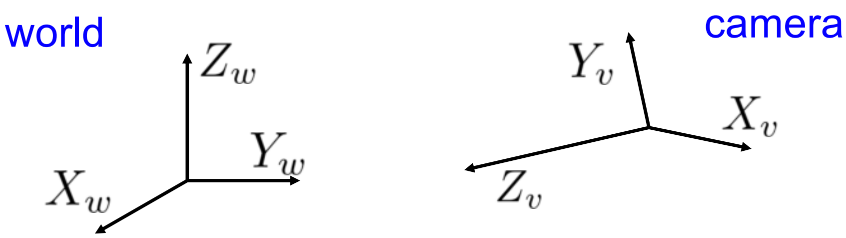

$$\begin{pmatrix} X_v \\ Y_v \\ Z_v \end{pmatrix} = \underline{\underline{R}} \begin{pmatrix} X_w \\ Y_w \\ Z_w \end{pmatrix} + \underline{T}$$

Rotation matrix $\underline{\underline{R}}$

Translation vector $\underline{T}$

Calibration

- *Camera Parameters:*

$$R, T, f_{eff}, \text{and } k$$

- *Calibrate using 3D objects at known positions*

$$X_d = (1 + kr^2) f_{eff} \frac{R_{11}X_w + R_{12}Y_w + R_{13}Z_w + T_x}{R_{31}X_w + R_{32}Y_w + R_{33}Z_w + T_z}$$

$$Y_d = (1 + kr^2) f_{eff} \frac{R_{21}X_w + R_{22}Y_w + R_{23}Z_w + T_y}{R_{31}X_w + R_{32}Y_w + R_{33}Z_w + T_z}$$

Calibration

- Radial Alignment Constraint RAC (Tsai, 1985)

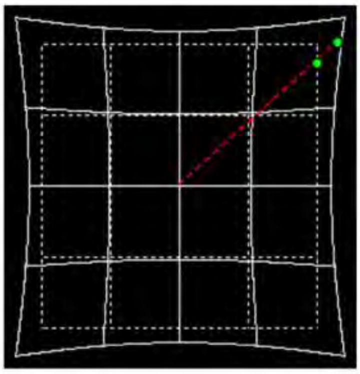

$$\begin{pmatrix} X_u \\ Y_u \end{pmatrix} \times \begin{pmatrix} X_d \\ Y_d \end{pmatrix} = 0$$

$$X_d\left(R_{21}X_w + R_{22}Y_w + R_{23}Z_w + T_y\right) - Y_d\left(R_{11}X_w + R_{12}Y_w + R_{13}Z_w + T_x\right) = 0$$

and $\underline{R_1} \times \underline{R_2} = \underline{R_3}$

Calibration masks

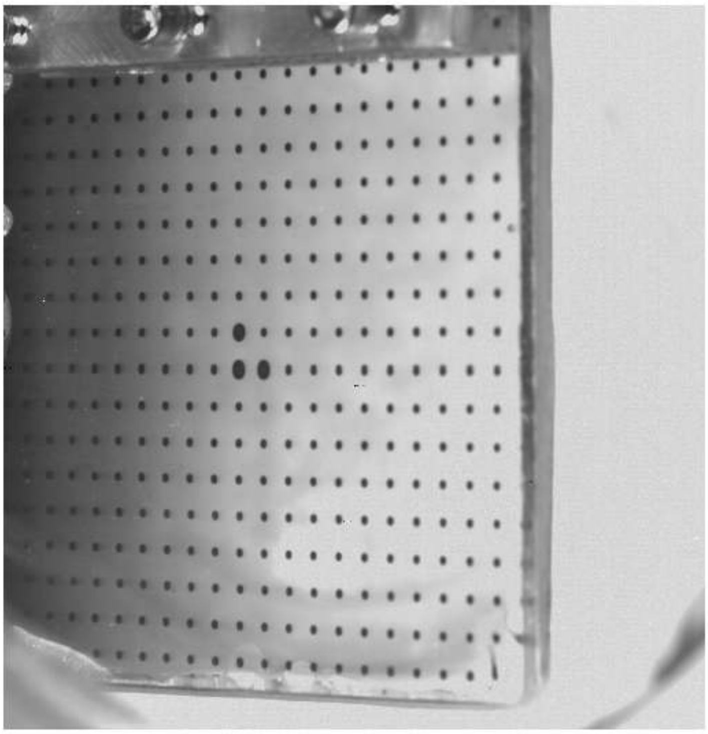

/mnt/raid/hd1/turb/raw_data/050328/calib/calib5.cam0.mcin

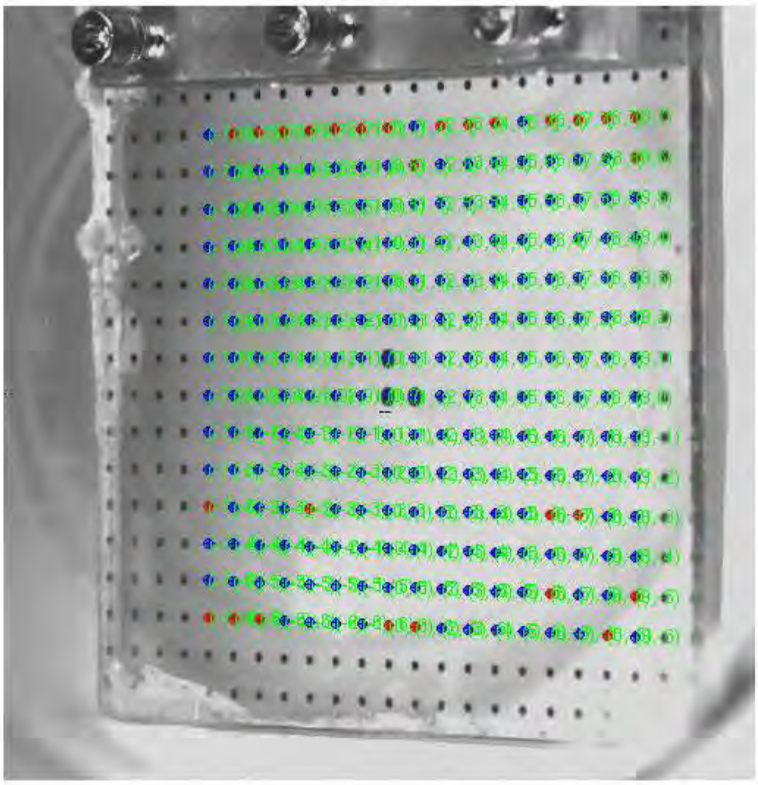

blue < 0.5 pixel

red > 0.5 pixel

1. *Imaging and camera model*
2. *2-d particle centre localization (Oullette)*
3. *3-d particle localization*
4. *tracking algorithm*
5. *drop out correction - segment connection*
6. *example.*

2-d particle centre localization

Issues:

Definition of a particle
Sub-pixel accuracy
Computational speed
Noise
Particle overlap

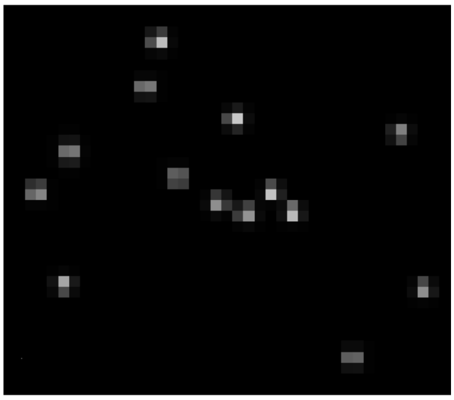

Weighted Averaging

- Center of mass style average
- Easy to implement, computationally efficient
- Comparatively poor accuracy

Maas *et al.*, Exp Fluids 1993

Gaussian Fitting

1D	2D
Fit two 1D Gaussians to each intensity maximum	Fit a single 2D Gaussian to each intensity maximum
Analytical solution: very efficient	Poor efficiency
Very good accuracy	Excellent accuracy

see e.g. Cowen & Monismith, Exp Fluids 1997

Mann *et al.*, Risø National Laboratory Report 1999

- No noise

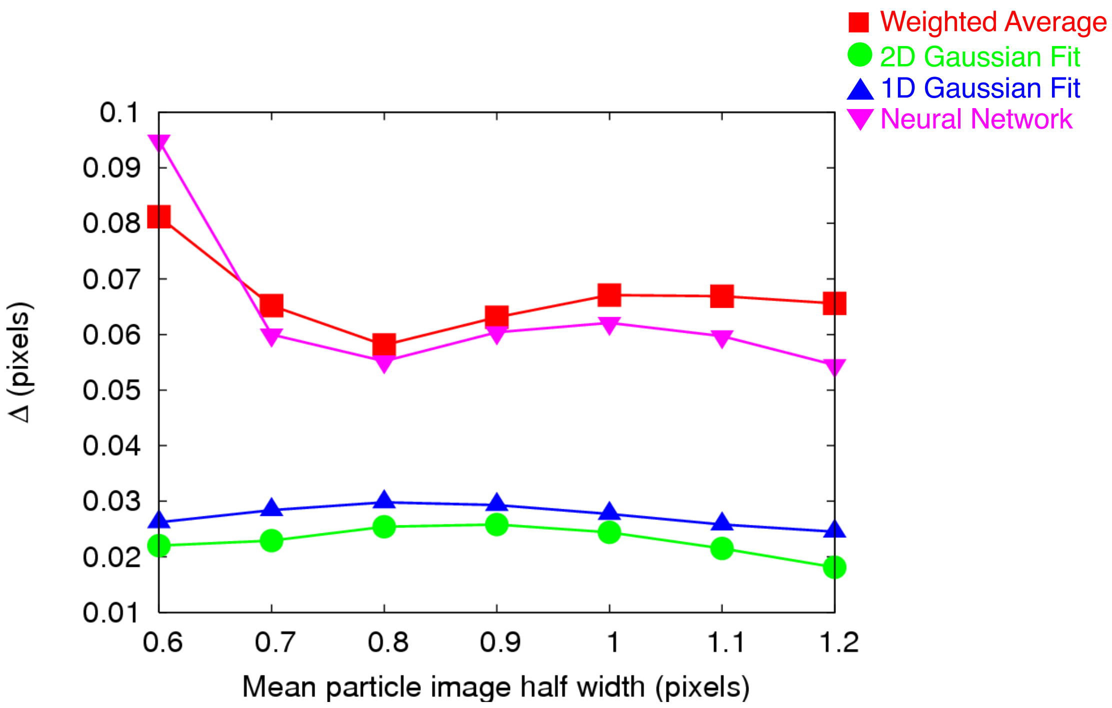

- Noise variance: 5.6
- Particle image half-width: 0.8 pixels

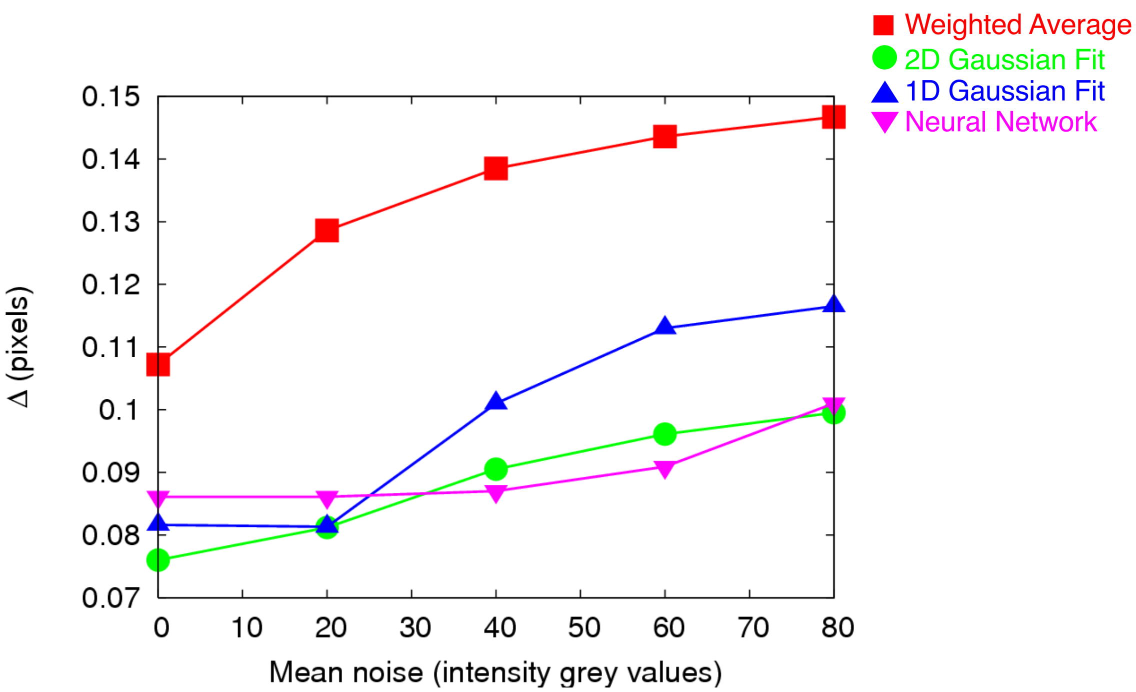

Experiments in Fluids. 40(2):301-313, 2006 Feb.

1. *Imaging and camera model*
2. *2-d particle centre localization*
3. *3-d particle localization (Xu)*
4. *tracking algorithm*
5. *drop out correction - segment connection*
6. *example.*

Ideal Camera Case

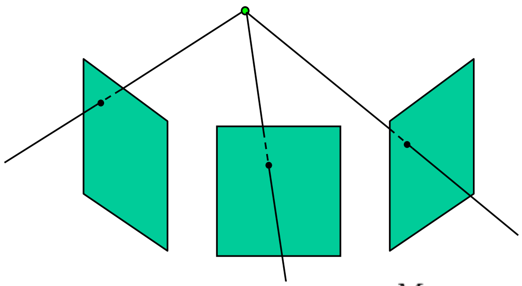

Intersection of “Ray of sight”: $\min\left(\sum_{i=1}^{M}\left(h_i^2\right)\right)$

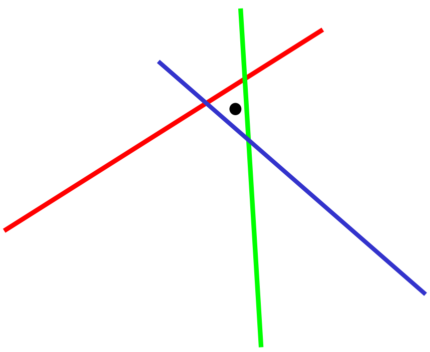

$$h \equiv \left[\frac{1}{M}\sum_{i=1}^{M}\left(h_i^2\right)\right]^{1/2}$$

$$h \le h_c$$

Brute-force Algorithm

- Consider all possible particle image combinations from all cameras
- Easy to program
- Computation cost

$$O(N^M)$$

N: average number of particles per image
M: number of cameras

Dracos Algorithm

Project "beam of sight" onto the other cameras

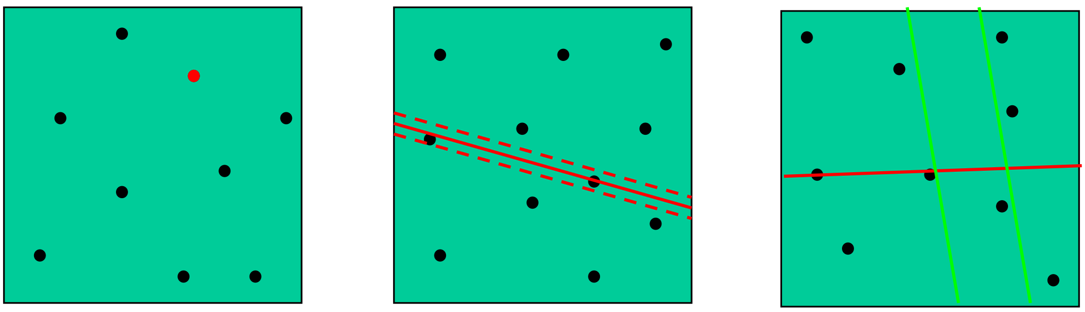

Computation cost: $$O(N^2 P^{M-2})$$

P: number of particle centers on image plane within tolerance ε_{2D}

Risoe Algorithm

- Working with pairs of cameras first
- Find a line in 3D space that is perpendicular to the two axes of cameras.
- Then project particle centers from image plane onto that line, use the projection as the generalized height-coordinate.

Computation cost $$O\left(N^2 P^{M-2}\right)$$

Our Algorithm

- Mixed Dracos and Risoe
- Working with camera pairs first
- Consider "common axis" on image plane

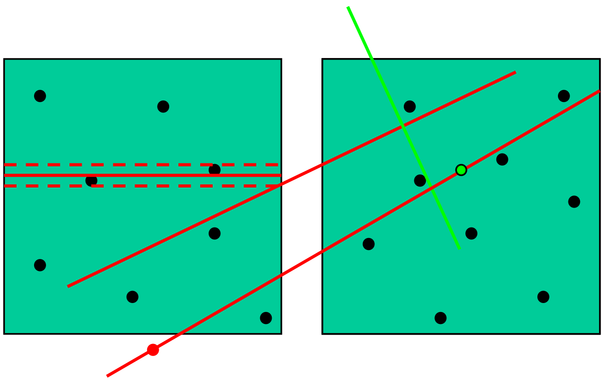

Computation cost $$O\left(N^2 P^{M-2}\right)$$

Camera with Distortion

- Correct distortion first, then using the same algorithm described before.

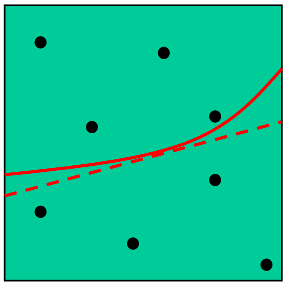

Distortion correction: $O(NM)$

Match

- Each pair of camera gives a list of possible matches.
- Search through the lists to find consistent list entries.
- Allow overlap.

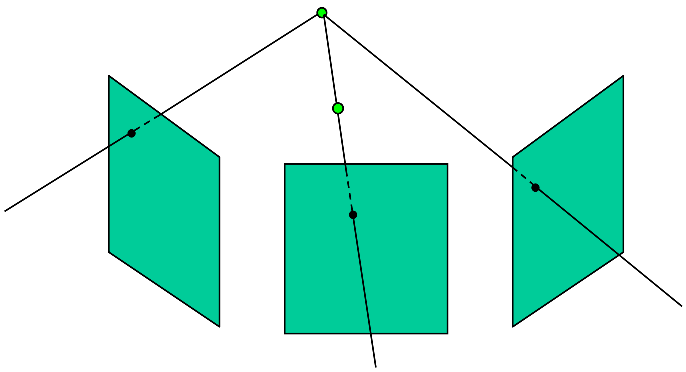

1. *Imaging and camera model*
2. *2-d particle centre localization*
3. *3-d particle localization*
4. *tracking algorithm (Ouellette, Xu)*
5. *drop out correction - segment connection*
6. *example.*

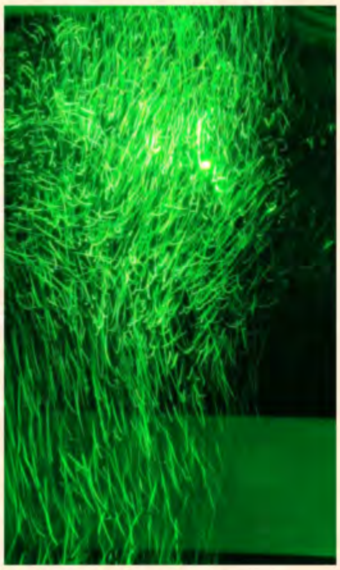

four-frame predictive algorithm

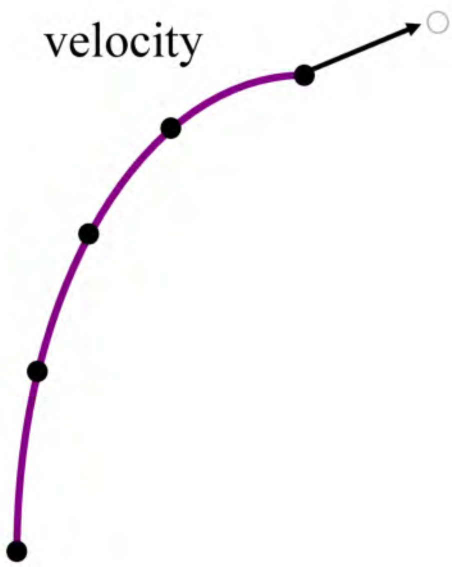

four-frame predictive algorithm

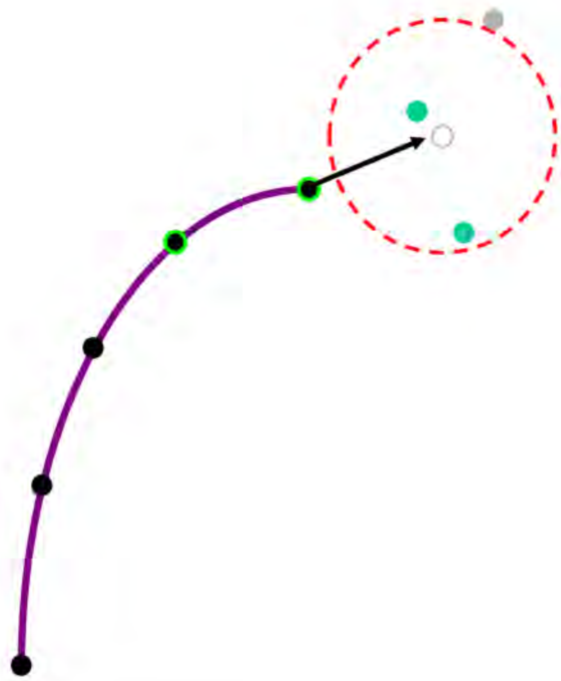

four-frame predictive algorithm

velocity & acceleration

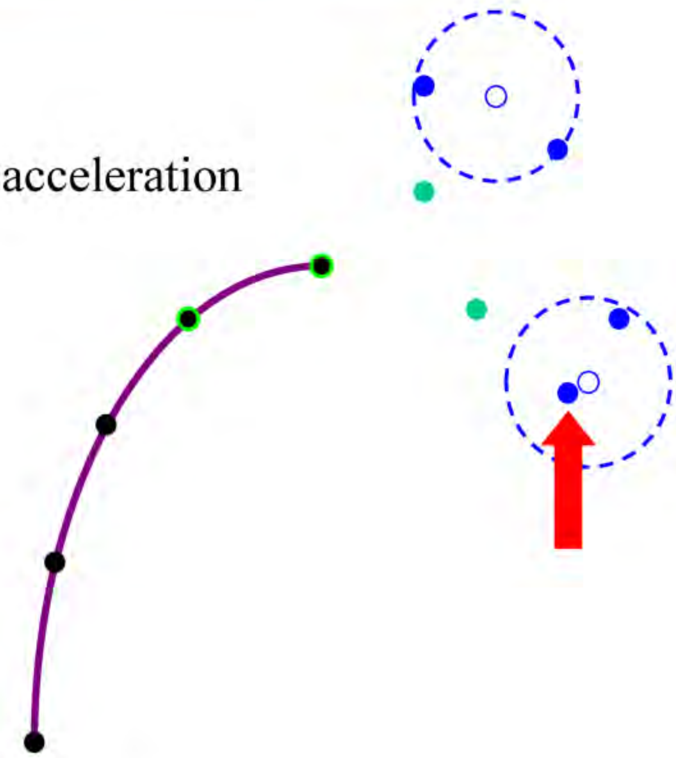

four-frame predictive algorithm

next particle location identified

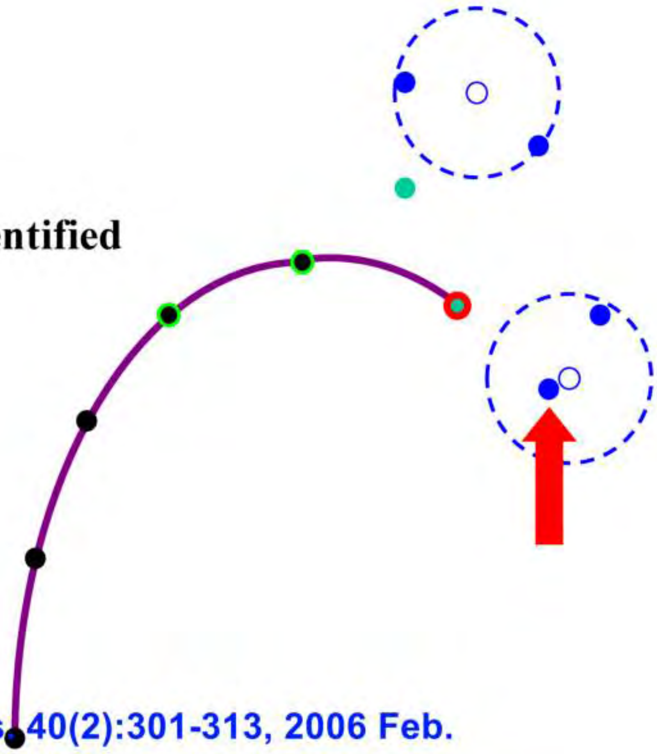

Experiments in Fluids, 40(2):301-313, 2006 Feb.

1. *Imaging and camera model*
2. *2-d particle centre localization*
3. *3-d particle localization*
4. *tracking algorithm (Ouellette, Xu)*
5. *drop out correction - segment connection (Xu)*
6. *example.*

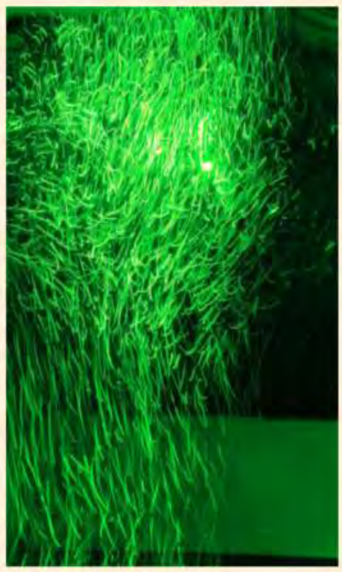

Broken Trajectories

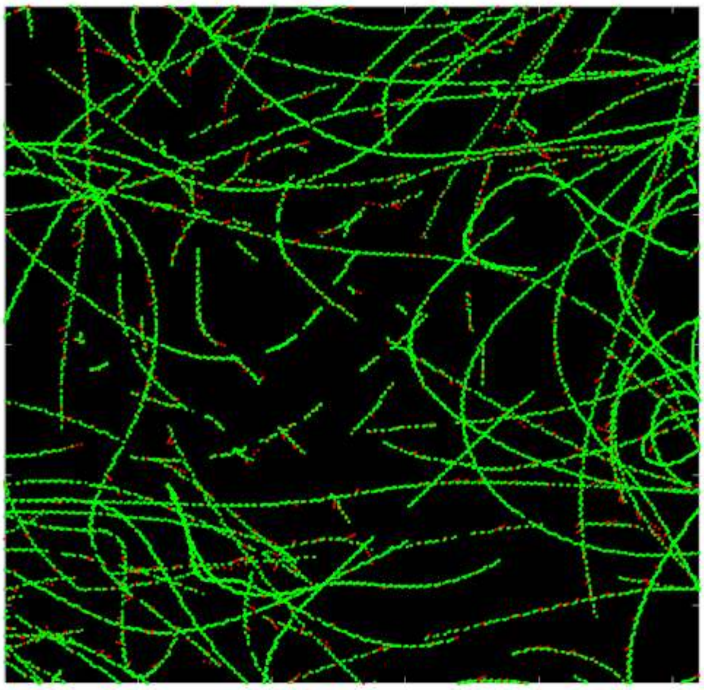

Causes of "particle drop-out"

- Fluctuations of the intensity of the light source
- Angular dependence of scattering intensity
- Presence of light-insensitive circuits on CMOS sensors
- "Cross-over" of trajectories
- Thermal, shot, and environmental noise

connect broken trajectories

Idea:

Treat each trajectory segment in
6-dimensional physical-velocity space

Advantages:

space sparse
Common algorithms applicable

Special considerations:

Segments are of different lengths
time intervals for successive segments are random

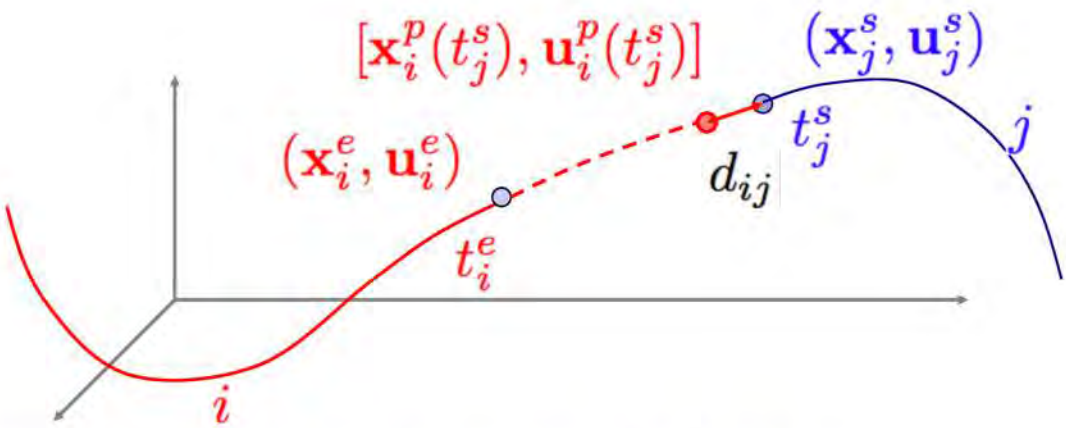

Distance between segments *i* and *j* in P-V space:

$$d_{ij} \equiv \sqrt{|\mathbf{x}_i^p(t_j^s) - \mathbf{x}_j^s|^2 + [|\mathbf{u}_i^p(t_j^s) - \mathbf{u}_j^s|(t_j^s - t_i^e)]^2}$$

with $\quad t_i^e < t_j^s$

Estimates:

$$\mathbf{x}_i^p = \mathbf{x}_i^e + \frac{1}{2}(\mathbf{u}_i^e + \mathbf{u}_j^s)(t_j^s - t_i^e)$$

$$\mathbf{u}_i^p = \mathbf{u}_i^e + w_a \frac{1}{2}(\mathbf{a}_i^e + \mathbf{a}_j^s)(t_j^s - t_i^e)$$

Segments *i* and *j* belong to the same trajectory if:

$$d_{ij} = \min_k(d_{ik} | d_{ik} \leq d_M), \quad (0 < t_k^s - t_i^e < T_s)$$

Results: connected trajectories

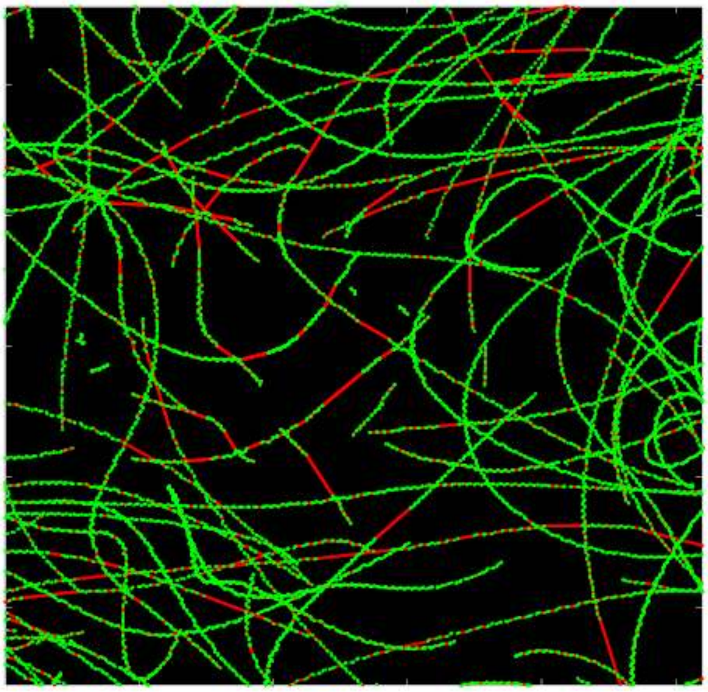

Results: trajectory length

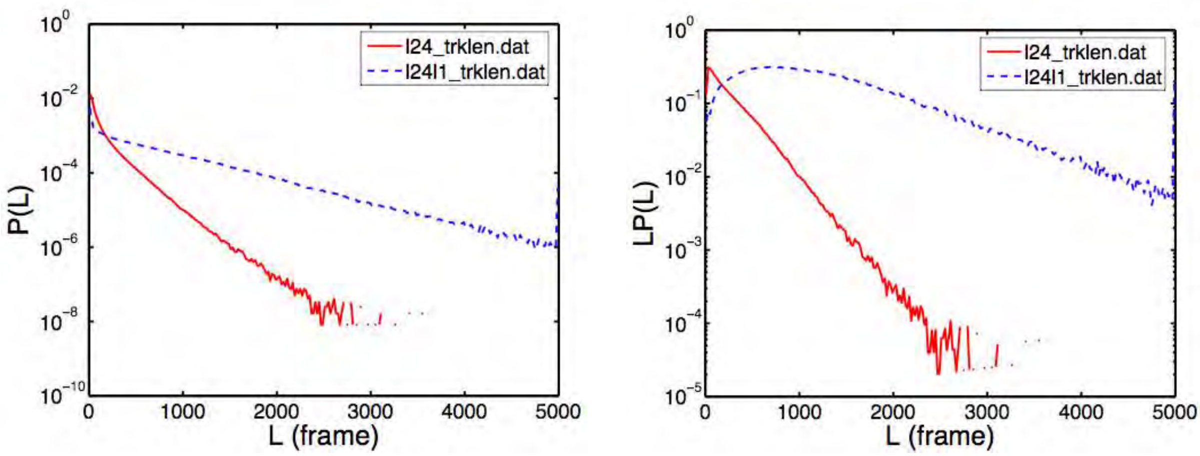

Average trajectory length increased by a factor of 5

Lagrangian trajectories

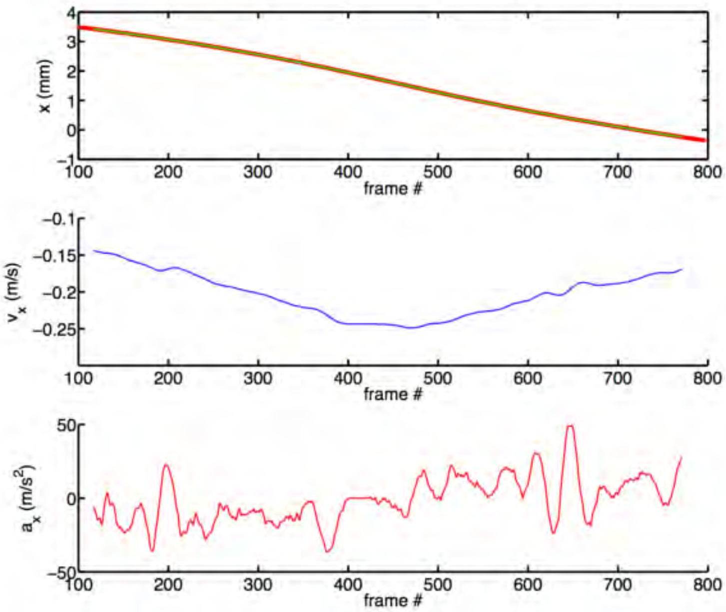

$\tilde{X}(t)$: measured trajectories

$$X(t) = \int f(\tau)\tilde{X}(t+\tau)d\tau$$

$$u(t) = \frac{dX(t)}{dt}$$

$$a(t) = \frac{d^2X(t)}{dt^2}$$

$$R_\lambda = 460$$

$P(a^+)$

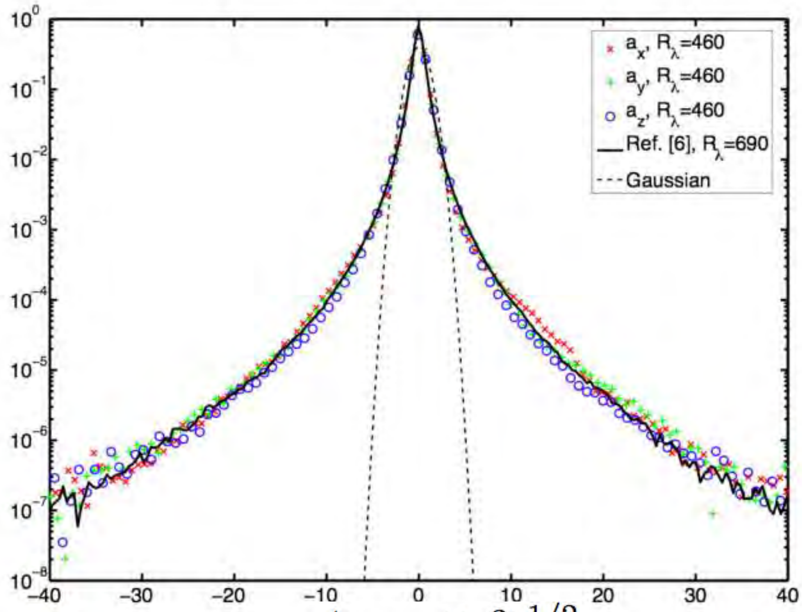

$a^+ \equiv a/\langle a^2\rangle^{1/2}$

$$R_\lambda = 460$$

$a^{+4}P(a^+)$

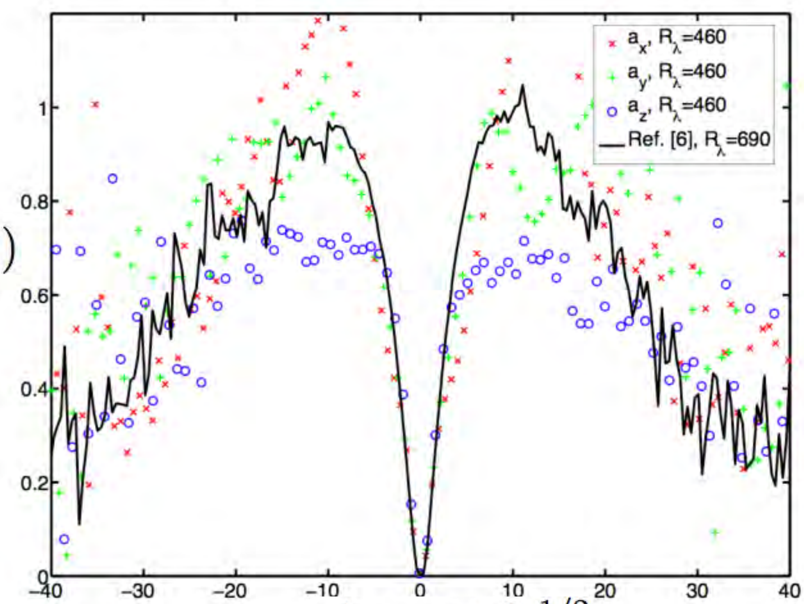

$a^+ \equiv a/\langle a^2\rangle^{1/2}$

Why Acceleration?

- Highly intermittent

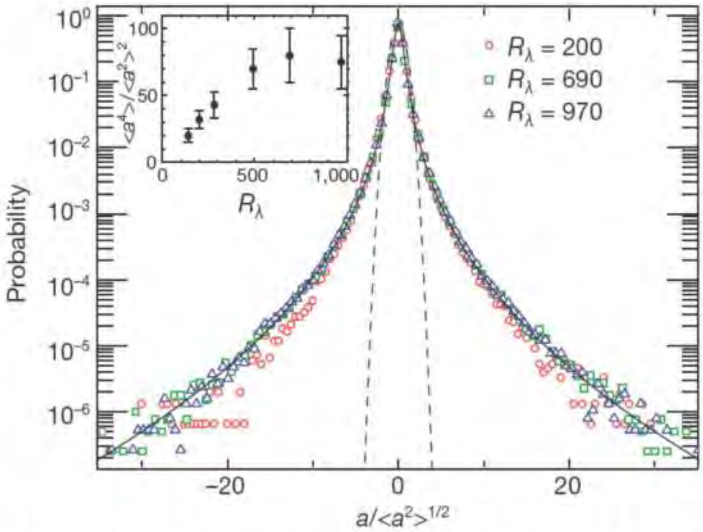

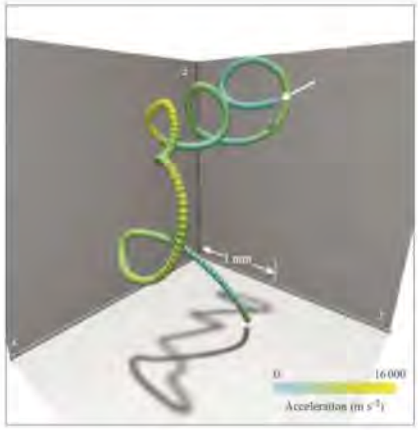

La Porta et al, **Nature** (2001); Voth et al, **J. Fluid Mech.** (2002); Biferale et al, **Phys. Fluids.** (2005)

Why Acceleration?

- Highly intermittent
- Related to pressure

$$\mathbf{a} = \frac{D\mathbf{u}}{Dt} = -\frac{1}{\rho}\nabla P + \nu\Delta\mathbf{u}$$

$$D_p(r) = 2\rho^2 \int_0^r r' R_{NN}(r')\mathrm{d}r'$$

Why Acceleration?

- Highly intermittent
- Related to pressure
- Heissenberg-Yaglom scaling

$$\langle a^2 \rangle \sim \epsilon^{3/2} \nu^{-1/2}$$

$$a_0 \equiv \frac{\langle a^2 \rangle}{\epsilon^{3/2} \nu^{-1/2}}$$

Acceleration Measurements

$$a_0 \equiv \frac{\langle a^2 \rangle}{\epsilon^{3/2} \nu^{-1/2}}$$

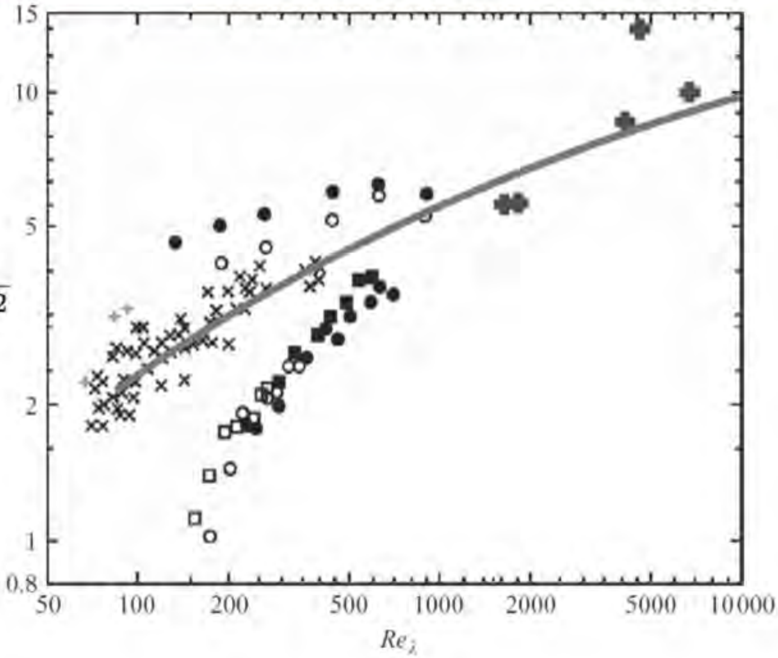

Figure from Gulitski et al, **J. Fluid Mech.** (2007)

Lagrangian Particle Tracking

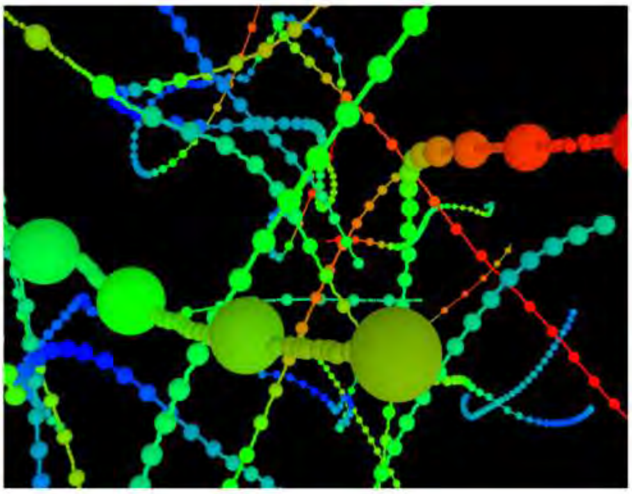

$$x(t) = \int f(\tau)\tilde{x}(t-\tau)\mathrm{d}\tau$$

$$a(t) = \frac{\mathrm{d}^2}{\mathrm{d}t^2}\int f(\tau)\tilde{x}(t-\tau)\mathrm{d}\tau$$

Acceleration Variance

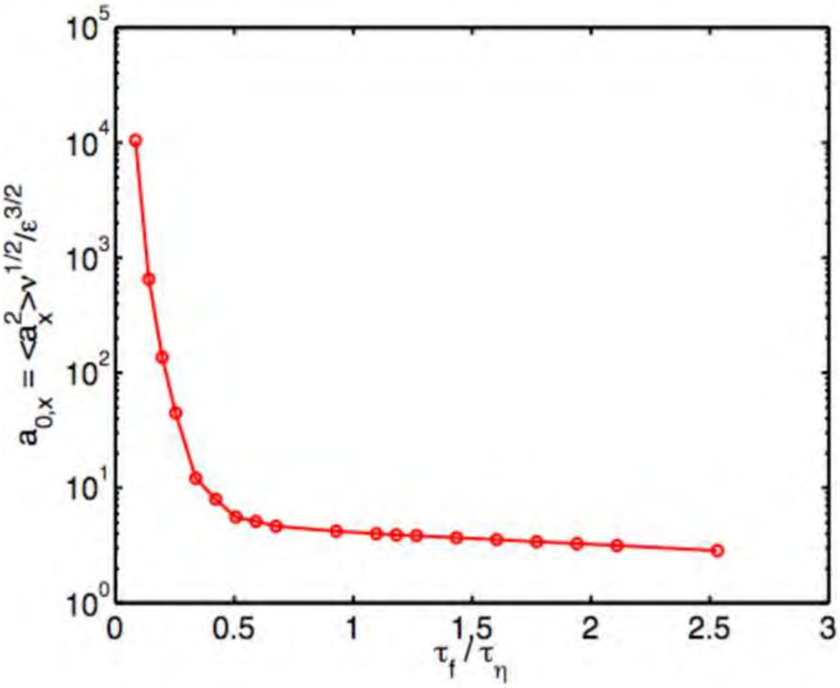

Acceleration Variance

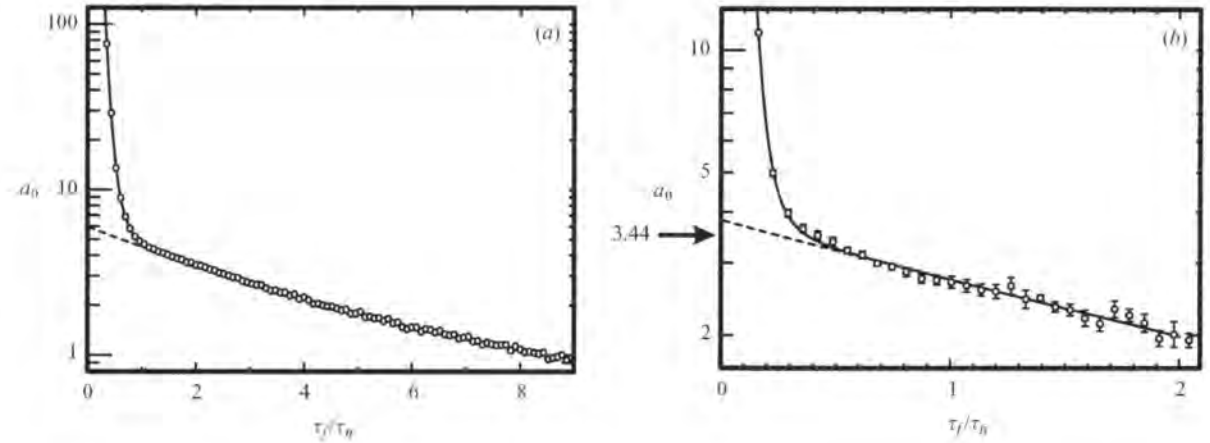

Voth et al, **J. Fluid Mech.** (2002)

Acceleration Autocorrelation

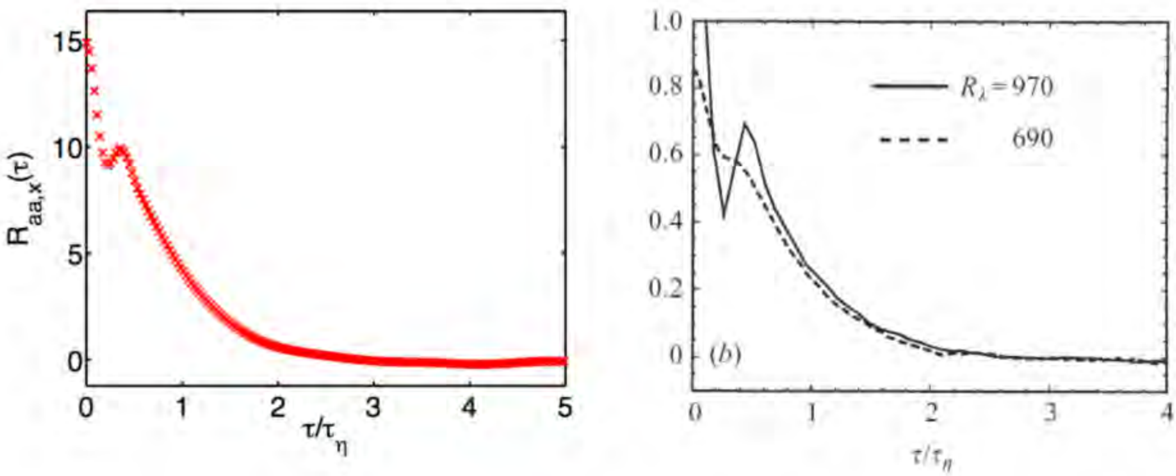

Voth et al, **J. Fluid Mech.** (2002)

Acceleration Autocorrelation

Measured position:

$$\tilde{x}(t) = x(t) + \xi(t)$$

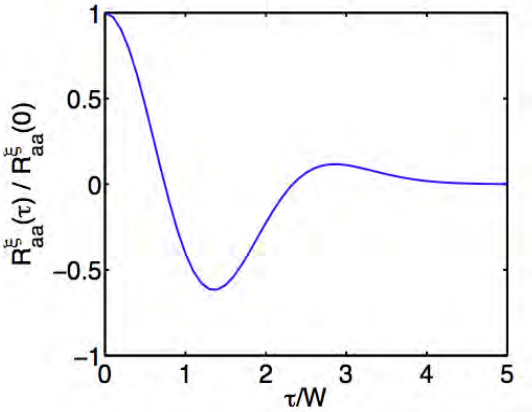

Acceleration Autocorrelation

$$\tilde{R}_{aa}(\tau) = R^{f}_{aa}(\tau) + R^{\xi}_{aa}(\tau)$$

?

$$R^{\xi}_{aa}(\tau) = \frac{\boxed{\sigma_\xi^2}}{\sqrt{2\pi}} W^{-5}\left(3 - \frac{6\tau^2}{W^2} + \frac{\tau^4}{W^4}\right) e^{-\frac{\tau^2}{2W^2}}$$

Corrected Acceleration Autocorrelation

$$\tilde{R}_{aa}(\tau; W_1) - \tilde{R}_{aa}(\tau; W_2) \approx R^{\xi}_{aa}(\tau; W_1) - R^{\xi}_{aa}(\tau; W_2)$$

$$= \frac{\sigma_\xi^2}{\sqrt{2\pi}}\left[W_1^{-5}\left(3 - \frac{6\tau^2}{W_1^2} + \frac{\tau^4}{W_1^4}\right) e^{-\frac{\tau^2}{2W_1^2}} - W_2^{-5}\left(3 - \frac{6\tau^2}{W_2^2} + \frac{\tau^4}{W_2^4}\right) e^{-\frac{\tau^2}{2W_2^2}}\right]$$

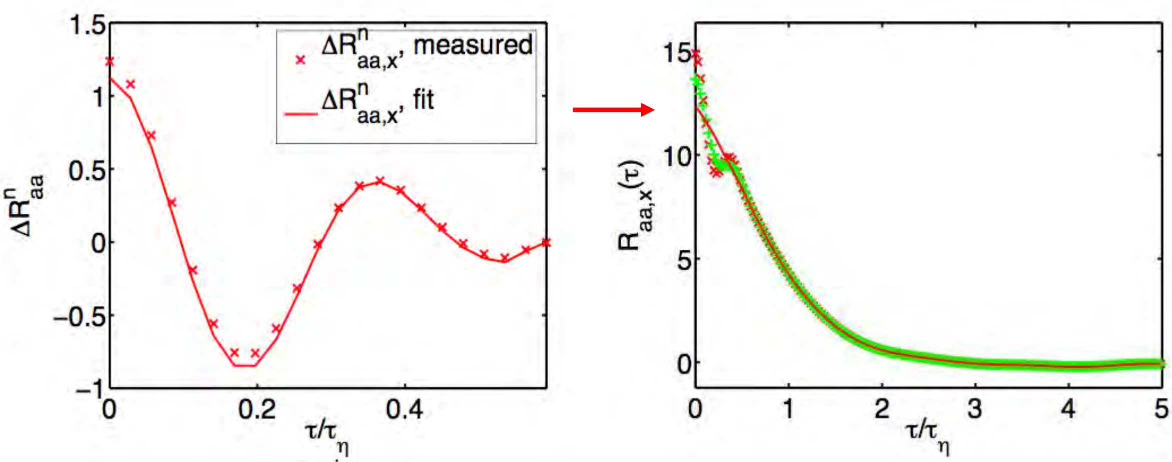

Test with DNS Data

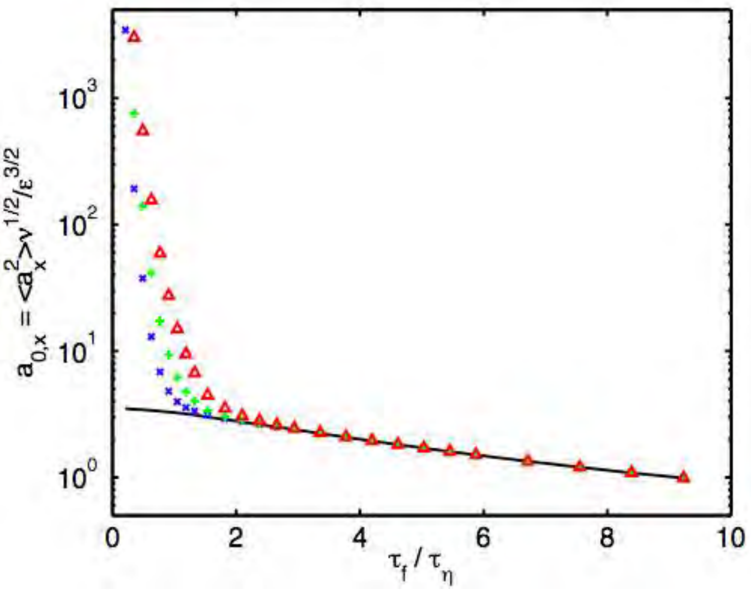

1024^3 DNS:

$$R_\lambda = 284$$

$$\eta/\Delta x = 0.8$$

$$\tau_\eta/\Delta t = 14.3$$

Biferale et al, **Phys. Fluids** (2005)

Test with DNS Data

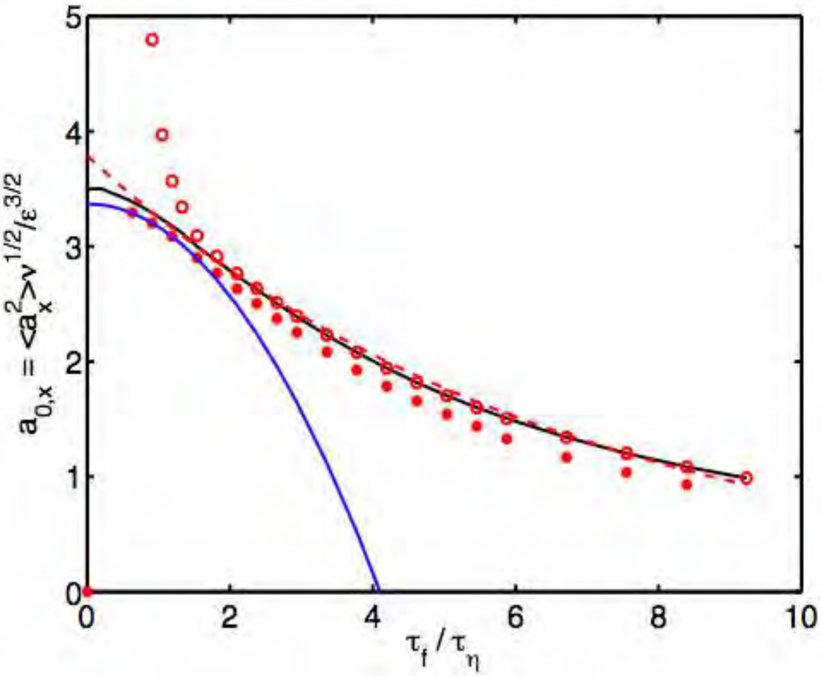

DNS: $a_0 = 3.5$

Exponential fit: $a_0 = 3.79$

Our technique: $a_0 = 3.37$

Experimental Data

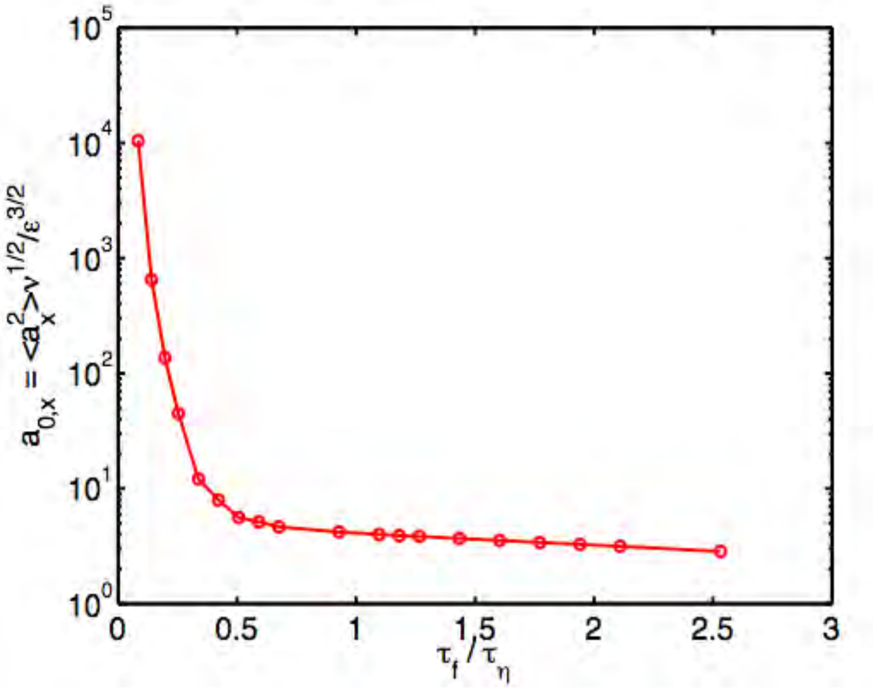

$R_\lambda = 350$

Experimental Data

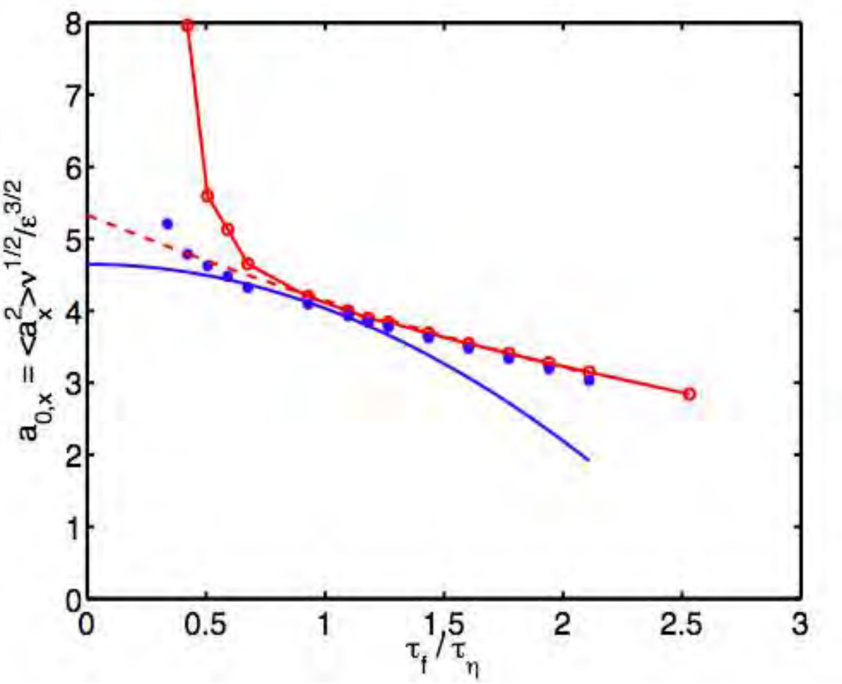

$R_\lambda = 350 \quad a_0 = 4.59$

Acceleration Variance

$$a_0 \equiv \frac{\langle a^2 \rangle}{\epsilon^{3/2}\nu^{-1/2}}$$

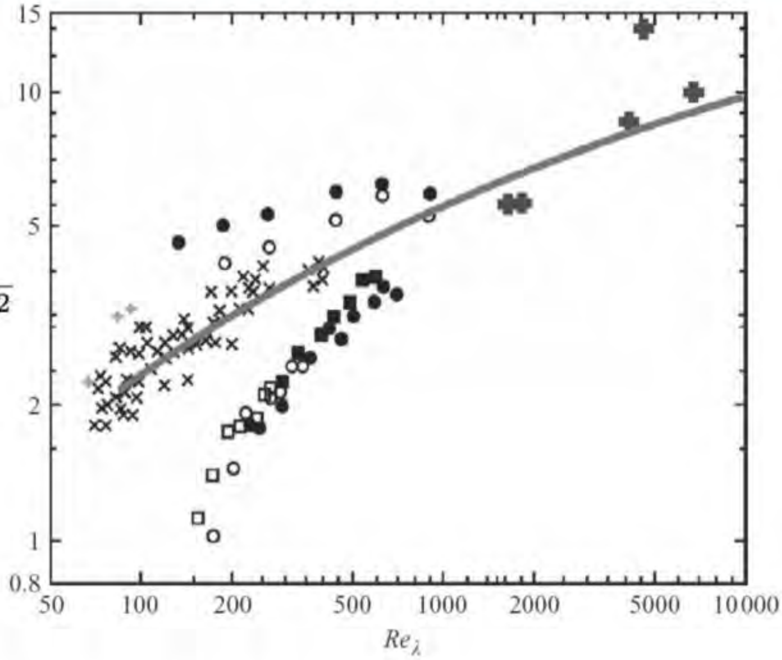

Figure from Gulitski et al, **J. Fluid Mech.** (2007)

Acceleration Variance

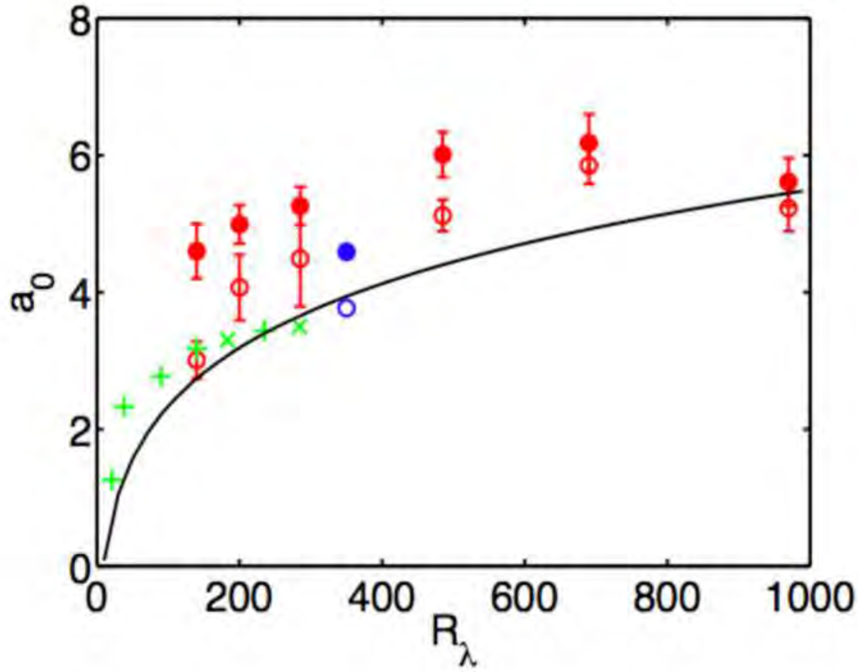

Thank you!

Particle Tracking and Clustering of Cloud Droplets at Zugspitze

Jan Moláček[1]

Gholamhossein Bagheri[1]

Guus Bertens[1]

Haitao Xu[1,2]

Eberhard Bodenschatz[1]

1 MPI for Dynamics & Self-Organization, Göttingen, GER
2 Tsinghua University, Beijing, CHN

MAX-PLANCK-GESELLSCHAFT

Particle Tracking

0. Calibration / Map from world coords to sensor coords

1. **Get particle image properties on sensor**
   - **1a. Get candidate image position**
   - **1b. Get first estimate of image properties**
   - **1c. Iteratively improve image properties by Levenberg-Marquardt**

2. **Triangulate (particle images -> particle woorld coords)**
   - **2a. Search all candidate image combinations**
   - **2b. Apply additional constraints to remove ghosts**
   - **2c. Enforce uniqueness**

3. **Track in time**

0. Calibration

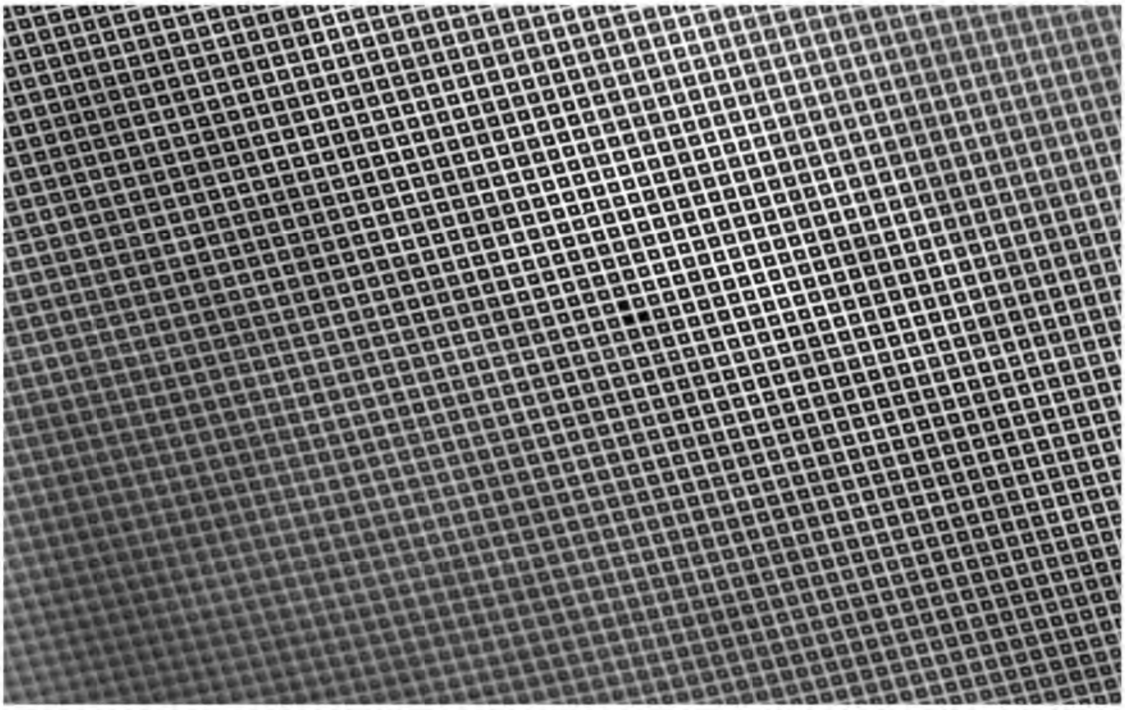

0. Camera Model

- Parallel orthogonal projection
- Pinhole model
- Two slit model
- ....
- + lens distortion parametrization

1. Fitting particle images

Triangulation

- Candidate 3D points selected based on triangulation error
- Number of ghost particles increases as $(\varepsilon N)^3$

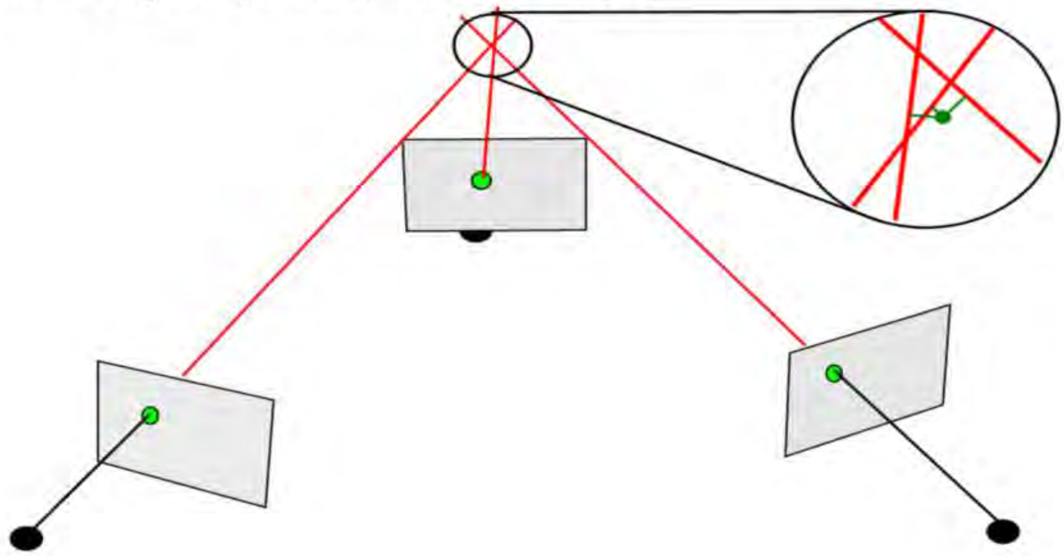

Tracking in time

- Nearest neighbour
- Minimum acceleration
- Minimum jerk (change in acceleration)
- ...

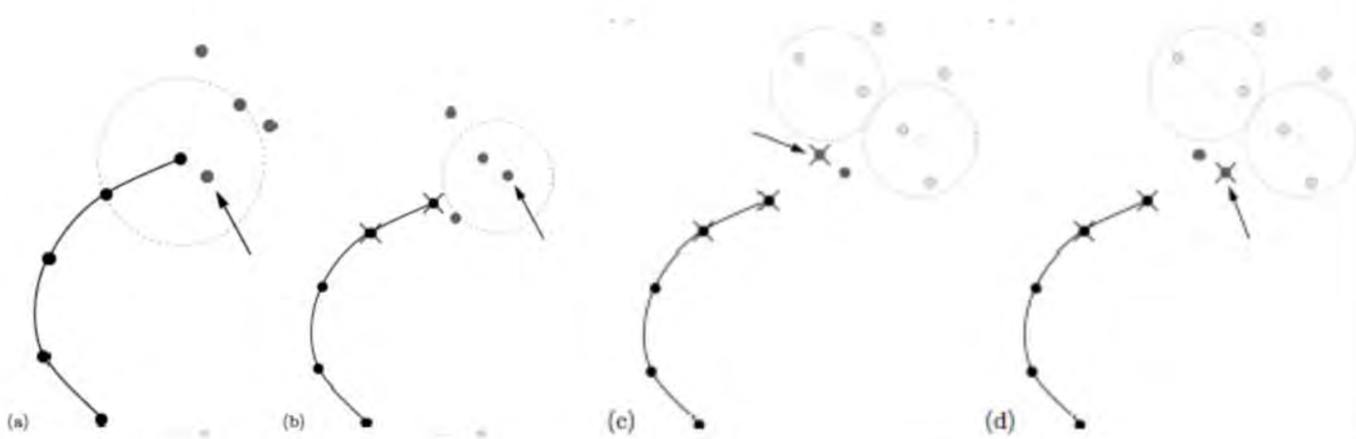

Movable platform – "Seesaw"

- Length 7.1m, travel length 5.1m, adjustable pitch +-13.5°
- F_{max}=3800N, v_{max}=7.5m/s, a_{max}=28m/s^2, A_{max}=106.7A

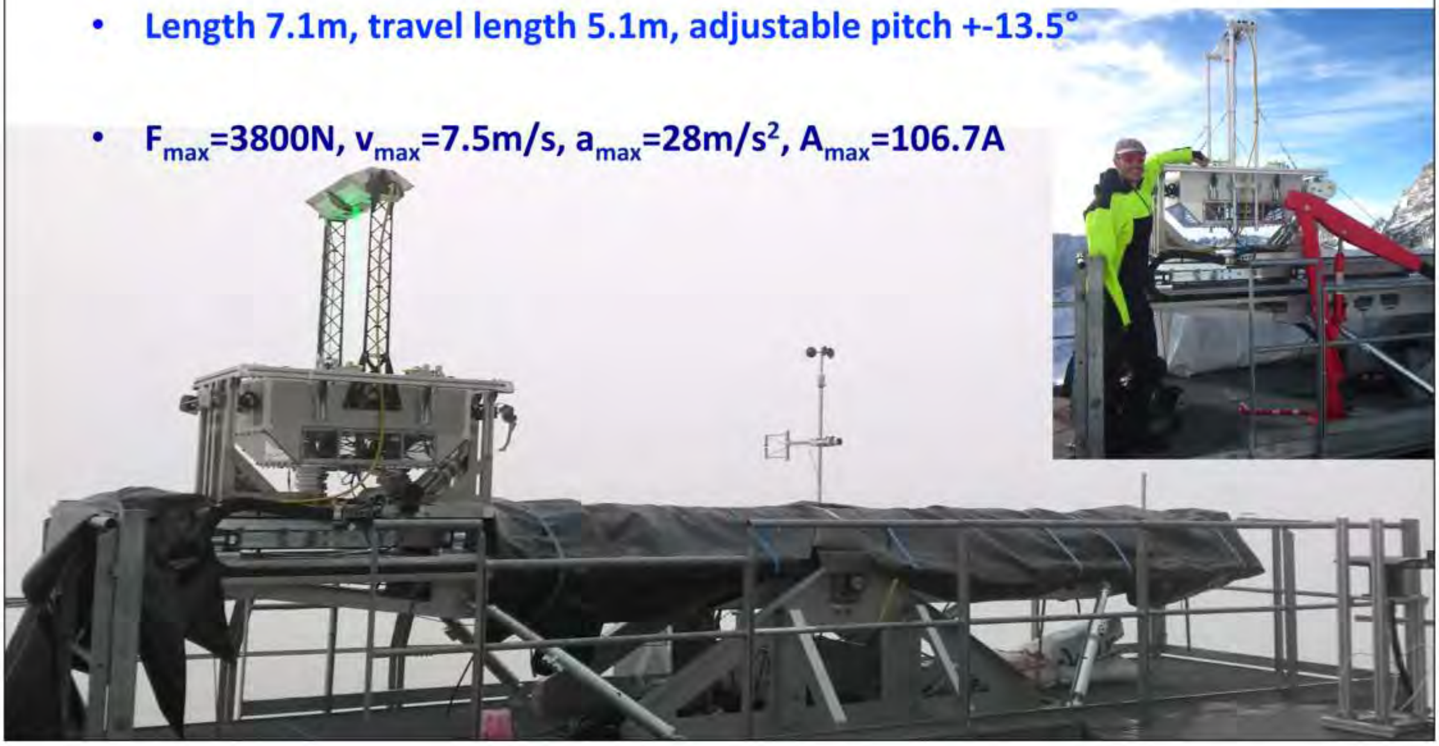

3rd generation Camera Box

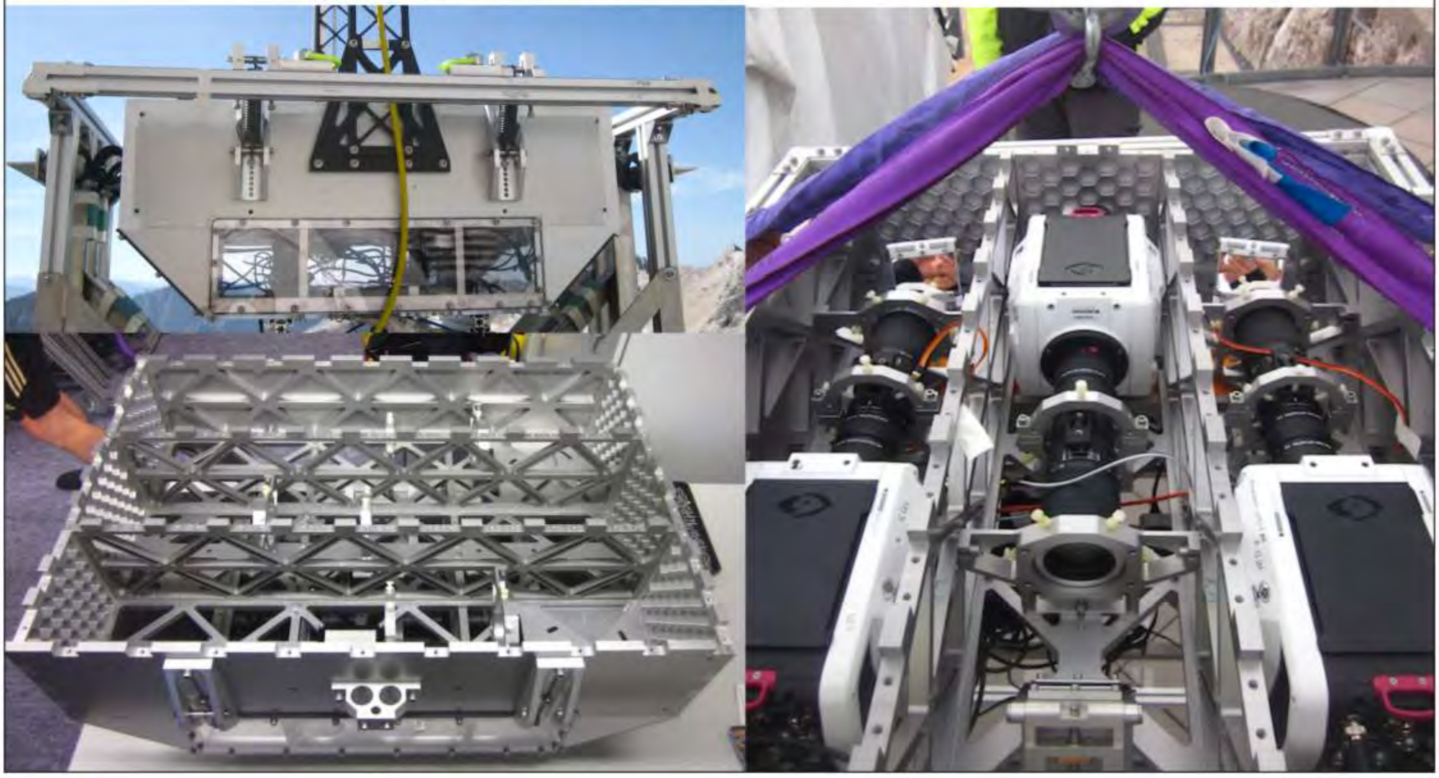

Illumination

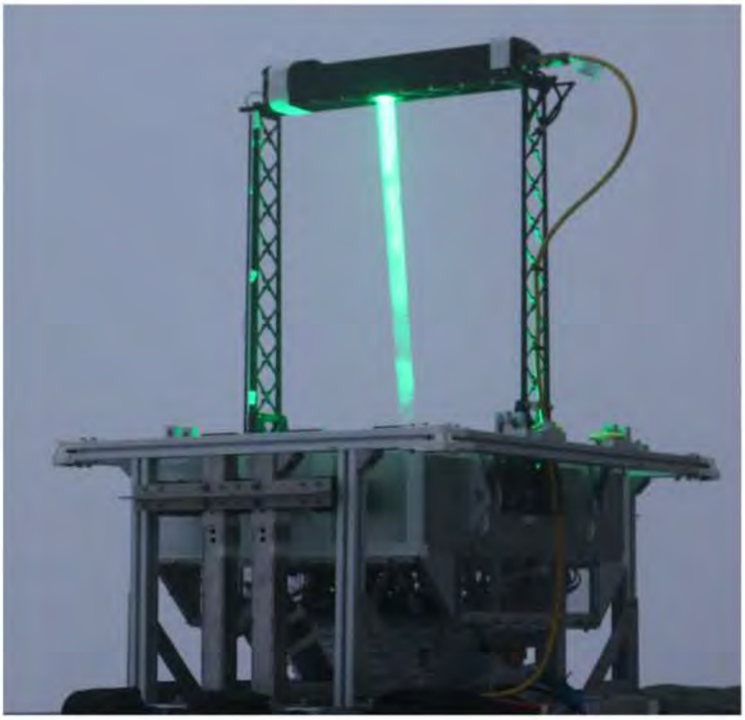

Illumination

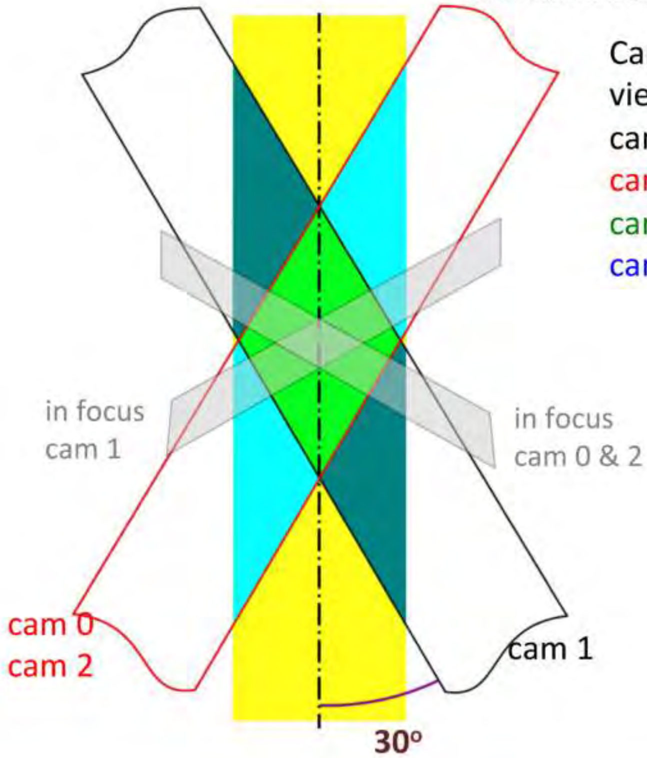

Camera common view volumes:
cam 012: 15.5cm^3
cam 01: 2.9cm^3
cam 02: 25.2cm^3
cam 12: 3.1cm^3

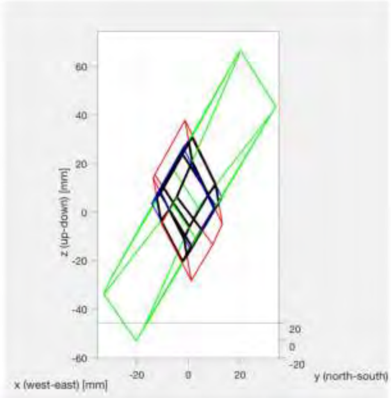

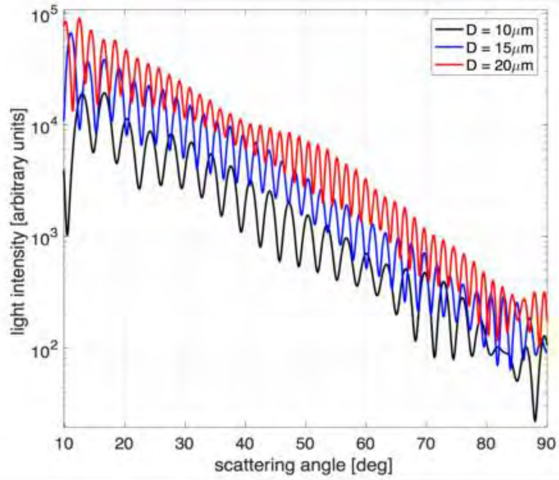

Illumination

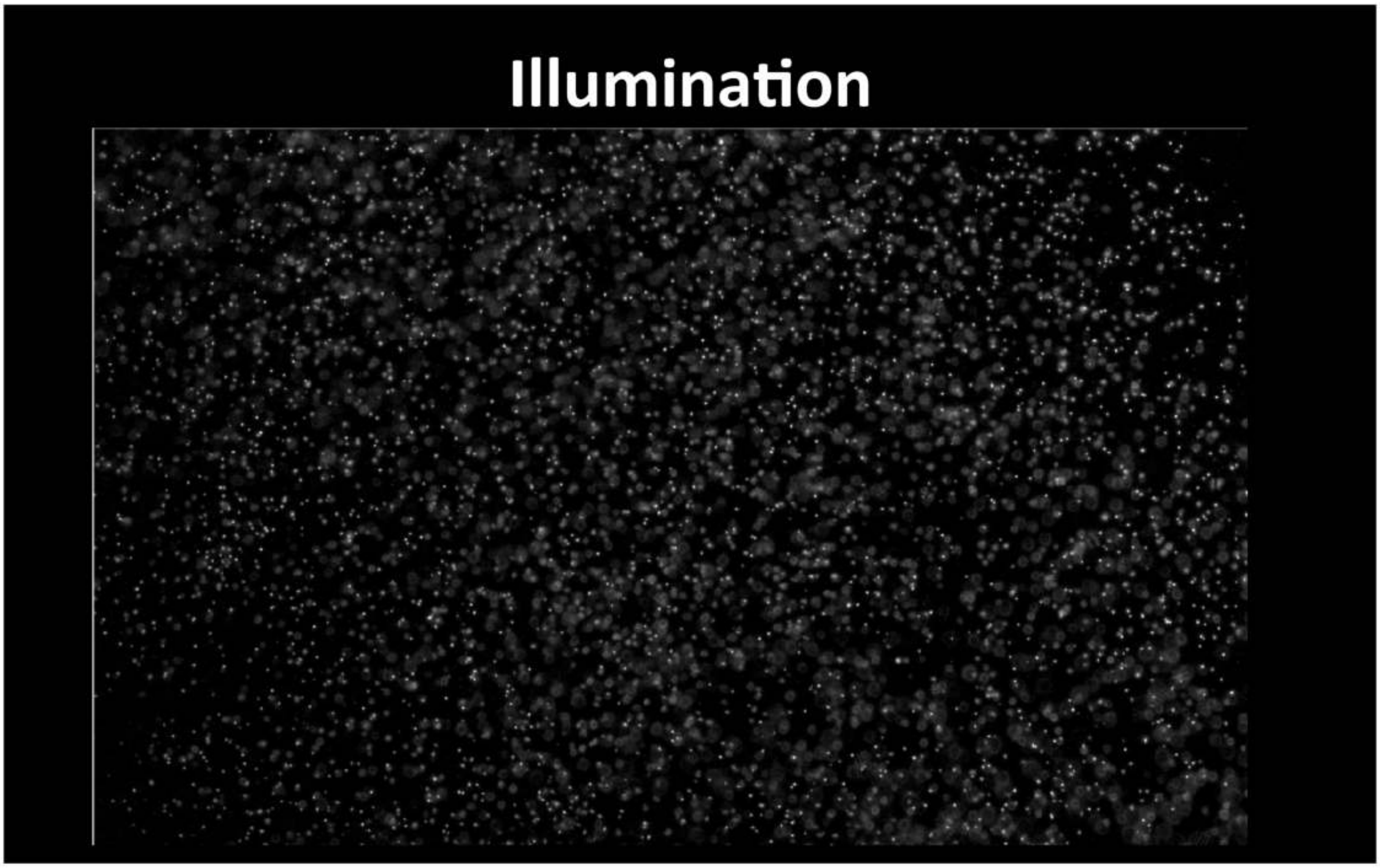
Illumination

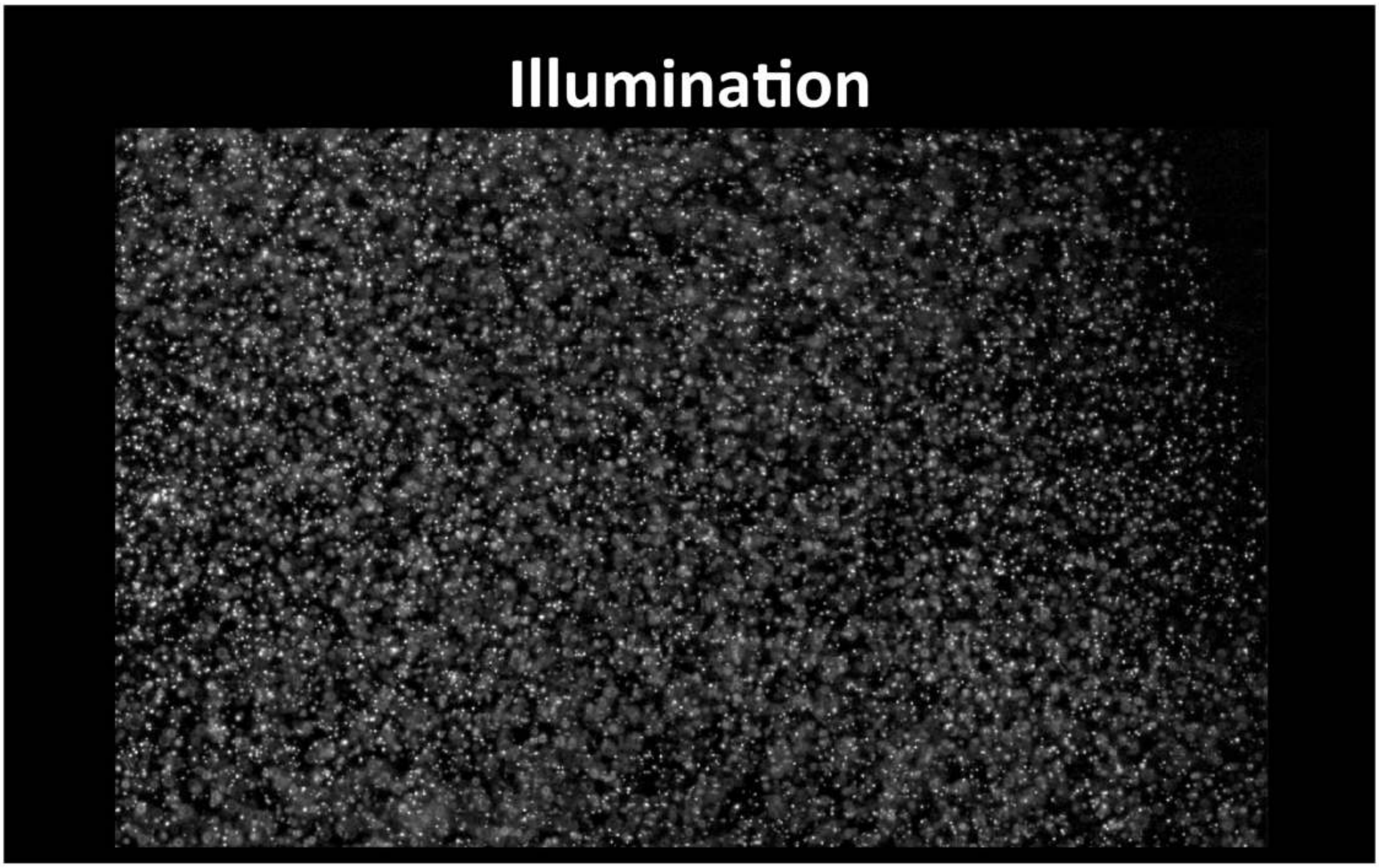
Illumination

Illumination

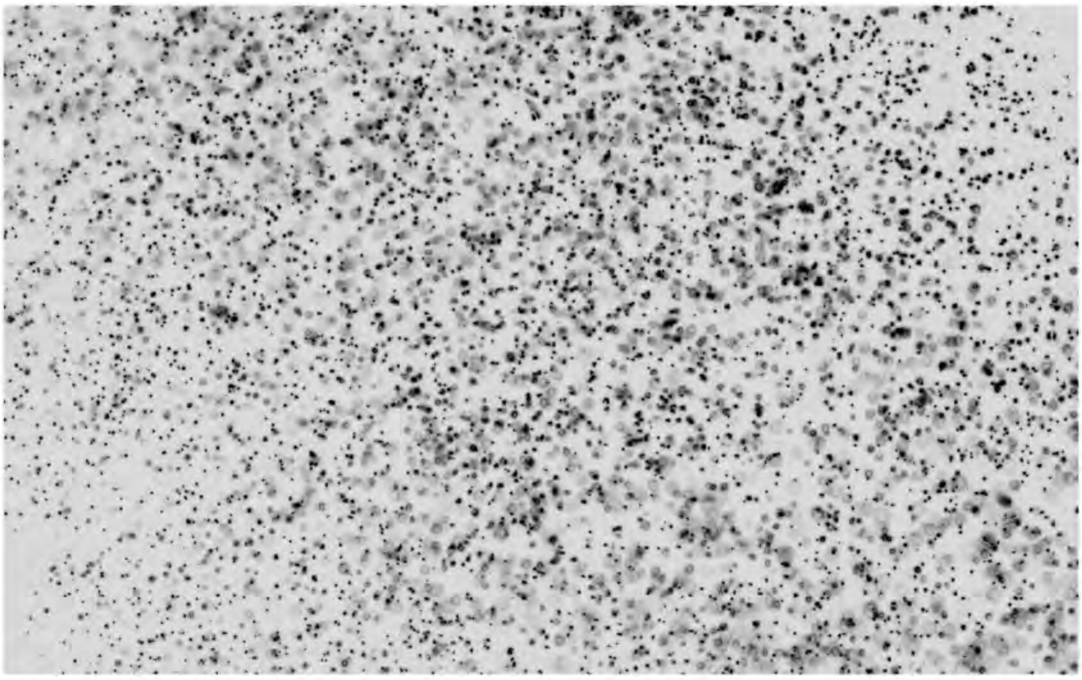

Tracking using OTF

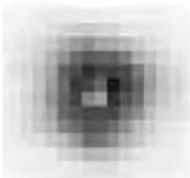

Tracking using OTF

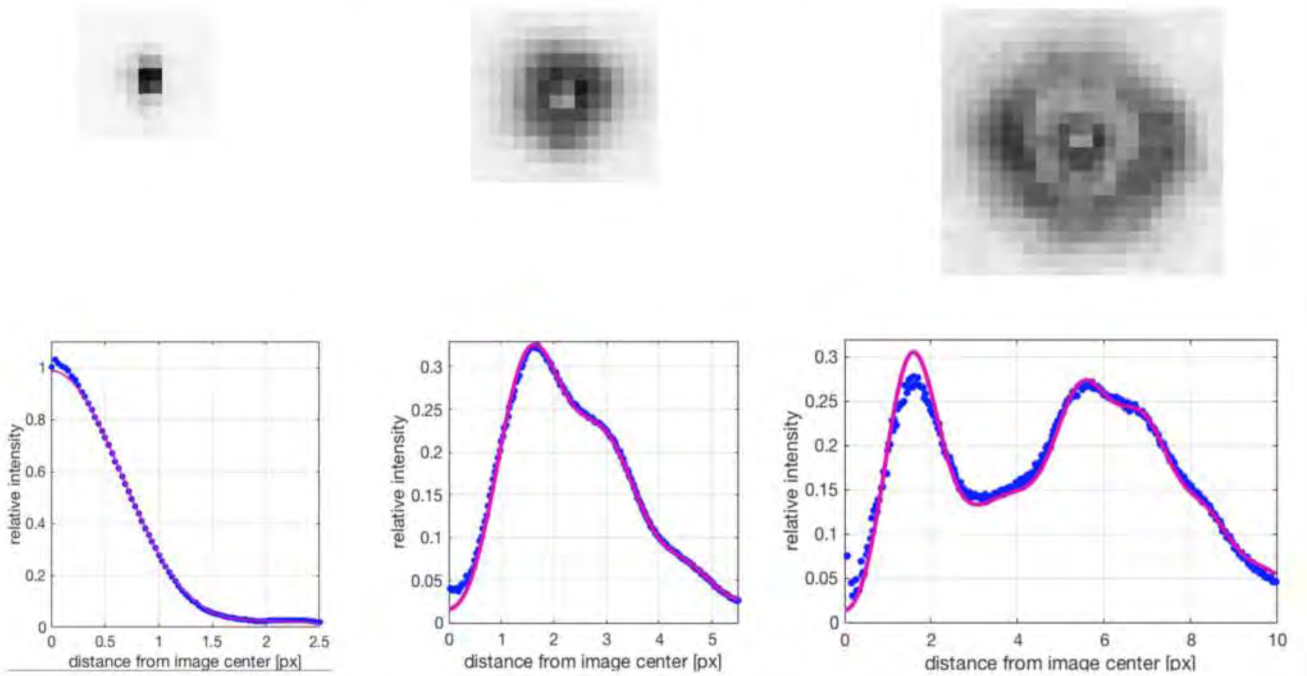

Tracking using OTF

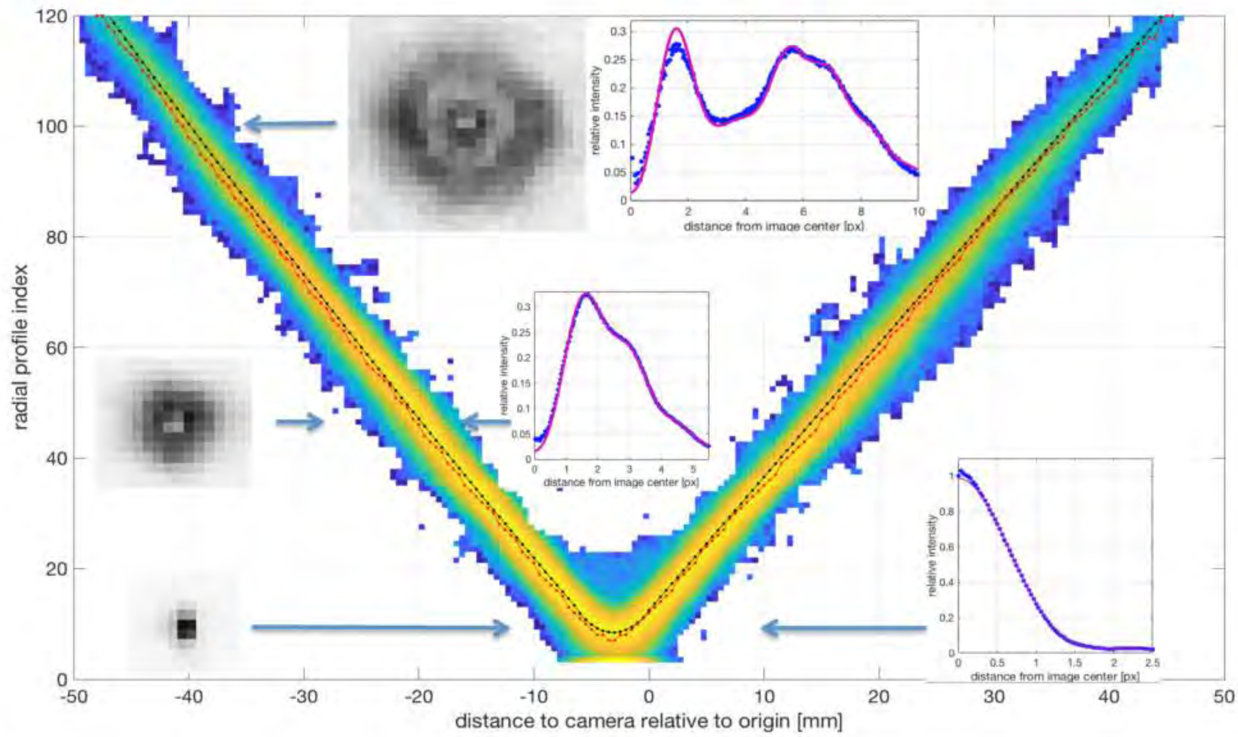

Tracking using OTF

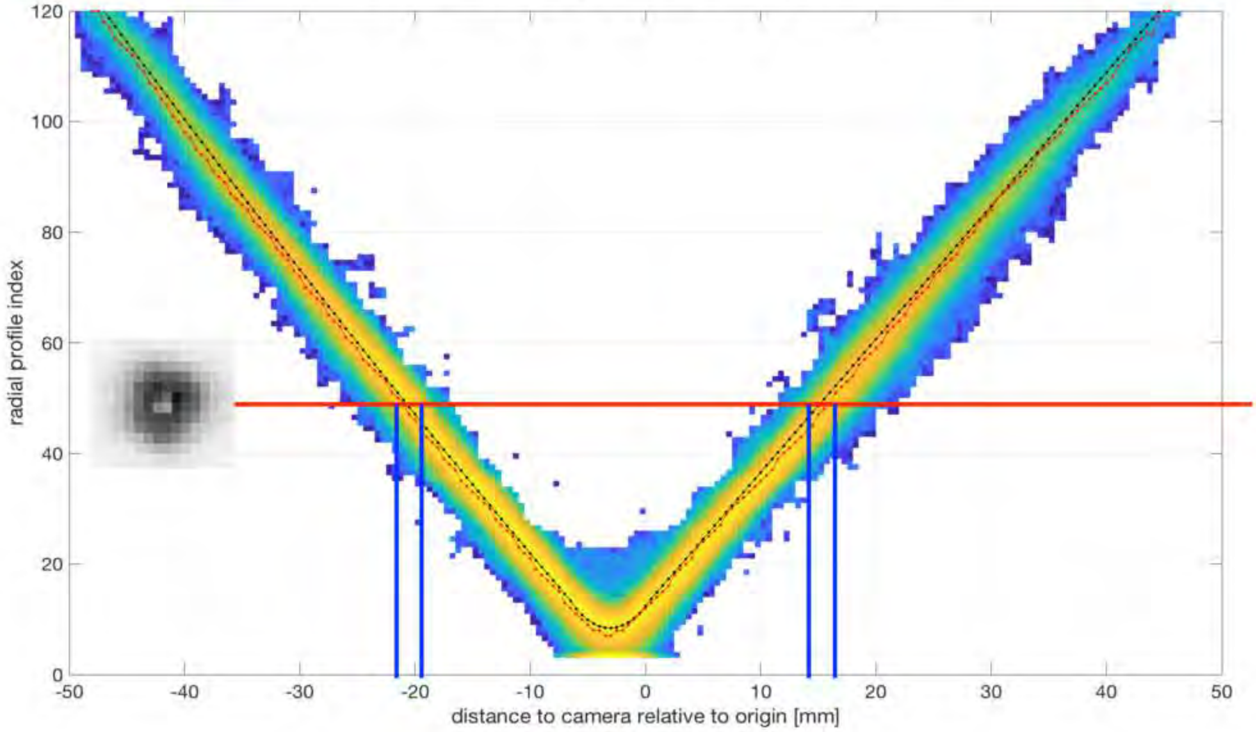

Tracking using OTF

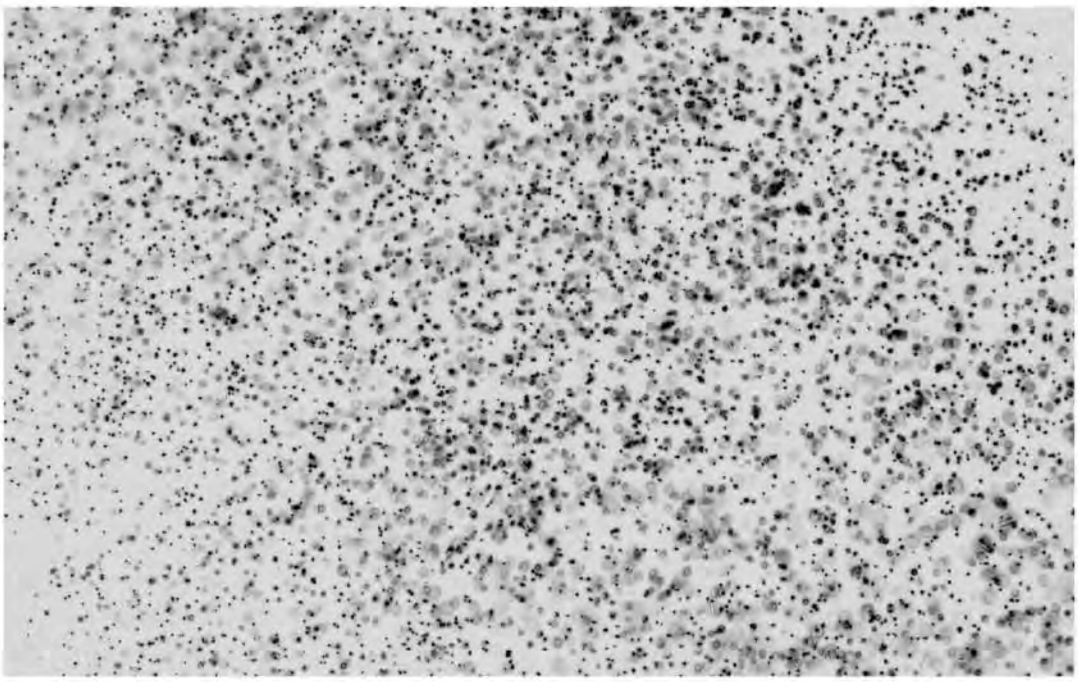

Tracking using OTF

Tracking using OTF

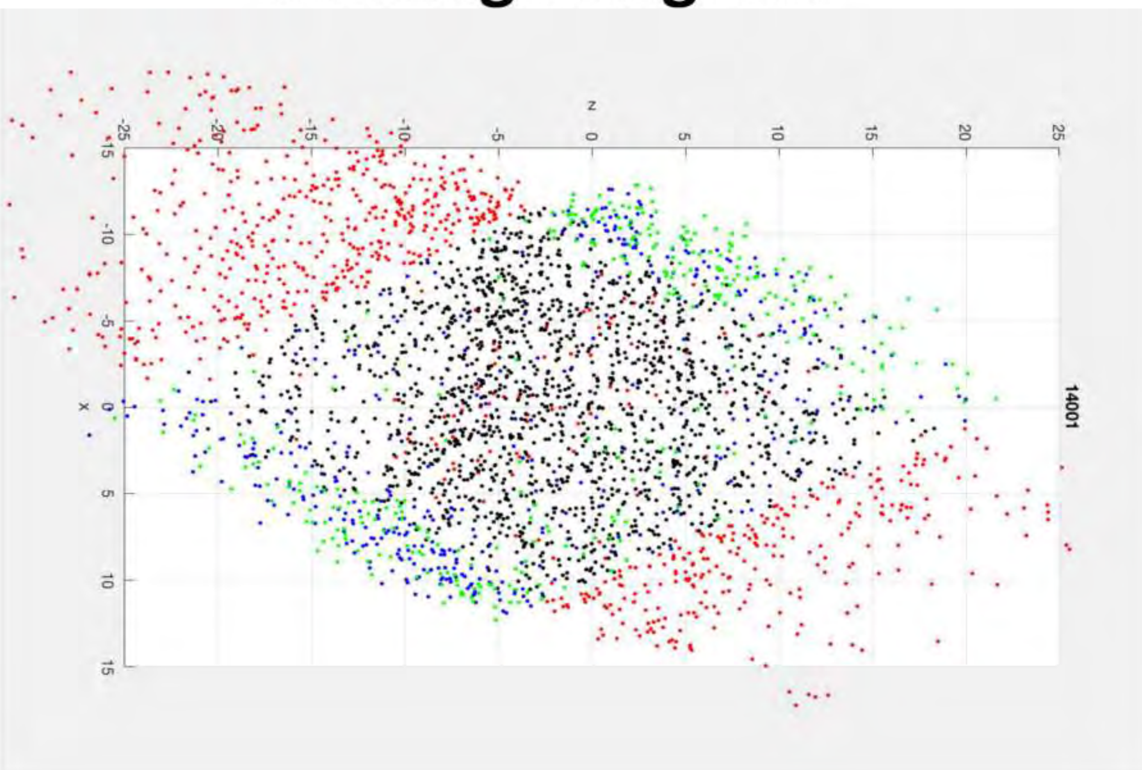

Background intensity

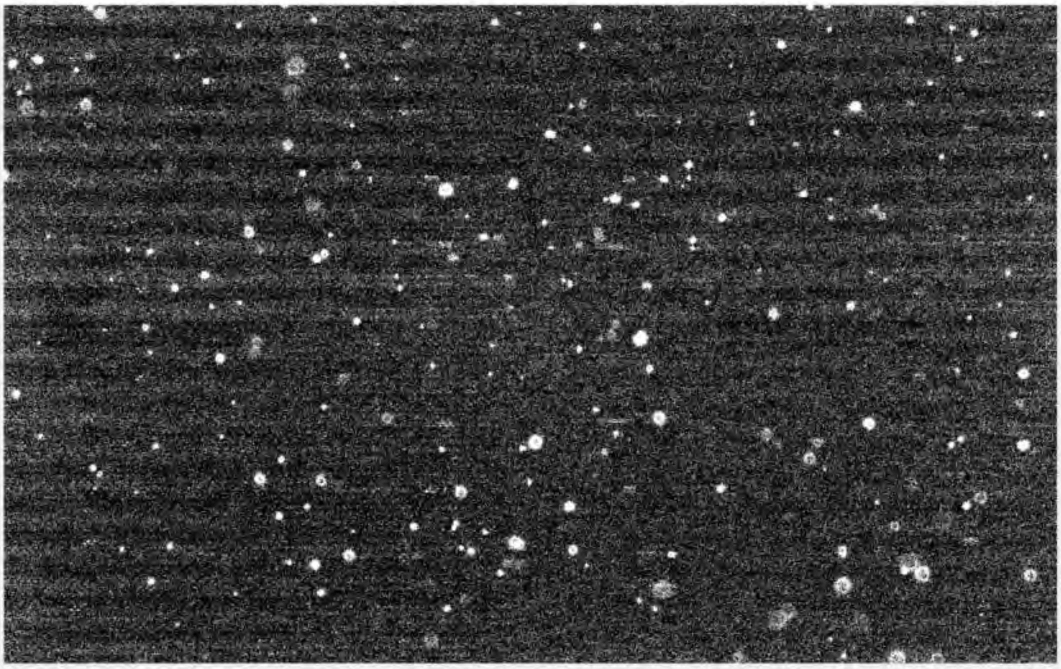

Data 2017

- **11 days with clouds:**

Day	T^{rec}_{TOT} [s]	Drop D [µm]
2017-06-04	125	7-35 (18)
2017-06-05	75	TBD
2017-07-20	347	12-26 (19)
2017-07-22	197	4-19 (9 & 13)
2017-07-23	421	10-35 (27)
2017-07-24	70	10-20 (17)
2017-08-19	486	20-35 [a.m.]
		10-30 [p.m.]
2017-08-20	40	4-15 (9)
2017-08-22	502	8-30 (15) [a.m.]
		6-18 (10) [p.m.]
2017-08-24	29	5-17 (9)
2017-08-28	42	9-26 (17)
TOTAL:	2334	

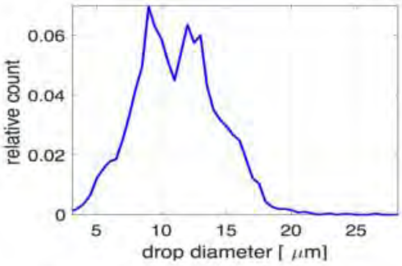

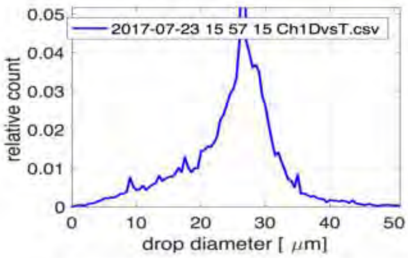

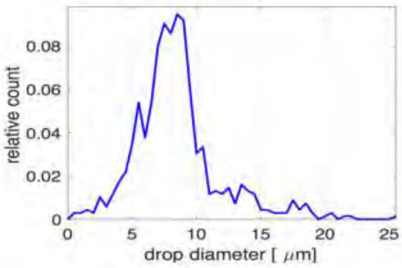


Thank you for your attention
• We gratefully acknowledge financial support from the
Bavarian Ministry for Environment and Consumer Protection

EnviSens Technologies

GNSS fundamentals

COMPLETE MSCA-ETN

HORIZON 2020

2nd Summer School on
Microphysics and Dynamics of Clouds
July 09 – 14, 2018

Eng. Marco Allegretti
marco.allegretti@polito.it

EnviSens Technologies (EST) s.r.l.
C.so Ciro Menotti 4, 10138 Torino, Italy.
Ph. +39-011 0904200 - Fax. +39-011 0904200 - www.envisens.com

Summary

- The navigation problem
- GNSS basic concepts
- Error sources
- Signal Propagation
- Signal Reception
- GNSS system examples: GPS - GALILEO
- Applications

EnviSens Technologies (EST) s.r.l.
C.so Ciro Menotti 4, 10138 Torino, Italy.
Ph. +39-011 0904200 - Fax. +39-011 0904200 - www.envisens.com

The problem

We want to know the position of an **object** with respect to a **reference frame.**

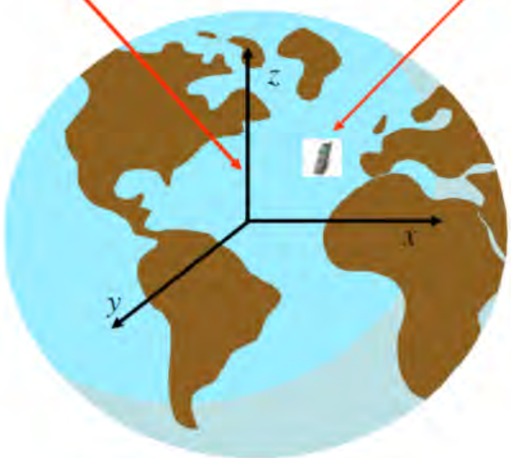

EnviSens Technologies (EST) s.r.l.
C.so Ciro Menotti 4, 10138 Torino, Italy.
Ph. +39-011 0904200 - Fax. +39-011 0904200 - www.envisens.com

Global Navigation Satellite System (GNSS)

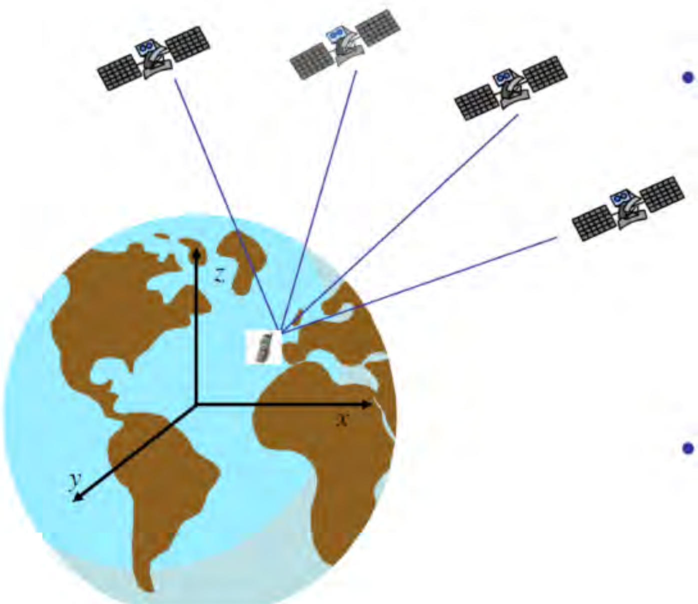

- A **Global Navigation Satellite System** (GNSS) consists of a constellation of satellites, whose payloads are especially designed to provide positioning of objects with global coverage.
- GNSSs implement the trilateration method.

EnviSens Technologies (EST) s.r.l.
C.so Ciro Menotti 4, 10138 Torino, Italy.
Ph. +39-011 0904200 - Fax. +39-011 0904200 - www.envisens.com

GNSS orbits

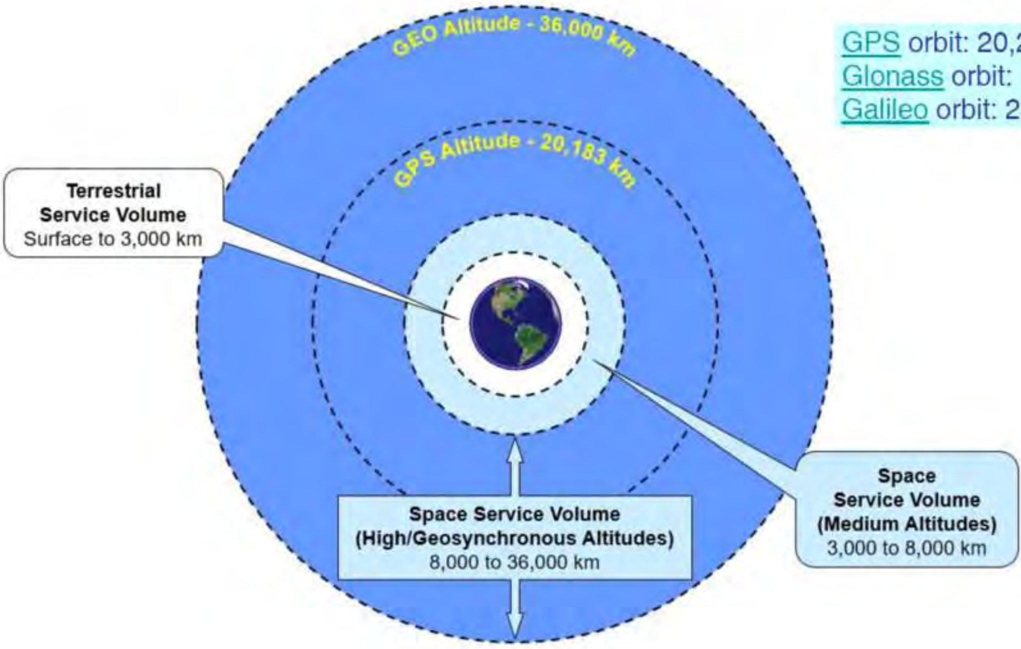

GPS orbit: 20,200 km
Glonass orbit: 19,100 km
Galileo orbit: 23,222 km

EnviSens Technologies (EST) s.r.l.
C.so Ciro Menotti 4, 10138 Torino, Italy.
Ph. +39-011 0904200 - Fax. +39-011 0904200 - www.envisens.com

CONCEPT 1: range measurements by TOA

- If a source transmits a pulse at t_0, and the pulse is received at time $t_0+\tau$, the distance between TX and RX (range) can be estimated as:

$$R = c \cdot \tau$$

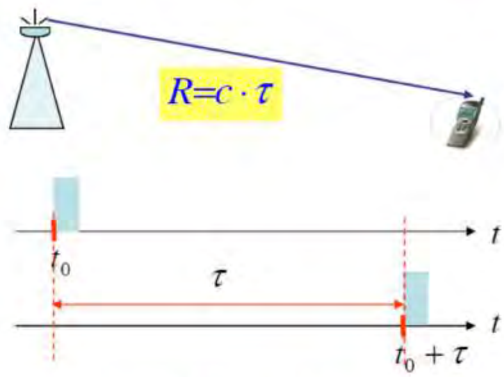

where c is the speed of light

- If both the clocks are perfect the measurement of $t_0+\tau$ allows for R determination
- In this case the range is the result of a TOA (Time of arrival) measurement.

EnviSens Technologies (EST) s.r.l.
C.so Ciro Menotti 4, 10138 Torino, Italy.
Ph. +39-011 0904200 - Fax. +39-011 0904200 - www.envisens.com

CONCEPT 2: trilateration principle

The observer is able to measure the TOA (*Time Of Arrival*)

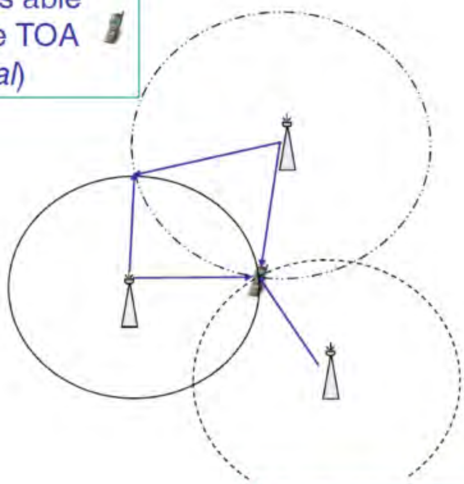

Transmitters are in known positions

The receiver is in an unknown position

Trilateration by GNSS satellites

The transmitters are onboard the satellites.

The satellites are at known positions, as we know the orbits, and the satellite time.

The satellites are equipped with atomic clocks.

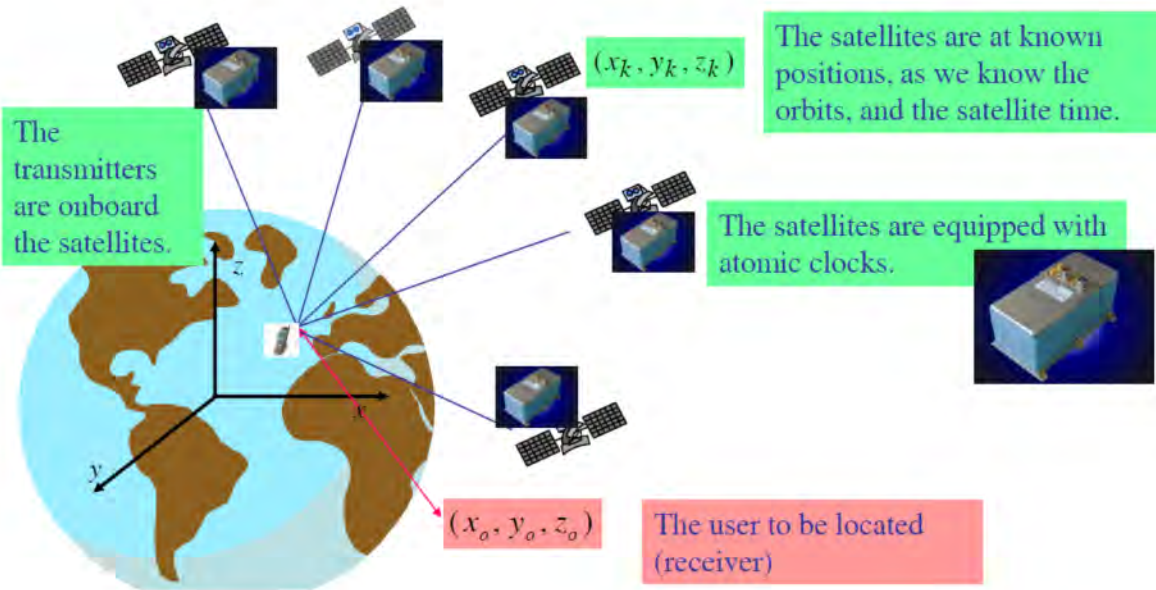

The user to be located (receiver)

EnviSens Technologies (EST) s.r.l.
C.so Ciro Menotti 4, 10138 Torino, Italy.
Ph. +39-011 0904200 - Fax. +39-011 0904200 - www.envisens.com

CONCEPT 3: the clock

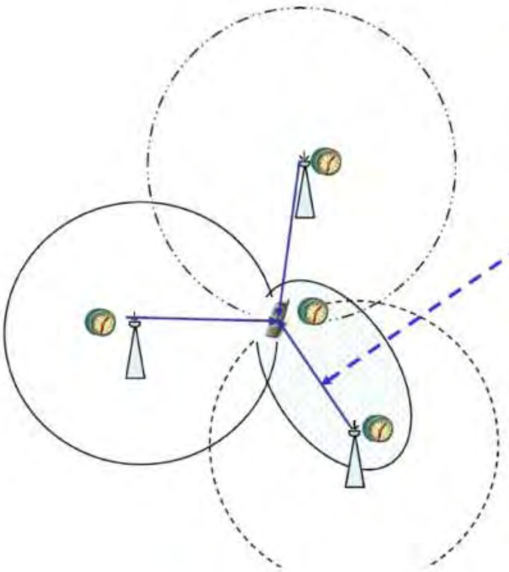

The observer measures the TOA (*Time Of Arrival*).
Then transmitters and receivers have to be equipped with clocks.

The basic requirement:
the clocks must be synchronized

Very onerous requirement !!

Synchronization error of $1\mu s$
Error of 300 m in distance

EnviSens Technologies (EST) s.r.l.
C.so Ciro Menotti 4, 10138 Torino, Italy.
Ph. +39-011 0904200 - Fax. +39-011 0904200 - www.envisens.com

Clocks (e.g GALILEO)

On-board clocks

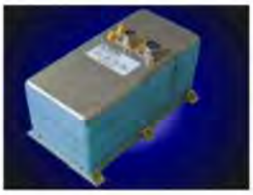

Rubidium Atomic Frequency Standard
3.2 Kg mass
30 W power

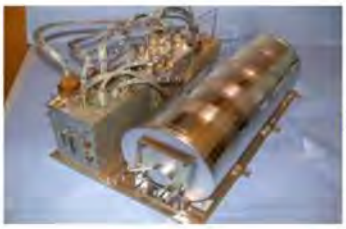

Passive Hydrogen Maser
18 Kg mass
70 W power

Frequency Standards

Rubidium
- Cheaper and Smaller
- Better short-term stability (less than 10 nsec per day)
- Subject to larger frequency variation caused by environment conditions

Passive H-Maser
- outstanding short-term and long term frequency stability (less than 1 nsec per day)
- frequency drift

EnviSens Technologies (EST) s.r.l.
C.so Ciro Menotti 4, 10138 Torino, Italy.
Ph. +39-011 0904200 - Fax. +39-011 0904200 - www.envisens.com

CONCEPT 4: the 4° satellite

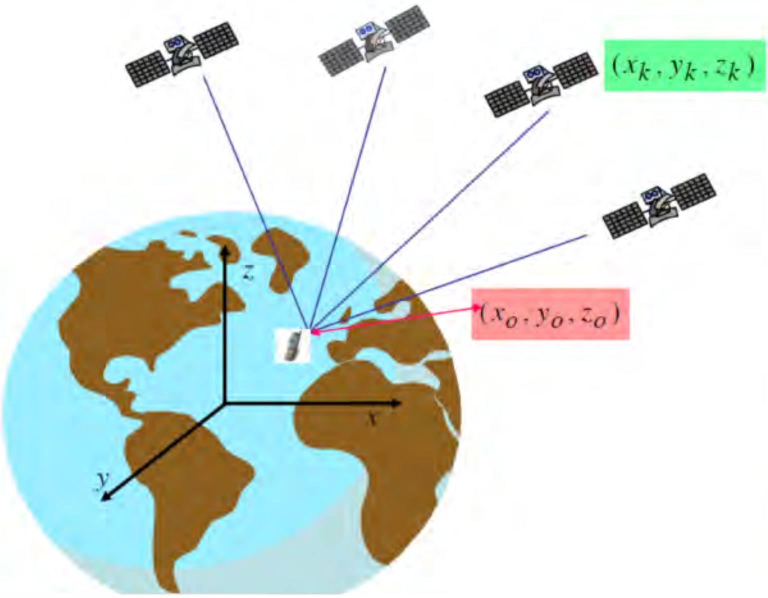

Why four satellites?

To sidestep the synchronisation requirement

EnviSens Technologies (EST) s.r.l.
C.so Ciro Menotti 4, 10138 Torino, Italy.
Ph. +39-011 0904200 - Fax. +39-011 0904200 - www.envisens.com

CONCEPT 5: the pseudorange

To sidestep the synchronisation requirement four satellites are needed

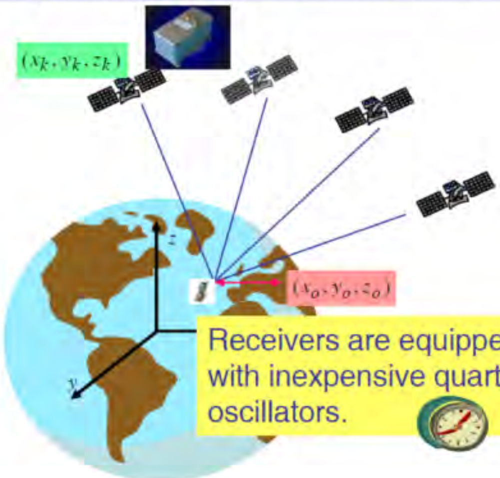

Receivers are equipped with inexpensive quartz oscillators.

TOA measurements at the receiver are affected by the same clock bias (b_c)

$(b_c) \longrightarrow (b_r)$

The range bias (b_r) becomes the fourth unknown to be estimated

Because of the bias (b_r) pseudoranges are measured instead of ranges

EnviSens Technologies (EST) s.r.l.
C.so Ciro Menotti 4, 10138 Torino, Italy.
Ph. +39-011 0904200 - Fax. +39-011 0904200 - www.envisens.com

THE NAVIGATION EQUATION

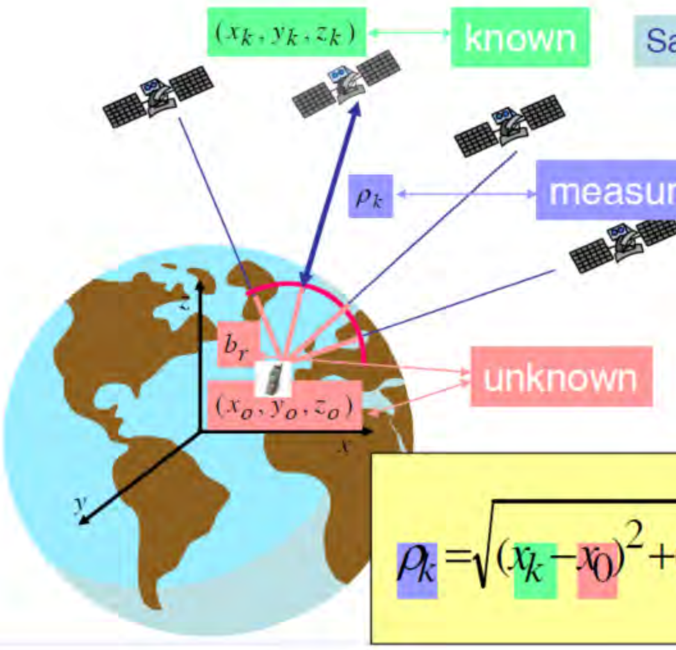

Satellite clocks are sync.

Receiver has a clock bias vs satellite clocks

$$\rho_k = \sqrt{(x_k - x_0)^2 + (y_k - y_0)^2 + (z_k - z_0)^2} - b_r$$

EnviSens Technologies (EST) s.r.l.
C.so Ciro Menotti 4, 10138 Torino, Italy.
Ph. +39-011 0904200 - Fax. +39-011 0904200 - www.envisens.com

The navigation equations

$$\begin{cases} \rho_1 = \sqrt{(x_0 - x_{s1})^2 + (y_0 - y_{s1})^2 + (z_0 - z_{s1})^2} + c \cdot \delta t_u \\ \rho_2 = \sqrt{(x_0 - x_{s2})^2 + (y_0 - y_{s2})^2 + (z_0 - z_{s2})^2} + c \cdot \delta t_u \\ \rho_3 = \sqrt{(x_0 - x_{s3})^2 + (y_0 - y_{s3})^2 + (z_0 - z_{s3})^2} + c \cdot \delta t_u \\ \rho_4 = \sqrt{(x_0 - x_{s4})^2 + (y_0 - y_{s4})^2 + (z_0 - z_{s4})^2} + c \cdot \delta t_u \end{cases}$$

measured

Known (written in the navigation message)

$x_0, y_0, z_0, \delta t_u$

4 unknowns

EnviSens Technologies (EST) s.r.l.
C.so Ciro Menotti 4, 10138 Torino, Italy.
Ph. +39-011 0904200 - Fax. +39-011 0904200 - www.envisens.com

A General GNSS system: architecture

- GNSS satellite systems consists of three major components or “segments:
  - Space Segment
  - Control Segment
  - User Segment

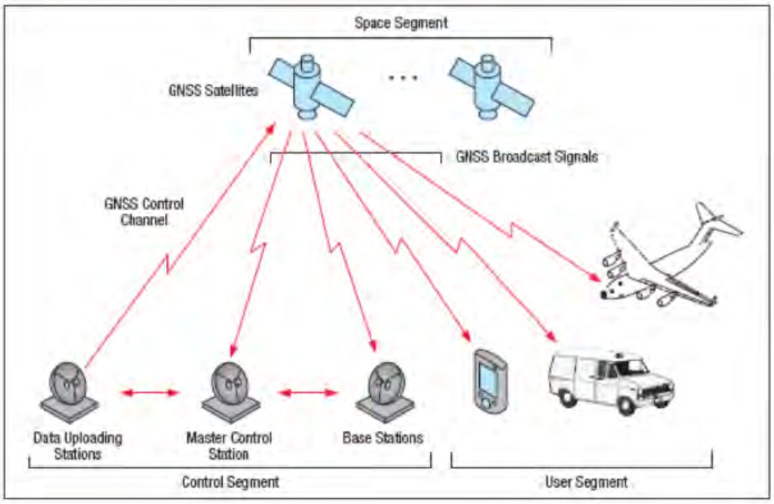

EnviSens Technologies (EST) s.r.l.
C.so Ciro Menotti 4, 10138 Torino, Italy.
Ph. +39-011 0904200 - Fax. +39-011 0904200 - www.envisens.com

A General GNSS system: space segment

- Consists of GNSS satellites, orbiting about 20,000 km above the earth. Each GNSS has its own constellation of satellites

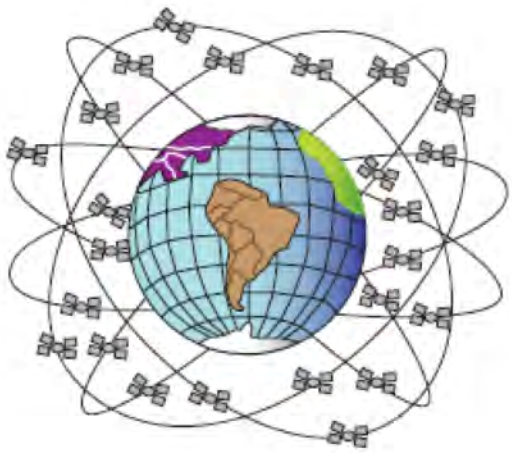

EnviSens Technologies (EST) s.r.l.
C.so Ciro Menotti 4, 10138 Torino, Italy.
Ph. +39-011 0904200 - Fax. +39-011 0904200 - www.envisens.com

A General GNSS system: control segment

- The control segment comprises of a ground-based network of master control stations, data uploading stations, and monitor stations.
- Master control stations adjust the satellites' orbit parameters and on-board high-precision clocks when necessary to maintain accuracy.
- Monitor stations monitor the satellites' signal and status, and relay this information to the master control station.
- Uploading stations uploads any change in satellite status back to the satellites

EnviSens Technologies (EST) s.r.l.
C.so Ciro Menotti 4, 10138 Torino, Italy.
Ph. +39-011 0904200 - Fax. +39-011 0904200 - www.envisens.com

A General GNSS system: user segment

- User segment consists of GNSS antennas and receivers used to determine information such as position, velocity, and time

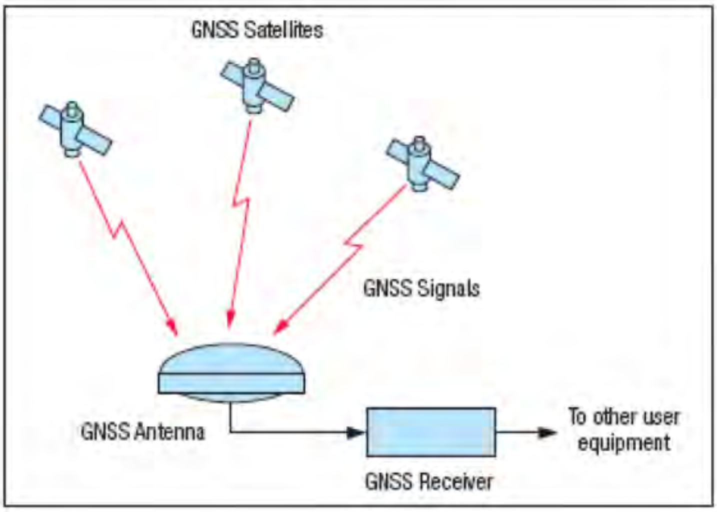

EnviSens Technologies (EST) s.r.l.
C.so Ciro Menotti 4, 10138 Torino, Italy.
Ph. +39-011 0904200 - Fax. +39-011 0904200 - www.envisens.com

GNSS error sources

- **Satellite errors**
  Errors in modeling clock offset
  Errors in Keplerian representation of ephemeris
  Latency in tracking

- **Atmospheric propagation errors**
  Through the ionosphere, carrier experiences phase advance and the code experiences group delay
  Dependent on:
    Geomagnetic latitude
    Time of the day
    Elevation of the satellite

Propagation

- GNSS signals pass through the near-vacuum of space, then through the various layers of the atmosphere to the earth, as illustrated in the figure below:

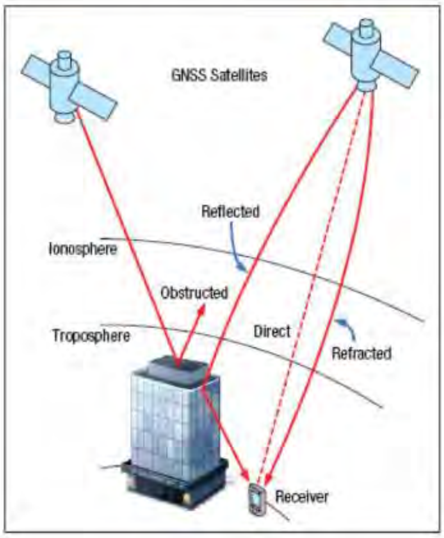

EnviSens Technologies (EST) s.r.l.
C.so Ciro Menotti 4, 10138 Torino, Italy.
Ph. +39-011 0904200 - Fax. +39-011 0904200 - www.envisens.com

Propagation

- To determine accurate positions, we need to know the range to the satellite. This is the direct path distance from the satellite to the user equipment.
- The signal will "bend" when traveling through the earth's atmosphere.
- This "bending" increases the amount of time the signal takes to travel from the satellite to the receiver.
- The computed range will contain this propagation time error, or atmospheric error.
- Since the computed range contains errors and is not exactly equal to the actual range, we refer to it as a "pseudorange"

EnviSens Technologies (EST) s.r.l.
C.so Ciro Menotti 4, 10138 Torino, Italy.
Ph. +39-011 0904200 - Fax. +39-011 0904200 - www.envisens.com

Propagation

- The ionosphere contributes to most of the atmospheric error. It resides at 70 to 1000 km above the earth's surface.
- Free electrons resides in the ionosphere, influencing electromagnetic wave propagation.
- Ionospheric delay are frequency dependent. It can be virtually eliminated by calculating the range using two frequencies.
- The troposphere, the lowest layer of the Earth's atmosphere, contributes to delays due to local temperature, pressure and relative humidity.
- Tropospheric delay cannot be eliminated the way ionospheric delay can be.
- It is possible to model the tropospheric delay then predict and compensate for much of the error.

EnviSens Technologies (EST) s.r.l.
C.so Ciro Menotti 4, 10138 Torino, Italy.
Ph. +39-011 0904200 - Fax. +39-011 0904200 - www.envisens.com

Propagation

- Signals can be reflected on the way to the receiver. This is called "multipath propagation".
- These reflected signals are delayed from the direct signal, and if strong enough, can interfere with the direct signal.
- Techniques have been developed whereby the receiver only considers the earliest-arriving signals and ignore multipath signals, which arrives later.
- It cannot be entirely eliminated

EnviSens Technologies (EST) s.r.l.
C.so Ciro Menotti 4, 10138 Torino, Italy.
Ph. +39-011 0904200 - Fax. +39-011 0904200 - www.envisens.com

Reception

- Receivers need at least 4 satellites to obtain a position. If more are available, these additional observations can be used to improve the position solution.
- GNSS signals are modulated by a unique pseudorandom digital sequence, or code. Each satellite uses a different pseudorandom code.
- Pseudorandom means that the signal appears random, but actually repeats itself after a period of time.
- Receivers know the pseudorandom code for each satellite. This allows receivers to correlate (synchronize) with the GNSS signal to a particular satellite.
- Through code correlation, the receiver is able to recover the signal and the information they contain

EnviSens Technologies (EST) s.r.l.
C.so Ciro Menotti 4, 10138 Torino, Italy.
Ph. +39-011 0904200 - Fax. +39-011 0904200 - www.envisens.com

Reception

- For each satellite tracked, the receiver determines the propagation time

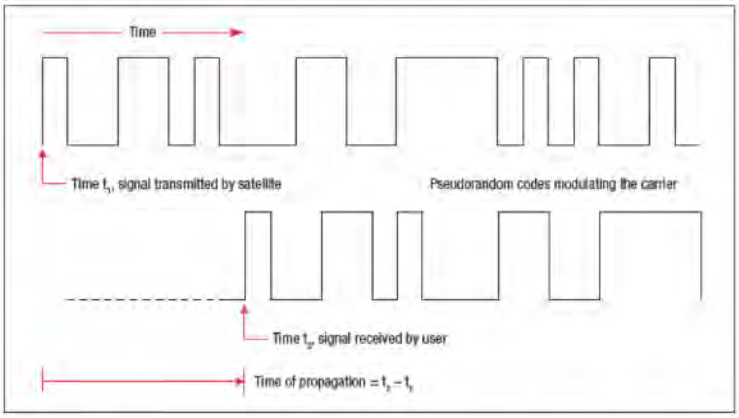

- The above figure shows the transmission of a pseudorandom code from a satellite. The receiver can determine the time of propagation by comparing the transmit time to the receive time

EnviSens Technologies (EST) s.r.l.
C.so Ciro Menotti 4, 10138 Torino, Italy.
Ph. +39-011 0904200 - Fax. +39-011 0904200 - www.envisens.com

Computation

- Range measurements from at least 4 satellites are needed to determine position.
- For each satellite tracked, the receiver calculates how long the satellite signal took to reach it, which in turn, determines the distance to the satellite:
  - Propagation Time = Time Signal Reached Receiver – Time Signal Left Satellite
  - Distance to Satellite = Propagation Time * Speed of Light
- Receiver now knows where the satellite was at the time of transmission through the use of orbit ephemerides.
- Through trilateration, the receiver calculates its position.

EnviSens Technologies (EST) s.r.l.
C.so Ciro Menotti 4, 10138 Torino, Italy.
Ph. +39-011 0904200 - Fax. +39-011 0904200 - www.envisens.com

Computation

- When we compute the pseudorange of the satellites, the points will not intersect to a single computed position.

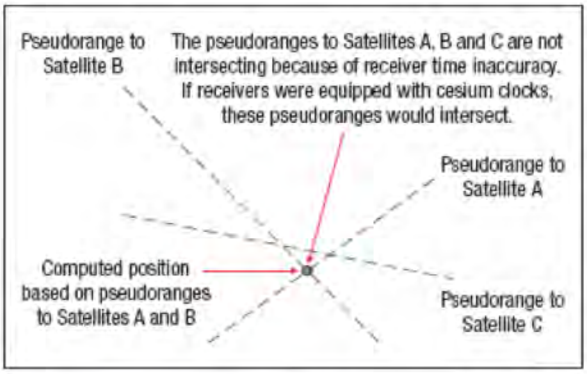

- The receiver knows that the pseudoranges to the three satellites do not intersect due to receiver clock errors.
- Receiver clocks are not nearly as accurate as satellite clocks. Their typical accuracy is only about 5 parts per million.
- When multiplied by the speed of light, the resulting accuracy is within +/- 1500 meters

EnviSens Technologies (EST) s.r.l.
C.so Ciro Menotti 4, 10138 Torino, Italy.
Ph. +39-011 0904200 - Fax. +39-011 0904200 - www.envisens.com

Computation

- Here are the GNSS error sources that affect the accuracy of pseudorange calculation:

Contributing Source	Error Range
Satellite clocks	±2 m
Orbit errors	±2.5 m
Ionospheric delays	±5 m
Tropospheric delays	±0.5 m
Receiver noise	±0.3 m
Multipath	±1 m

- The degree with which the above pseudorange errors affect positioning accuracy depends largely on the geometry of the satellites being used. This will be discussed later in this training.

EnviSens Technologies (EST) s.r.l.
C.so Ciro Menotti 4, 10138 Torino, Italy.
Ph. +39-011 0904200 - Fax. +39-011 0904200 - www.envisens.com

GNSS systems

- Currently, the following GNSS systems are operational
  - GPS (United States)
  - GLONASS (Russia)
- The following GNSS systems are planned and are in varying stages of development
  - Galileo (European Union)
  - BeiDou (China)
- The following regional navigation satellite systems are planned and are in varying stages of development:
  - IRNSS (India)
  - QZSS (Japan)

EnviSens Technologies (EST) s.r.l.
C.so Ciro Menotti 4, 10138 Torino, Italy.
Ph. +39-011 0904200 - Fax. +39-011 0904200 - www.envisens.com

GNSS system: GPS

- GPS (Global Positioning System) or NAVSTAR, as it is officially called, is the first GNSS system.
- Launched in the late 1970's and early 1980's for the US Department of Defense.
- Since the initial launch, several generations, referred to as "Blocks", of GPS satellites have been launched.
- GPS was initially launched for military use, but opened up to civilian use in 1983

EnviSens Technologies (EST) s.r.l.
C.so Ciro Menotti 4, 10138 Torino, Italy.
Ph. +39-011 0904200 - Fax. +39-011 0904200 - www.envisens.com

GNSS system: GPS space segment

- The GPS space segment is summarized in the table below:

Satellites	21 plus 3 spares
Orbital planes	6
Orbit inclination	55 degrees
Orbit radius	26,560 km

- The orbital period of each satellite is approximately 12 hours.
- At any point in time, a GPS receiver will have at least 6 satellites in view at any point on Earth under open sky conditions.

EnviSens Technologies (EST) s.r.l.
C.so Ciro Menotti 4, 10138 Torino, Italy.
Ph. +39-011 0904200 - Fax. +39-011 0904200 - www.envisens.com

GNSS system: GPS satellites

- GPS orbits approximately 26,560 km above the Earth.
- GPS satellites continuously broadcast their identification, ranging signals, satellite status and corrected ephemerides (orbit parameters).
- Each satellite is identified by their Space Vehicle Number (SVN) and their PseudoRandom code Number (PRN)

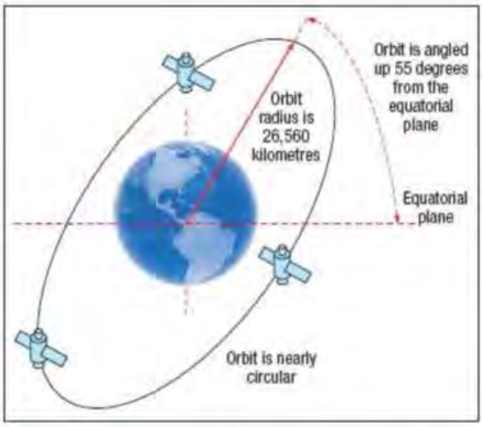

EnviSens Technologies (EST) s.r.l.
C.so Ciro Menotti 4, 10138 Torino, Italy.
Ph. +39-011 0904200 - Fax. +39-011 0904200 - www.envisens.com

GNSS system: GPS frequencies

Designation	Frequency	Description
L1	1575.42 MHz	L1 is modulated by the C/A code (Coarse/Acquisition) and the P-code (Precision) which is encrypted for military and other authorized users.
L2	1227.60 MHz	L2 is modulated by the P-code and, beginning with the Block IIR-M satellites, the L2C (civilian) code. L2C, which is considered "under development", is discussed below, under "GPS Modernization".
L5	1176.45 MHz	At the time of writing, L5 is available for demonstration on one GPS satellite. The L5 signal is discussed below, under "GPS Modernization".

GNSS system: GPS frequencies

- GPS Control Segment consists of a master control station and a backup master control station, in addition to monitor stations throughout the world.

- The monitor stations tracks the satellite broadcast signal and pass them on to the master control station where the ephemerides are recalculated. The resulting ephemerides and timing corrections are transmitted back to the satellites through data up-loading stations.

EnviSens Technologies (EST) s.r.l.
C.so Ciro Menotti 4, 10138 Torino, Italy.
Ph. +39-011 0904200 - Fax. +39-011 0904200 - www.envisens.com

GNSS system: GPS modernization

- GPS space segment modernization has included new signals, as well as improvements in atomic clock accuracy, satellite signal strength and reliability.
- Control segment modernization includes improved ionospheric and trophospheric modelling and in-orbit accuracy, and additional monitoring stations.
- Latest generation of GPS satellites has the capability to transmit new civilian signal, designated L2C.
- L2C will be easier for the user segment to track and will provide improved navigation accuracy.
- It will also provide the ability to directly measure and remove the ionospheric delay error for a particular satellite, using the civilian signals on both L1 and L2.

EnviSens Technologies (EST) s.r.l.
C.so Ciro Menotti 4, 10138 Torino, Italy.
Ph. +39-011 0904200 - Fax. +39-011 0904200 - www.envisens.com

GNSS system: GPS modernization

- A new GPS L5 frequency (1176.45 MHz) is slowly being added to new satellites.
- The first NAVSTAR GPS satellite to transmit L5, on a demonstration basis, was launched in 2009.
- L5 signal is added to meet the requirements of critical safety-of-life applications.
- GPS satellite modernization will also include a new military signal and an improved L1C which will provide greater civilian interoperability with Galileo.

EnviSens Technologies (EST) s.r.l.
C.so Ciro Menotti 4, 10138 Torino, Italy.
Ph. +39-011 0904200 - Fax. +39-011 0904200 - www.envisens.com

GNSS system: GALILEO

- Europe's global navigation system.
- Guaranteed global positioning service under civilian control.
- Guaranteed availability of service under all but the most extreme circumstances.
- Suitable for applications where safety is crucial, such as air and ground transportation.

Satellites	27 operational and three active spares
Orbital planes	3
Orbital inclination	56 degrees
Orbit radius	23,616 km

EnviSens Technologies (EST) s.r.l.
C.so Ciro Menotti 4, 10138 Torino, Italy.
Ph. +39-011 0904200 - Fax. +39-011 0904200 - www.envisens.com

GNSS system: GALILEO implementation plan

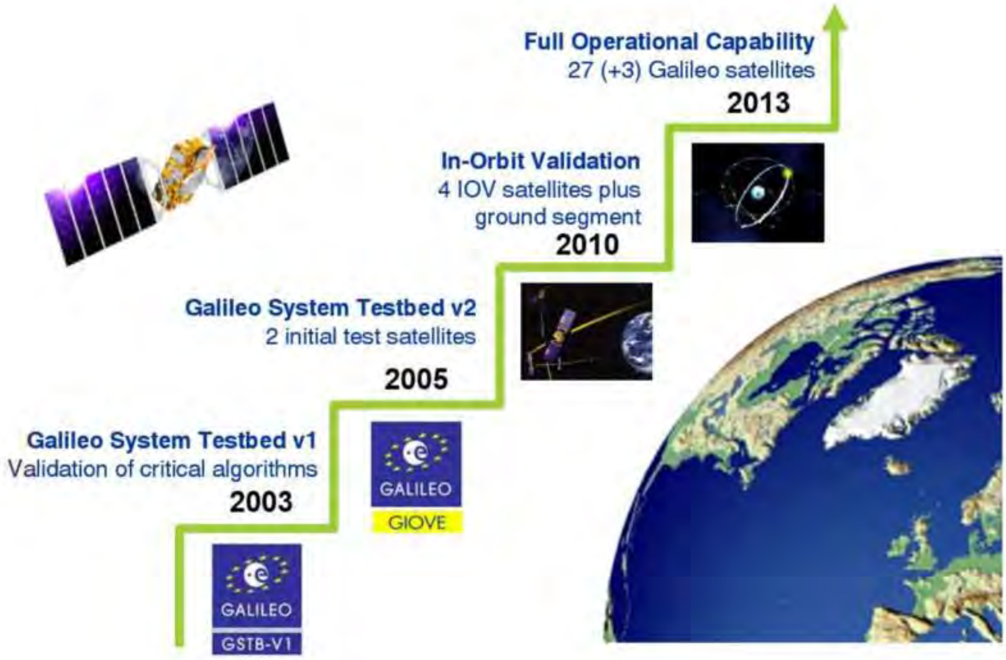

EnviSens Technologies (EST) s.r.l.
C.so Ciro Menotti 4, 10138 Torino, Italy.
Ph. +39-011 0904200 - Fax. +39-011 0904200 - www.envisens.com

GNSS system: GALILEO characteristics

- Once the constellation is operational, Galileo navigation signals will provide coverage at all latitudes.
- Two Galileo Control Centers (GCC) will be located in Europe.
- Data recovered by a global network of twenty Galileo Sensor Stations (GSS) will be sent to the GCC.
- Galileo will provide global Search and Rescue (SAR) function.

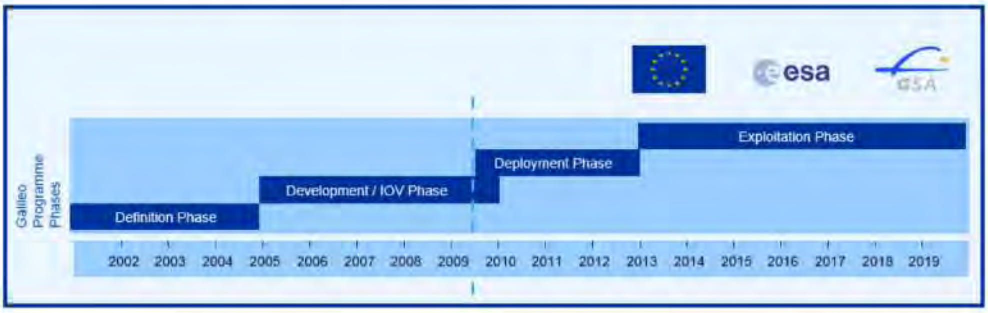

EnviSens Technologies (EST) s.r.l.
C.so Ciro Menotti 4, 10138 Torino, Italy.
Ph. +39-011 0904200 - Fax. +39-011 0904200 - www.envisens.com

GNSS system: GALILEO services

Service	Description
Free Open Service (OS)	Provides positioning, navigation and precise timing service. It will be available for use by any person with a Galileo receiver. No authorisation will be required to access this service. Galileo is expected to be similar to GPS in this respect.
Highly reliable Commercial Service (CS)	Service providers can provide added-value services, for which they can charge the end customer. The CS signal will contain data relating to these additional commercial services.
Safety-of-Life Service (SOL)	Improves on OS by providing timely warnings to users when it fails to meet certain margins of accuracy. A service guarantee will likely be provided for this service.
Government encrypted Public Regulated Service (PRS)	Highly encrypted restricted-access service offered to government agencies that require a high availability navigation signal.
Search and Rescue Service (SAR)	Public service designed to support search and rescue operations, which will make it possible to locate people and vehicles in distress.

EnviSens Technologies (EST) s.r.l.
C.so Ciro Menotti 4, 10138 Torino, Italy.
Ph. +39-011 0904200 - Fax. +39-011 0904200 - www.envisens.com

GNSS system: compatibility and interoperability

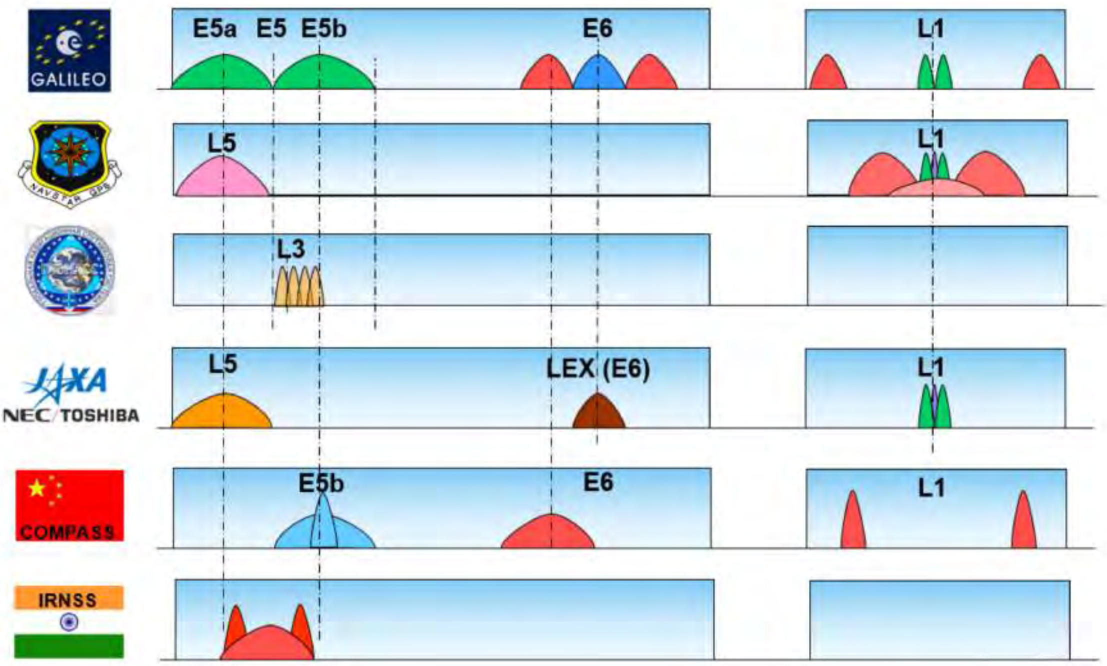

EnviSens Technologies (EST) s.r.l.
C.so Ciro Menotti 4, 10138 Torino, Italy.
Ph. +39-011 0904200 - Fax. +39-011 0904200 - www.envisens.com

GNSS application: transportation

- Portable navigation devices
- Air, marine, and ground based vehicle navigation

www.boeing.com

www.wellandcanal.ca

EnviSens Technologies (EST) s.r.l.
C.so Ciro Menotti 4, 10138 Torino, Italy.
Ph. +39-011 0904200 - Fax. +39-011 0904200 - www.envisens.com

GNSS application: machine control

NovAtel Inc.

Thomas Morley, NovAtel Inc.

GNSS application: surveying and civil engineering

NovAtel Inc.

Google Earth

EnviSens Technologies (EST) s.r.l.
C.so Ciro Menotti 4, 10138 Torino, Italy.
Ph. +39-011 0904200 - Fax. +39-011 0904200 - www.envisens.com

GNSS application: machine control

NovAtel Inc.

Thomas Morley, NovAtel Inc.

EnviSens Technologies (EST) s.r.l.
C.so Ciro Menotti 4, 10138 Torino, Italy.
Ph. +39-011 0904200 - Fax. +39-011 0904200 - www.envisens.com

GNSS application: GIS, DEM, cartography

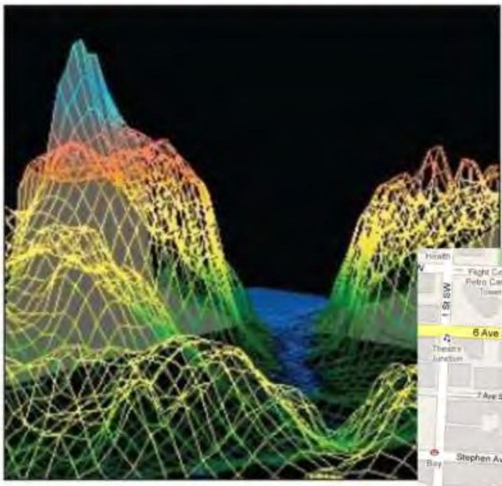

EnviSens Technologies (EST) s.r.l.
C.so Ciro Menotti 4, 10138 Torino, Italy.
Ph. +39-011 0904200 - Fax. +39-011 0904200 - www.envisens.com

GNSS application: automation, defence… etc!

EnviSens Technologies (EST) s.r.l.
C.so Ciro Menotti 4, 10138 Torino, Italy.
Ph. +39-011 0904200 - Fax. +39-011 0904200 - www.envisens.com

GNSS application: atmosferic studies

- Radio occultation.
- Tomography.
- Ionospheric scintillation studies.
- Atmospheric parameters studies (temperature, water vapour, refractive index…)
- Meteorology.
- …

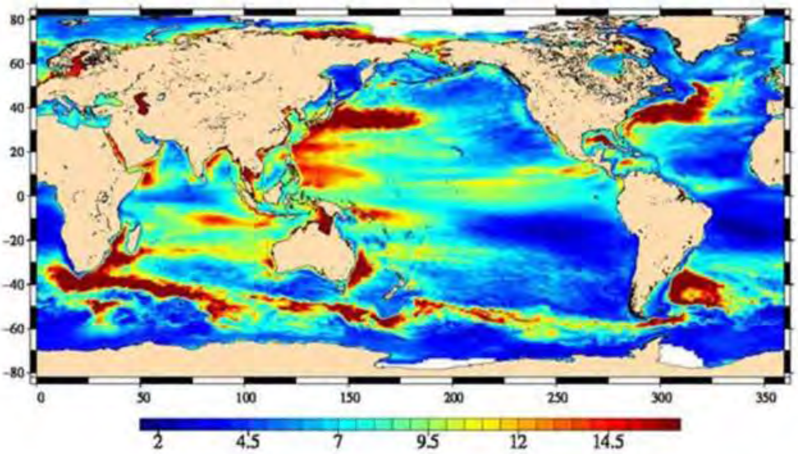

EnviSens Technologies (EST) s.r.l.
C.so Ciro Menotti 4, 10138 Torino, Italy.
Ph. +39-011 0904200 - Fax. +39-011 0904200 - www.envisens.com

HOWEVER… High precision!

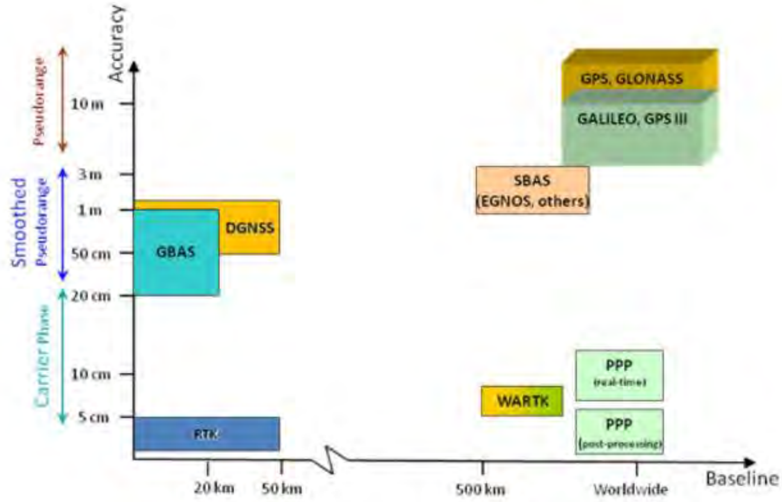

GBAS: Ground Based Augmentation System
EGNOS: European Geostationary Navigation Overlay System
DGNSS: Differential GNSS
PPP: Precise Point Positioning

SBAS: Satellite Base Augmentation System

RTK: Real Time Kinematic
WARTK: Wide Area RTK

EnviSens Technologies (EST) s.r.l.
C.so Ciro Menotti 4, 10138 Torino, Italy.
Ph. +39-011 0904200 - Fax. +39-011 0904200 - www.envisens.com

Envisens Technologies s.r.l. (EST)

Thank you!

Eng. Marco Allegretti
marco.allegretti@polito.it

Slides prepared by: Eng. M. Allegretti, Eng. S. Bertoldo, Prof. G. Perona

EnviSens Technologies (EST) s.r.l.
C.so Ciro Menotti 4, 10138 Torino, Italy.
Ph. +39-011 0904200 - Fax. +39-011 0904200 - www.envisens.com

Radarmeteorology - introduction

COMPLETE

MSCA-ETN

HORIZON 2020

2nd Summer School on
Microphysics and Dynamics of Clouds
July 09 – 14, 2018

Eng. Marco Allegretti
marco.allegretti@polito.it

Summary

- Introduction
- Microwave, water, meteorology
- Weather radar bands
- Radar for meteorology
- Example of weather radars

Radarmeteorology

- Precipitation
  - type: rain, snow, hail, etc.
  - rates or cumulative amounts

- Wind Shear Conditions (Airport Terminal Area)
  - Microburst
  - Gust Fronts

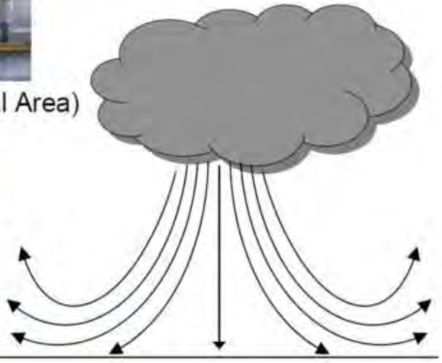

- Hazardous Conditions
  - Thunderstorms
    - Intensity
    - Location
    - Extent
    - Movement

  - Mesocyclones
    - Possible precursor to tornados

EnviSens Technologies (EST) s.r.l.
C.so Ciro Menotti 4, 10138 Torino, Italy.
Ph. +39-011 0904200 - Fax. +39-011 0904200 - www.envisens.com

Radarmeteorology

Radar: **R**adio **D**etection **A**nd **R**anging

An electronic instrument used for the detection and ranging of distant objects of such composition that they scatter or reflect radio energy.

Radar Meteorology:

The study of the atmosphere and weather using radar as the means of observation and measurement.

Meteorology:

The study of the physics, chemistry, and dynamics of the Earth's atmosphere.

Reference: AMS, American Meteorological Society

EnviSens Technologies (EST) s.r.l.
C.so Ciro Menotti 4, 10138 Torino, Italy.
Ph. +39-011 0904200 - Fax. +39-011 0904200 - www.envisens.com

Weather radar bands

HF	3 - 30	MHz
VHF	30 - 300	MHz
UHF	300 - 1000	MHz
L	1 - 2	GHz
S	2 - 4	GHz
C	4 - 8	GHz
X	8 - 12	GHz
Ku	12 - 18	GHz
K	18 - 27	GHz
Ka	27 - 40	GHz
V	40 - 75	GHz
W	75 - 110	GHz
mm	110 - 300	GHz

EnviSens Technologies (EST) s.r.l.
C.so Ciro Menotti 4, 10138 Torino, Italy.
Ph. +39-011 0904200 - Fax. +39-011 0904200 - www.envisens.com

Weather radar bands

UHF-Band (300MHz, 909MHz) (75 cm, 33 cm)
- Wind Profiler Radars
- Bragg Scattering

S-Band (2.0 to 4.0 GHz) (15 cm to 7.5 cm)
- Attenuation due to weather is minimal compared to higher frequency bands
- Good for ground based long range weather radars
- Note that the beamwidth is inversely proportional to the size of the antenna

C-Band (4.0 to 8.0 GHz)(7.5 cm to 3.75 cm)
- Generally, a compromise between S and X band
- Localized weather observation (e.g. airport terminal area)

X-Band (8.0 to 12.5 GHz) (3.75 cm to 2.4 cm)
- Radars in this band allow for a reduction in antenna size while maintaining the desired beamwidth for angular accuracy
- Used in weather avoidance airborne systems where antenna dimensions becomes a real issue and where attenuation is less of a factor due to reduced operating ranges.
- Attenuation can be significant

EnviSens Technologies (EST) s.r.l.
C.so Ciro Menotti 4, 10138 Torino, Italy.
Ph. +39-011 0904200 - Fax. +39-011 0904200 - www.envisens.com

Meteorological targets

- Are usually considered as clutter in other radar applications
- Occupy a large percentage of the volume of interest
- Vary in size, composition (gas, liquid, solid (ice)), and dielectric properties
- Represent a random process due to the dynamic nature of the scatterers which vary in size, relative location, and motion

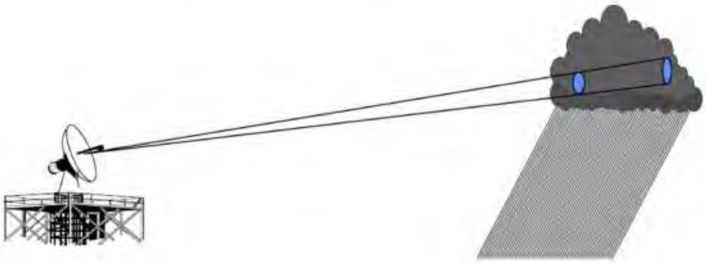

EnviSens Technologies (EST) s.r.l.
C.so Ciro Menotti 4, 10138 Torino, Italy.
Ph. +39-011 0904200 - Fax. +39-011 0904200 - www.envisens.com

What does a weather radar measure?

A weather radar can measure various quantities:

- the **radar reflectivity** (related to precipitation rates)
- the **Doppler phase shift** (related to radial component of wind vector)
- **polarimetric quantities** (related to shape and orientation of raindrops)

EnviSens Technologies (EST) s.r.l.
C.so Ciro Menotti 4, 10138 Torino, Italy.
Ph. +39-011 0904200 - Fax. +39-011 0904200 - www.envisens.com

Radar measurement principle

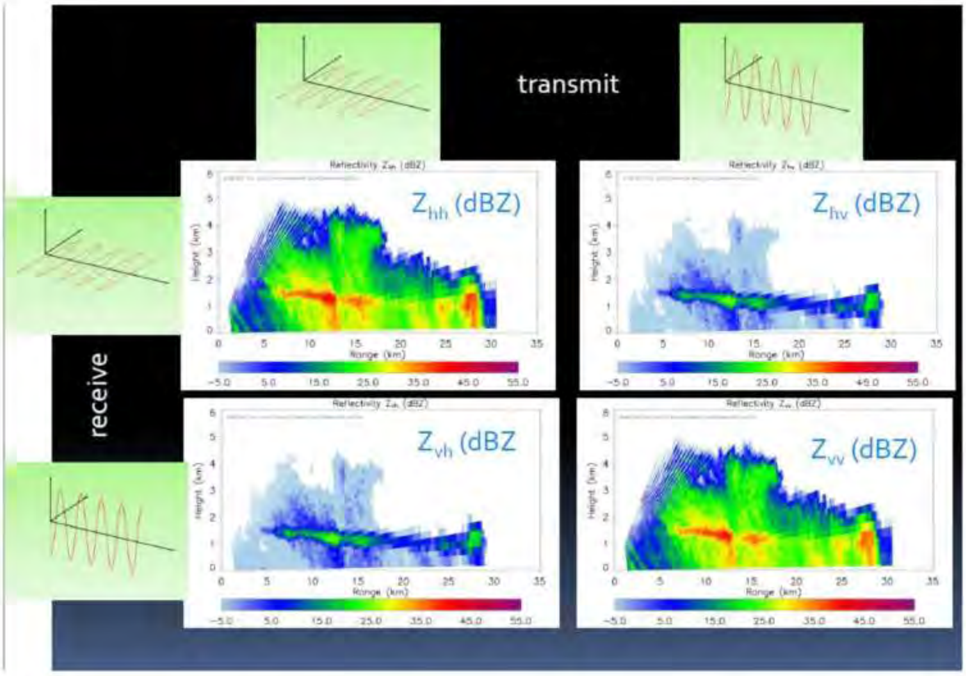

EnviSens Technologies (EST) s.r.l.
C.so Ciro Menotti 4, 10138 Torino, Italy.
Ph. +39-011 0904200 - Fax. +39-011 0904200 - www.envisens.com

Radar monitoring capabilities

- High spatial coverage
- High space-time resolution
- Complementary to others sensors (ground based or space based)
- Able to describe local phenomena
- Network - increase space-time description

EnviSens Technologies (EST) s.r.l.
C.so Ciro Menotti 4, 10138 Torino, Italy.
Ph. +39-011 0904200 - Fax. +39-011 0904200 - www.envisens.com

Radar monitoring capabilities

Respect other atmospheric observation techniques in situ, e.g. instruments carried by aircraft or balloons or rockets, passive, e.g. photographic or radiometric techniques, radar offers the following advantages:

- Visibility through optic opaque zone
- Active target identification
- Data may be collected in 3D
- Target is not perturbed by observation
- Data are immediately available

EnviSens Technologies (EST) s.r.l.
C.so Ciro Menotti 4, 10138 Torino, Italy.
Ph. +39-011 0904200 - Fax. +39-011 0904200 - www.envisens.com

Example of C-band radar

- ✓**Band : C**
- ✓**Polarimetric**
- ✓**Doppler**
- ✓**Peak power 250 KW**
- ✓**Ang. resol.: 1 deg**
- ✓**Antenna diameter: about 4,2 m**

Primary scan:

- ✓**Prf: 1090 Hz**
- ✓**8 elevations**
- ✓**Scan time: 5-10 minuti**
- ✓**Radial resol: 0.375 Km**
- ✓**Max dist.: 136 km**

Momenti: $Z_h, Z_{DR}, V_R, \Phi_{DP}, \rho_{HV}$

GPM250C System Selex-Gematronik

Operational 24h

Owners: 50% ARPAP, 50% Regione Liguria

Archive on DAT: only raw Polar Volume (long term)

Archive CF Liguria: rainfall fields 5/10 min. (long term)

Archive CF Liguria: CAPPI Z, Zdr 5/10 min. (30 days)

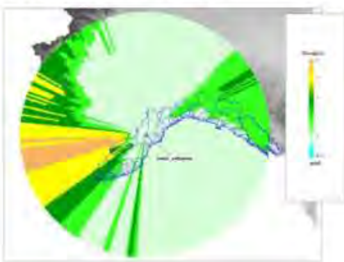

EnviSens Technologies (EST) s.r.l.
C.so Ciro Menotti 4, 10138 Torino, Italy.
Ph. +39-011 0904200 - Fax. +39-011 0904200 - www.envisens.com

Example of S-band radar

TDWR

Terminal Doppler Weather Radar

- Transmit Frequency 5.6 - 5.65 GHz
- Peak Power 250 kW
- Antenna Beamwidth < 0.55° (pencil beam)
- Pulse Width 1.1 usec
- PRF 2000 Hz (maximum)
- Range Resolution 165 meters
- Range of Observation
  - Radial Velocity 89 km
  - Reflectivity 460 km
- Maximum Unambiguous Doppler 53.6 m/sec

Colorado State University's CHILL and the National Center for Atmospheric Research's S-Pol radars

EnviSens Technologies (EST) s.r.l.
C.so Ciro Menotti 4, 10138 Torino, Italy.
Ph. +39-011 0904200 - Fax. +39-011 0904200 - www.envisens.com

Example of X-band radar

Non coherent – Non doppler – Pulsed
One polarization (Vertical)
Trasmitted power: 10 kW peak
PRF: 800 Hz (but configurable)
Pulse Duration: 400 ns (but configurable)
Antenna Gain: 34 dB – HPBW: 3.6° – 2.5° elevation
Maximun Range: 30 km
Space resolution of real time processed maps: 60 m
Time resolution for real time processed maps: 1 min

EnviSens Technologies

EnviSens Technologies (EST) s.r.l.
C.so Ciro Menotti 4, 10138 Torino, Italy.
Ph. +39-011 0904200 - Fax. +39-011 0904200 - www.envisens.com

Example of X-band weather radar network

Year: 2014

EnviSens Technologies

EnviSens Technologies (EST) s.r.l.
C.so Ciro Menotti 4, 10138 Torino, Italy.
Ph. +39-011 0904200 - Fax. +39-011 0904200 - www.envisens.com

Envisens Technologies s.r.l. (EST)

Thank you!

Eng. Marco Allegretti
marco.allegretti@polito.it

Slides prepared by: Eng. M. Allegretti, Eng. S. Bertoldo, Prof. G. Perona

EnviSens Technologies (EST) s.r.l.
C.so Ciro Menotti 4, 10138 Torino, Italy.
Ph. +39-011 0904200 - Fax. +39-011 0904200 - www.envisens.com

EnviSens Technologies

Atmospheric absorption, scattering and attenuation

COMPLETE
MSCA-ETN

HORIZON 2020

2nd Summer School on
Microphysics and Dynamics of Clouds
July 09 – 14, 2018

Eng. Marco Allegretti
marco.allegretti@polito.it

Summary

- Rain attenuation effects on communication systems
- Extinction cross section
- Scattering
- Absorption
- Attenuation

Rain attenuation effects on communication systems

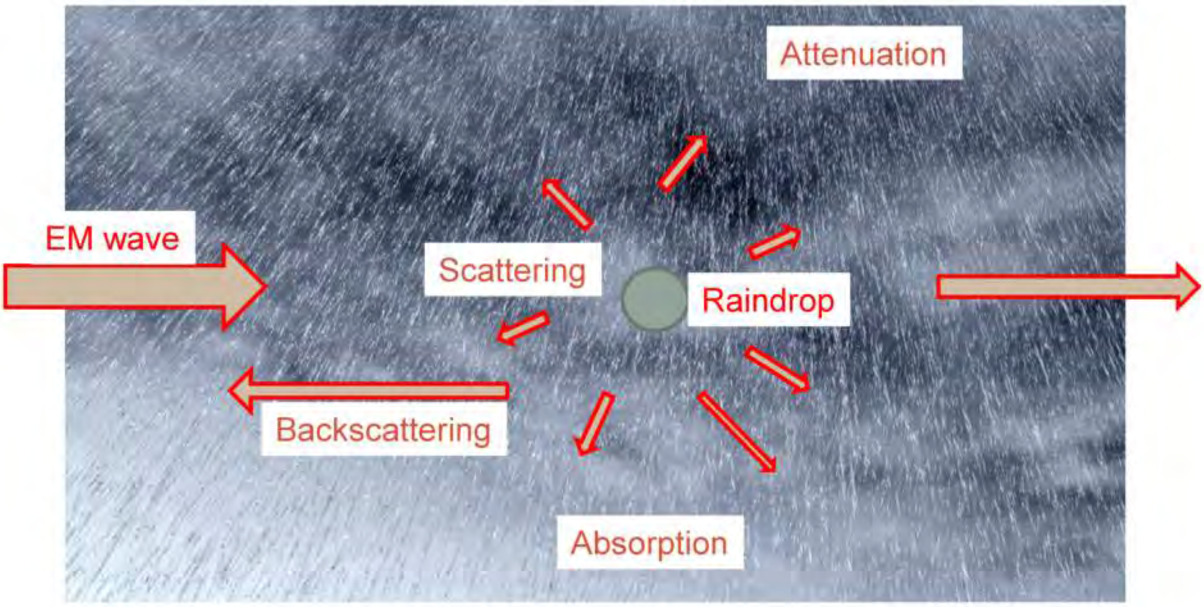

EnviSens Technologies (EST) s.r.l.
C.so Ciro Menotti 4, 10138 Torino, Italy.
Ph. +39-011 0904200 - Fax. +39-011 0904200 - www.envisens.com

Rain attenuation effects on communication systems

- In radar technology, all EM wave scattering effects of an object (target) are contained in a single parameter, the radar cross section, σ.
- RCS of an object accounts for the
  - amount of wave power intercepted by object,
  - amount of wave power reflected (scattered, not absorbed) by the object, and
  - amount of wave power directed back towards the radar.

EnviSens Technologies (EST) s.r.l.
C.so Ciro Menotti 4, 10138 Torino, Italy.
Ph. +39-011 0904200 - Fax. +39-011 0904200 - www.envisens.com

Extinction cross section - definition -

$$\sigma_{ext} = \frac{P}{\left.\frac{dP}{d\Sigma}\right|_{inc}} = 4\pi \cdot \frac{\frac{dP}{d\Omega}}{\left.\frac{dP}{d\Sigma}\right|_{inc}}$$

Extinction cross section [m^2]

Note that sometimes the *coefficient for unit of volume* are used. They are measured in [m^2/m^3].

EnviSens Technologies (EST) s.r.l.
C.so Ciro Menotti 4, 10138 Torino, Italy.
Ph. +39-011 0904200 - Fax. +39-011 0904200 - www.envisens.com

Extinction cross section - definition -

For a <u>single particle</u> we can write:

$$\sigma_{ext}=\sigma_{scat}+\sigma_{abs}$$

Where:

- σ_{ext}[m^2]: total extinction cross section, multiplied by the incident power density, gives the total power substracted from the coherent wave.
- σ_{scat}[m^2]: total extinction cross section, multiplied by the incident power density, gives the power substracted from the coherent wave by mean of scattering.
- σ_{abs}[m^2]: total extinction cross section, multiplied by the incident power density, gives the power substracted from the coherent wave by mean of absorption.

EnviSens Technologies (EST) s.r.l.
C.so Ciro Menotti 4, 10138 Torino, Italy.
Ph. +39-011 0904200 - Fax. +39-011 0904200 - www.envisens.com

Extinction cross section

What does σ_{ext} depend on ?

- Particle diameter and frequency (mainly D/λ)
- Particle complex dielectric constant ε-jσ (which in turn, in the case of water, introduces dependency on temperature and , frequency)
- Particle shape
- Polarization and elevation angle (for non spherical particles)

EnviSens Technologies (EST) s.r.l.
C.so Ciro Menotti 4, 10138 Torino, Italy.
Ph. +39-011 0904200 - Fax. +39-011 0904200 - www.envisens.com

Extinction cross section

Normalized extinction cross section in function of normalized drop diameter

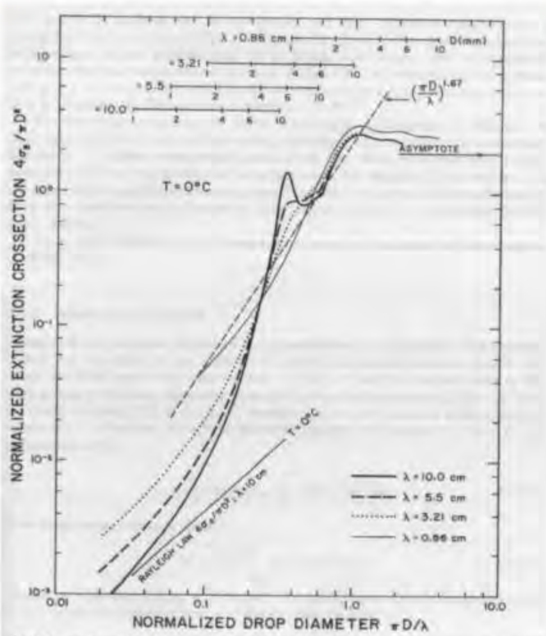

Fig. 3.4 The normalized extinction cross section versus normalized drop diameter for spherical water drops at a temperature of 0°C and at four wavelengths. (Data from Herman *et al.*, 1961.) The solid straight line is the asymptotic absorption cross section in the Rayleigh limit. The dashed straight line shows the power law that fits the data at $\lambda = 0.86$ cm (Section 8.4.2).

EnviSens Technologies (EST) s.r.l.
C.so Ciro Menotti 4, 10138 Torino, Italy.
Ph. +39-011 0904200 - Fax. +39-011 0904200 - www.envisens.com

Atmospheric efficiencies - definitions -

Absorbtion efficiency
$$\xi_{abs} = 4\chi \cdot \mathrm{Im}\{-k\} = \frac{2\pi \cdot r}{\lambda_0}\sqrt{\varepsilon_r}\,\mathrm{Im}\left\{\frac{\varepsilon_r - 1}{\varepsilon_r + 2}\right\} = \frac{\sigma_a}{\pi \cdot r^2}$$

Scattering efficiency
$$\xi_{scat} = \frac{8}{3}\chi^4 |k|^2 = \left(\frac{2\pi \cdot a}{\lambda_0}\right)^4 \frac{8}{3}\varepsilon_r^2 \left|\frac{\varepsilon_r - 1}{\varepsilon_r + 2}\right|^2 = \frac{\sigma_s}{\pi \cdot a^2}$$

Back-Scattering efficiency
$$\xi_b = \frac{\sigma_b}{\pi r^2} = 4\chi^4 |K|^2 \qquad \text{with } |n\chi| < 0.5$$

Raindrop perimeter normalized with respect to wavelength
$$\chi = \frac{(2\pi r)}{\lambda} = \frac{(2\pi r)}{\lambda_0}\sqrt{\varepsilon_r}$$

EnviSens Technologies (EST) s.r.l.
C.so Ciro Menotti 4, 10138 Torino, Italy.
Ph. +39-011 0904200 - Fax. +39-011 0904200 - www.envisens.com

Atmospheric absorption cross section

Absorbtion cross section depends on:

- Imaginary part of refraction index (n)
- the content of liquid water of the atmosphere
- the raindrop size according to the following law.

$$\xi_{abs} \propto r^3$$

EnviSens Technologies (EST) s.r.l.
C.so Ciro Menotti 4, 10138 Torino, Italy.
Ph. +39-011 0904200 - Fax. +39-011 0904200 - www.envisens.com

Atmospheric absorption

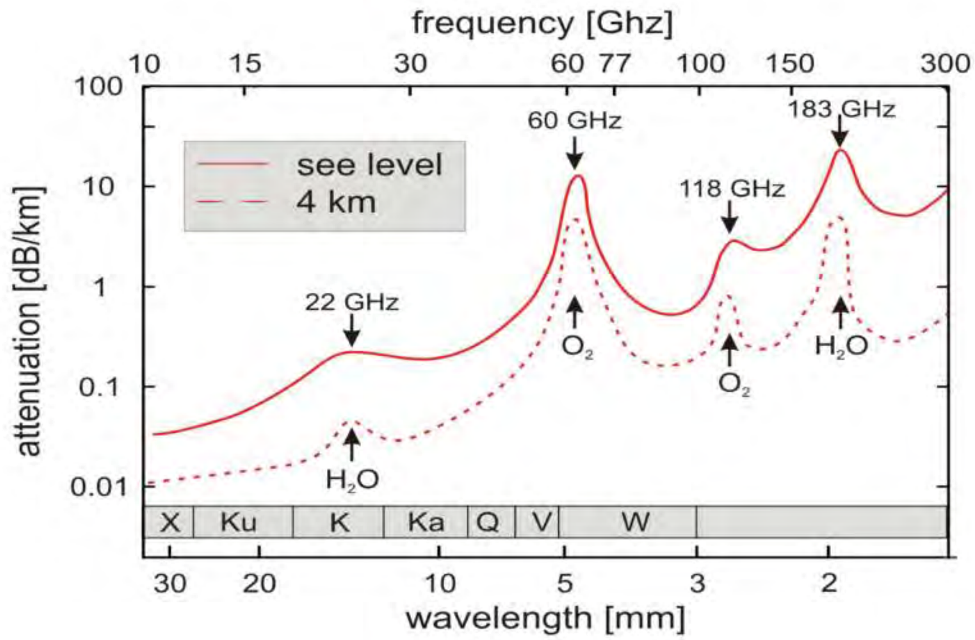

EnviSens Technologies (EST) s.r.l.
C.so Ciro Menotti 4, 10138 Torino, Italy.
Ph. +39-011 0904200 - Fax. +39-011 0904200 - www.envisens.com

Microwave & meteorology – remind –

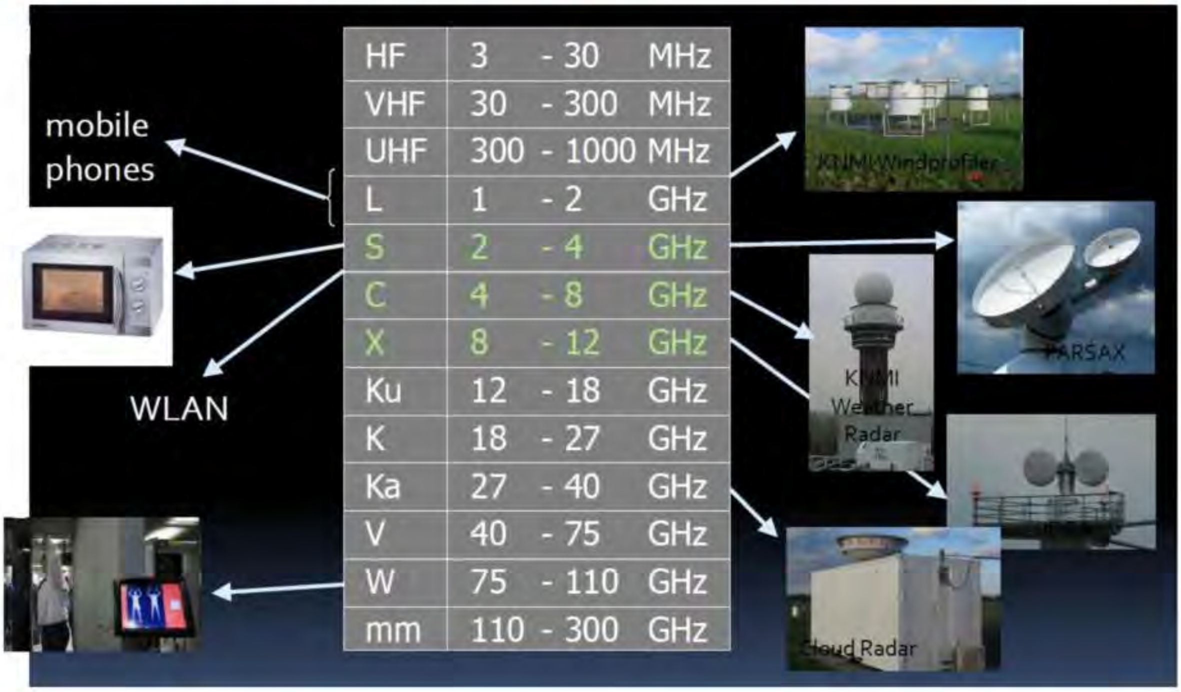

HF	3 - 30	MHz
VHF	30 - 300	MHz
UHF	300 - 1000	MHz
L	1 - 2	GHz
S	2 - 4	GHz
C	4 - 8	GHz
X	8 - 12	GHz
Ku	12 - 18	GHz
K	18 - 27	GHz
Ka	27 - 40	GHz
V	40 - 75	GHz
W	75 - 110	GHz
mm	110 - 300	GHz

EnviSens Technologies (EST) s.r.l.
C.so Ciro Menotti 4, 10138 Torino, Italy.
Ph. +39-011 0904200 - Fax. +39-011 0904200 - www.envisens.com

Atmospheric absportion

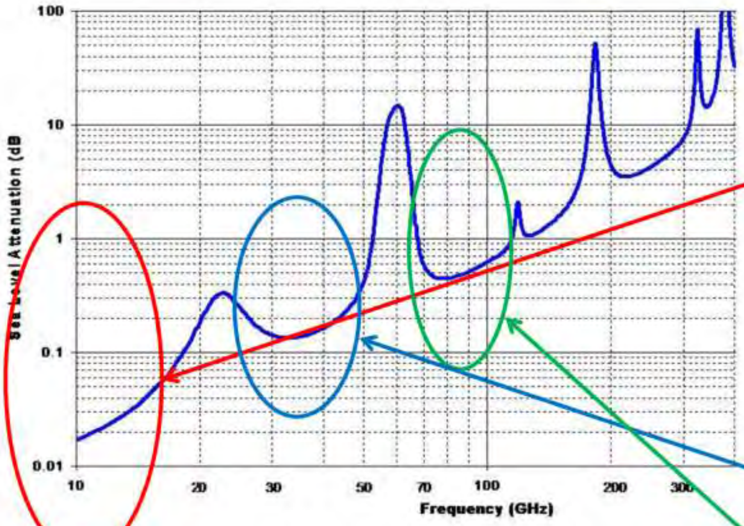

HF	3	- 30	MHz
VHF	30	- 300	MHz
UHF	300	- 1000	MHz
L	1	- 2	GHz
S	2	- 4	GHz
C	4	- 8	GHz
X	8	- 12	GHz
Ku	12	- 18	GHz
K	18	- 27	GHz
Ka	27	- 40	GHz
V	40	- 75	GHz
W	75	- 110	GHz
mm	110	- 300	GHz

EnviSens Technologies (EST) s.r.l.
C.so Ciro Menotti 4, 10138 Torino, Italy.
Ph. +39-011 0904200 - Fax. +39-011 0904200 - www.envisens.com

Atmospheric transmittance

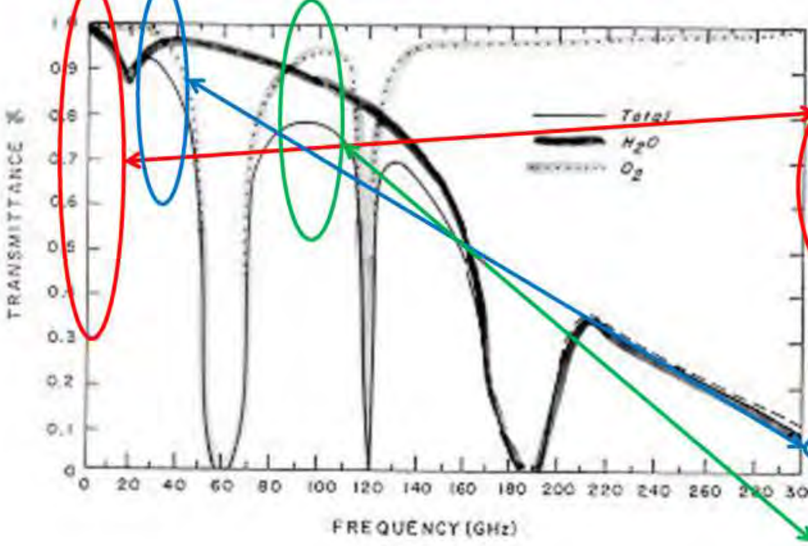

HF	3	- 30	MHz
VHF	30	- 300	MHz
UHF	300	- 1000	MHz
L	1	- 2	GHz
S	2	- 4	GHz
C	4	- 8	GHz
X	8	- 12	GHz
Ku	12	- 18	GHz
K	18	- 27	GHz
Ka	27	- 40	GHz
V	40	- 75	GHz
W	75	- 110	GHz
mm	110	- 300	GHz

EnviSens Technologies (EST) s.r.l.
C.so Ciro Menotti 4, 10138 Torino, Italy.
Ph. +39-011 0904200 - Fax. +39-011 0904200 - www.envisens.com

Attenuation

Specific attenuation α_R measured in dB/km:

$$\alpha_R = KR^a$$

If we know the coefficients for vertical and horizontal polarization (k_V, α_V and k_H, α_H), it can be shown that for an arbitrary polarization (k, α):

$$k = \{k_H + k_V + [k_H - k_V]\cos^2\vartheta\cos 2\tau\}/2$$
$$\alpha = \{k_H\alpha_H + k_V\alpha_V + [k_H\alpha_H - k_V\alpha_V]\cos^2\vartheta\cos 2\tau\}/2k$$

Where θ is the elevation angle and τ is polarization tilt (τ=45° for circular polarization)

Recommendation ITU-P.838-3 (03/05), *Specific attenuation model for rain for use in prediction method*

Attenuation

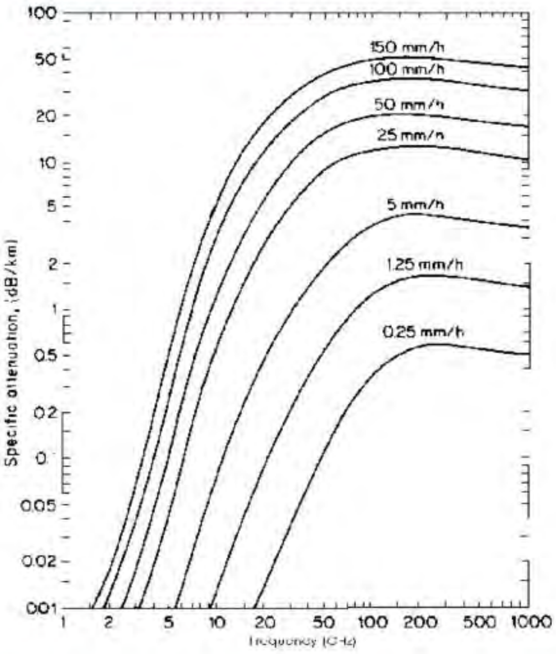

Table 4.1 *Regression coefficients for estimating the attenuation coefficients for the specific attenuation γ, where $\gamma = kR^a$ (from Table 1 of Reference 6)*

Frequency (GHz)	k_H	k_V	α_H	α_V
1	0·0000387	0·0000352	0·912	0·880
2	0·000154	0·000138	0·963	0·923
4	0·000650	0·000591	1·121	1·075
6	0·00175	0·00155	1·308	1·265
7	0·00301	0·00265	1·332	1·312
8	0·00454	0·00395	1·327	1·310
10	0·0101	0·00887	1·276	1·264
12	0·0188	0·0168	1·217	1·200
15	0·0367	0·0335	1·154	1·128
20	0·0751	0·0691	1·099	1·065
25	0·124	0·113	1·061	1·030
30	0·187	0·167	1·021	1·000
35	0·263	0·233	0·979	0·963
40	0·350	0·310	0·939	0·929
45	0·442	0·393	0·903	0·897
50	0·536	0·479	0·873	0·868
60	0·707	0·642	0·826	0·824
70	0·851	0·784	0·793	0·793
80	0·975	0·906	0·769	0·769
90	1·06	0·999	0·753	0·754
100	1·12	1·06	0·743	0·744
120	1·18	1·13	0·731	0·732
150	1·31	1·27	0·710	0·711
200	1·45	1·42	0·689	0·690
300	1·36	1·35	0·688	0·689
400	1·32	1·31	0·683	0·684

Laws and Parsons dropsize distribution [7]
Gunn and Ginzer terminal velocities [8]
Index of refraction of water at 20°C after Ray [9]
Values of k_H, k_V, α_H, and α_V for spheroidal drops [10, 11] in the range 1–150 mm/h
(Copyright © 1986 ITU, reproduced with permission)

Absorption + Attenuation

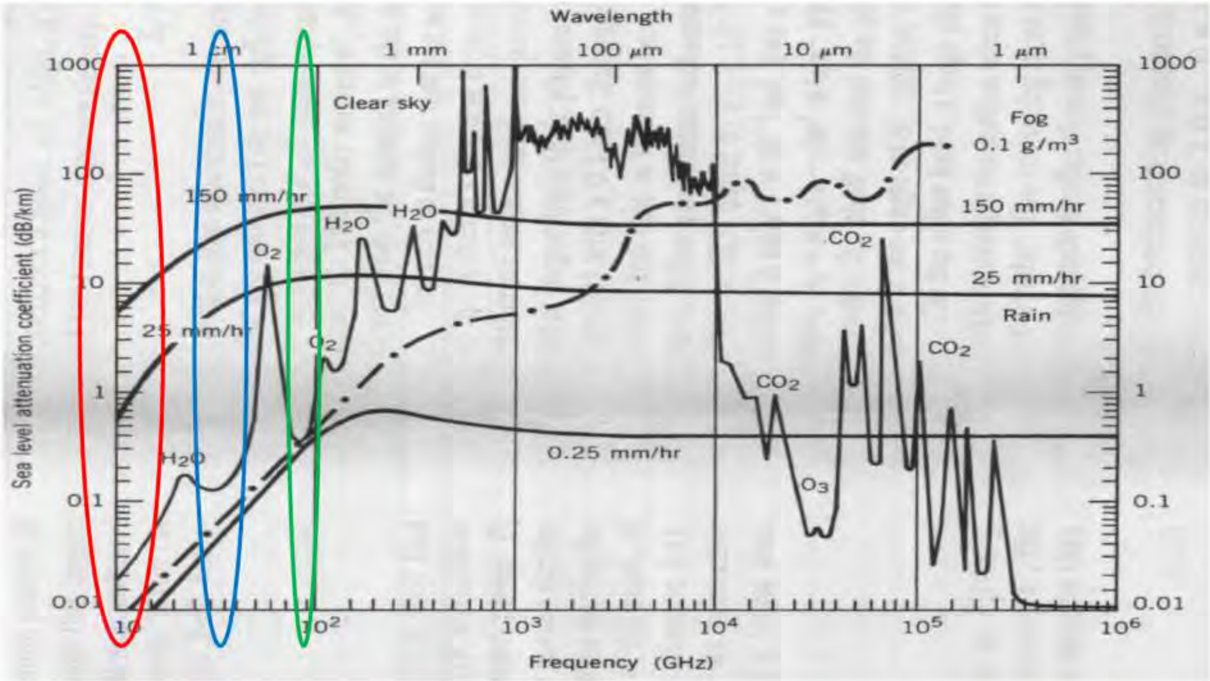

Envisens Technologies s.r.l. (EST)

Thank you!

Eng. Marco Allegretti
marco.allegretti@polito.it

Slides prepared by: Eng. M. Allegretti, Eng. S. Bertoldo, Prof. G. Perona

Radar equation for volume scattering
Radar equation for meteorological targets
Rain estimation

COMPLETE
HORIZON 2020

MSCA-ETN

2nd Summer School on
Microphysics and Dynamics of Clouds
July 09 – 14, 2018

Eng. Marco Allegretti
marco.allegretti@polito.it

Summary

- Radar equation for point target
- Radar equation for volumetric scattering
- Radar equation for meteorological targets
- Radar reflectivity factor (Z)
- Rain estimation
- Z-R equation

Radar equation for point target

Monostatic radar

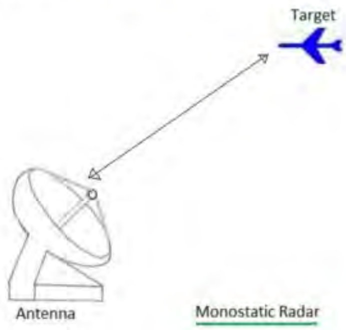

$$P_{RX} = \frac{P_{TX} \cdot G_{TX} \cdot A_{TX}}{\left(4\pi \cdot r^2\right)^2} \cdot \sigma$$

Remember that the radar resolution for a pulsed radar, with pulse druration equal to τ is:

$$\Delta r = \frac{c\tau}{2}$$

Radar equation for volumetric target

Given the return power from a volume of scatterers within the radar beam,

$$P_r = \frac{P_t G^2 \lambda^2 \sigma}{(4\pi)^3 R^4}$$ **Traditional Radar Range Equation**

the total radar cross section, s, associated with scatterers contained in a volume V can be expressed as

$$\sigma = \eta V$$

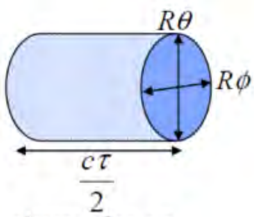

where

$$\eta = \frac{1}{\Delta V} \sum_{i=1}^{N} \sigma_i$$

is the backscattering cross-section per unit volume, and the volume for an elliptically shaped beam can be approximated as

$$V \approx \pi\left(R\frac{\theta}{2} R\frac{\phi}{2}\frac{C\tau}{2}\right)$$

EnviSens Technologies (EST) s.r.l.
C.so Ciro Menotti 4, 10138 Torino, Italy.
Ph. +39-011 0904200 - Fax. +39-011 0904200 - www.envisens.com

Radar equation for volumetric target

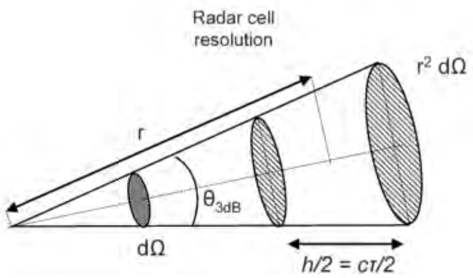

Let us assume that all EM energy is insed a cone: it is possible to exploit the relation between the angle θ_{3dB} and the solid angle Ω:

$$d\Omega = \frac{\pi}{4}\theta_{3dB}^2$$

The radar volumetric cell is therefore:

$$V = \frac{h}{2} r^2 d\Omega = \frac{\pi}{4}\theta_{3dB}^2 r^2 \frac{c\tau}{2}$$

Assuming the radar operating with a ideal «top hat» antenna

EnviSens Technologies (EST) s.r.l.
C.so Ciro Menotti 4, 10138 Torino, Italy.
Ph. +39-011 0904200 - Fax. +39-011 0904200 - www.envisens.com

Radar equation for volumetric target

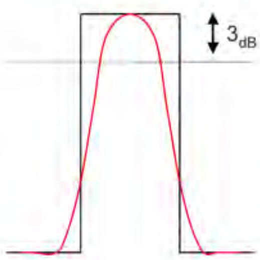

Ideal «top hat» antenna and «gaussian shape» antenna

Let us consider a «gaussian shape» antenna

The volumetric radar cell is: $V = \dfrac{\pi \vartheta_{3dB}\phi_{3dB}}{8\ln 2} r^2 \dfrac{c\tau}{2}$

EnviSens Technologies (EST) s.r.l.
C.so Ciro Menotti 4, 10138 Torino, Italy.
Ph. +39-011 0904200 - Fax. +39-011 0904200 - www.envisens.com

Radar equation for volumetric target

The radar equation becomes:

$$P_{RX} = P_{TX} \cdot \frac{1}{(4\pi)^3 r^4} \cdot G_{TX}^2 \cdot \lambda^2 \cdot \sigma_0 \cdot \int dV$$

$$P_{RX} = P_{TX} \cdot \frac{1}{(4\pi)^3 r^4} \cdot G_{TX}^2 \cdot \lambda^2 \cdot \sigma_0 \cdot V$$

$$P_{RX} = P_{TX} \cdot \frac{1}{(4\pi)^3 r^4} \cdot G_{TX}^2 \cdot \lambda^2 \cdot \sigma_0 \cdot \frac{\pi \vartheta_{3dB} \phi_{3dB}}{8 \ln 2} r^2 \frac{c\tau}{2}$$

$$\boxed{P_{RX} = \left(\frac{P_{TX} \; G_{TX}^2 \lambda^2 \theta_{3dB} \phi_{3dB} c\tau}{1024 \cdot \pi^2 \cdot \ln 2 \cdot r^2} \right) \sigma_0}$$

(σ_0 is the RCS, Radar Cross Section, of the elementary drop within the radar volumetric cell)

EnviSens Technologies (EST) s.r.l.
C.so Ciro Menotti 4, 10138 Torino, Italy.
Ph. +39-011 0904200 - Fax. +39-011 0904200 - www.envisens.com

Radar equation: consideration

- **Point target**: P_{RX} depends on r^{-4}

$$P_{RX} = \frac{P_{TX} G_{TX}^2 \lambda^2}{(4\pi)^3 r^4} \sigma_0$$

- **Surface target**: P_{RX} depends on r^{-3}

- **Volumetric target**: P_{RX} depends on r^{-2}

$$P_{RX} = \left(\frac{P_{TX} \; G_{TX}^2 \lambda^2 \theta_{3dB} \phi_{3dB} c\tau}{1024 \cdot \pi^2 \cdot \ln 2 \cdot r^2} \right) \sigma_0$$

EnviSens Technologies (EST) s.r.l.
C.so Ciro Menotti 4, 10138 Torino, Italy.
Ph. +39-011 0904200 - Fax. +39-011 0904200 - www.envisens.com

Radar equation for meteorological targets

- Inside a radar volume are present a huge number of radar targets.
- Total power received by radar is the convolution of single scatter signal.

$$P_{tot} = \sum_{V} P_{\text{singlescatter}}$$

- Single scatter signal is proportional to its backscattering section

$$P_{tot} \propto \sum_{V} \sigma_B$$

EnviSens Technologies (EST) s.r.l.
C.so Ciro Menotti 4, 10138 Torino, Italy.
Ph. +39-011 0904200 - Fax. +39-011 0904200 - www.envisens.com

Radar equation for meteorological targets

$$\sum_{V} \sigma_B = V\left(\sum_{V} \frac{\sigma_B}{V}\right) = V\eta$$

Radar reflectivity

$$\eta = \sum_{V} \frac{\sigma_B}{V}$$

Mean backscattering section over radar volume

$[m^2\ m^{-3}]$($o\ cm^{-1}$)

EnviSens Technologies (EST) s.r.l.
C.so Ciro Menotti 4, 10138 Torino, Italy.
Ph. +39-011 0904200 - Fax. +39-011 0904200 - www.envisens.com

Radar reflectivity factor (Z)

Note that Z is an intrinsic property of the distribution of drops under analysis (if Rayleigh's conditions are respected). It does not depend on the wavelength used. On the other hand η depend on the frequency used.

If we consider the DSD (Drop size Distribution):

$$Z = \Sigma \, n_i \, D_i^6$$

Where n_i is the drop concentration of the i^esima category
Z [mm^6 / m^3], represent the drop contrantation in the volume unit as a function of drop diameter.

Please note the difference between *radar reflectivity* and *radar reflectivity factor*

Be aware that in the day-to-day practice these two terms are used as synonymous.

EnviSens Technologies (EST) s.r.l.
C.so Ciro Menotti 4, 10138 Torino, Italy.
Ph. +39-011 0904200 - Fax. +39-011 0904200 - www.envisens.com

Backscattering from meteorological particles

When the ratio of the sphere radius, a, to the wavelength, l, is small

$$\frac{2\pi a}{\lambda} << 1$$

the radar cross section associated with the i-th scatterer can be expressed as

$$\sigma_i = \frac{\pi^5 |K|^2 D_i^6}{\lambda^4}$$

where D_i is the drop diameter usually given in millimeters and K is defined as

$$K = \frac{m^2 - 1}{m^2 + 1}$$

where m is the complex index of refraction

$|K|^2 \approx 0.93$ Water

$|K|^2 \approx 0.197$ Ice

wavelengths between **3 cm** and **10 cm** and temperatures between **0°** and **20°** C

EnviSens Technologies (EST) s.r.l.
C.so Ciro Menotti 4, 10138 Torino, Italy.
Ph. +39-011 0904200 - Fax. +39-011 0904200 - www.envisens.com

Backscattering from meteorological particles

Strong dependence to λ and particle dimension

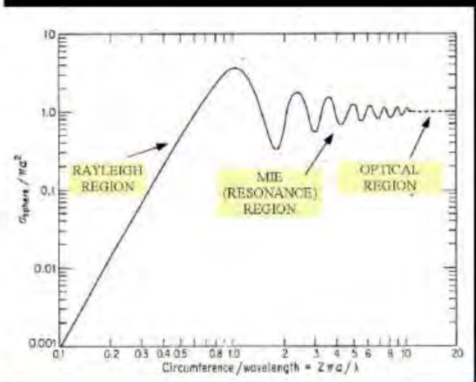

- d << λ ⇒ Rayleigh Regime:

$$\sigma_b = \frac{\lambda^2 \alpha^6}{\pi} |K|^2$$

- d ≈ λ ⇒ Mie Regime:
  σ very complicated calculation
- d >> λ ⇒ Optic region:
  σ ≈ geometric section

Rayleigh limit :

S band (10 cm)	D < 7 mm
C band (5 cm)	D < 3.5 mm
X band (3 cm)	D < 2.1 mm
K band (1 cm)	D < 0.7 mm
W band (0.4 cm)	D < 0.25 mm

S band radar - roughly always in Raiyleigh (except for hailstones).

Higher frequency radar are in Mie Region for rainDrops.

Backscattering from meteorological particles

Radar equation for meteorological target (Probert-Jones Equation)

$$P_r = \left(\frac{P_t \pi^3 G_0^2 \theta_{3dB} \phi_{3dB} c\tau}{\lambda^2 1024 \ln 2} \right) L^2 |K|^2 \frac{Z}{r^2} \longrightarrow P_r \cong Konst \frac{Z}{r^2}$$

Konst = Radar Constant

Z = Radar Reflectivity Factor due to the radar cell [$mm^6 mm^{-3}$].

The radar equation in meteorology

By J. R. PROBERT-JONES
*Meteorological Office, Bracknell, Berks.**

(Manuscript received 29 January 1962; in revised form 18 June 1962)

SUMMARY

While meteorologists can obtain much useful information by using radar in a qualitative manner, great benefit can be derived by obtaining quantitative measurements. However, these measurements have been found, in general, to be below values calculated from radar theory by a factor of between two and five, and there has been no satisfactory explanation for this discrepancy. In this paper, the radar equation for a meteorological target is derived, particular attention being devoted to the effect of the shape of the main lobe of the beam, and of the radiation outside it. It is shown that previous theoretical expressions for both the gain and the echoing volume have been too large, and hence that previous equations overestimated the received power. The present equation gives good agreement with all the experimental data.

Backscattering from meteorological particles

Radar equation for meteorological target (Probert-Jones Equation)

$$P_r = \left(\frac{P_t \pi^3 G_0^2 \theta_{3dB} \phi_{3dB} c\tau}{\lambda^2 1024 \ln 2} \right) L^2 |K|^2 \frac{Z}{r^2} \longrightarrow P_r \cong Konst \frac{Z}{r^2}$$

Note that this formulation is valid only under these conditions:

- Rayleigh approximation
- The beam is uniformly filled by targets
- The targets are isotropically distributed in the volume

EnviSens Technologies (EST) s.r.l.
C.so Ciro Menotti 4, 10138 Torino, Italy.
Ph. +39-011 0904200 - Fax. +39-011 0904200 - www.envisens.com

Backscattering from meteorological particles

Radar equation for meteorological target (Probert-Jones Equation)

$$P_r = \left(\frac{P_t \pi^3 G_0^2 \theta_{3dB} \phi_{3dB} c\tau}{\lambda^2 1024 \ln 2} \right) L^2 |K|^2 \frac{Z}{r^2} \longrightarrow P_r \cong Konst \frac{Z}{r^2}$$

Z is measured in $\frac{mm^6}{m^3}$

To obtain coherent muesurments unit it is necessary to multiply by 10^{-18} the equation.

Usually:

$dBZ = 10 \log_{10}(Z/Z_0)$,

$Z_0 = 1\ mm^6 m^{-3}$

E.g. "0 dBZ" = "1 mm^6m^{-3}"

EnviSens Technologies (EST) s.r.l.
C.so Ciro Menotti 4, 10138 Torino, Italy.
Ph. +39-011 0904200 - Fax. +39-011 0904200 - www.envisens.com

But…

Drop Size Distributions (DSDs)

Normalized Logarithmic Distribution

$$N(D) = \frac{N_T}{\sqrt{2\pi}\, D \ln\sigma} \exp - \left(\frac{\ln^2\left(\frac{D}{D_g}\right)}{2 \ln^2 \sigma} \right)$$

Modified Gamma Distribution

$$N(D) = N_0 D^{\mu} e^{-\Lambda D}$$

Marshall – Palmer Distribution (MP)

$$N(D) = 8000\, e^{-D\left(4{,}1 R^{-0{,}21}\right)}$$

$$[N(D)] = \frac{N}{m^3 mm}$$

Rain rate (R)

$$R = \frac{\pi}{6} \int_{D\,min}^{D\,max} N(D)\, D^3\, v(D)\, dD$$

$$[R] = \frac{m}{s} \propto \frac{mm}{h}$$

EnviSens Technologies (EST) s.r.l.
C.so Ciro Menotti 4, 10138 Torino, Italy.
Ph. +39-011 0904200 - Fax. +39-011 0904200 - www.envisens.com

But…

Drop Size Distributions (DSDs)

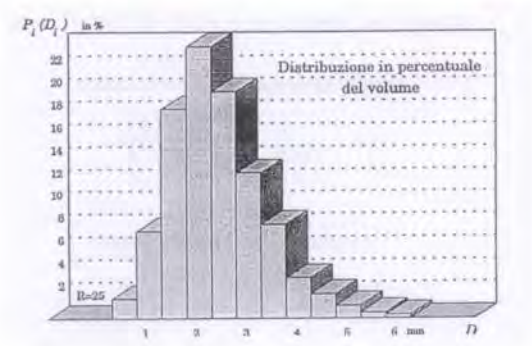

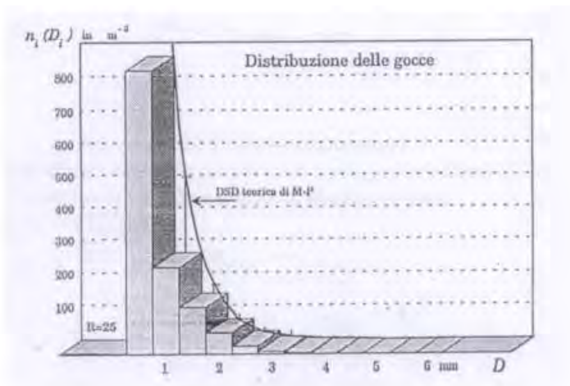

EnviSens Technologies (EST) s.r.l.
C.so Ciro Menotti 4, 10138 Torino, Italy.
Ph. +39-011 0904200 - Fax. +39-011 0904200 - www.envisens.com

And in addition…

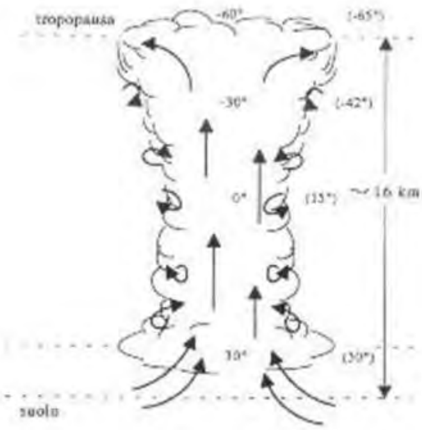

Raindrops characteristics

Diametro mm	Velocità m/s
0,5	2,10
1,0	3,90
1,5	5,30
2,0	6,40
2,5	7,30
3,0	7,90
3,5	8,35
4,0	8,70
4,5	9,00
5,0	9,20
5,5	9,35
> 6,0	9,50

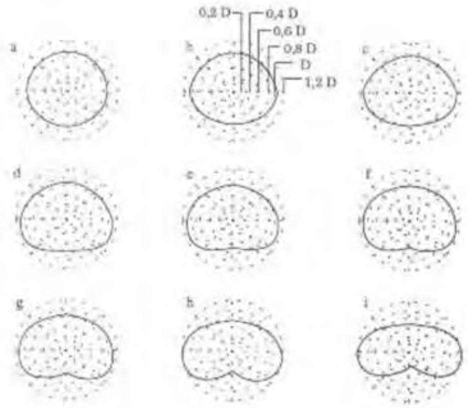

EnviSens Technologies (EST) s.r.l.
C.so Ciro Menotti 4, 10138 Torino, Italy.
Ph. +39-011 0904200 - Fax. +39-011 0904200 - www.envisens.com

Rain estimation: history

1940s post-WWII

- J. Stewart Marshall
  - Met Walter Palmer while working in Ottawa
- Stormy Weather Group focused on precipitation and cloud microphysics
- Investigation of Z – R relationships
  - Wexler and Swingle (1947): "Radar storm detection"
  - Marshall et al. (1947): "Measurement of rainfall by radar"
  - Marshall and Palmer (1948): "The distribution of raindrops with size"
- Marshall and Palmer (1948) seminal work in the field

EnviSens Technologies (EST) s.r.l.
C.so Ciro Menotti 4, 10138 Torino, Italy.
Ph. +39-011 0904200 - Fax. +39-011 0904200 - www.envisens.com

Rain estimation: history

1940s post-WWII

- More on Marshall-Palmer distribution and Z – R relationships
  - $Z = 200 * R^{1.6}$ (Marshall and Palmer 1948)
  - "It may be possible therefore to determine with useful accuracy the intensity of rainfall at a point quite distant (say 100 km) by the radar echo from that point."
  - Many other researchers suspicious of their computations due to simplicity
  - Other papers like Twomey (1953), Imai et al. (1955), Atlas and Chmela (1957), and Fujiwara (1960, 1965) derived other relationships in which reflectivity for a given rain rate differed by up to 38%, but they also remarked that there were physical explanations for the differences; could choose a relationship based on physical explanation and for a particular situation

Z-R equation

AUGUST 1948 SHORTER CONTRIBUTIONS 165

SHORTER CONTRIBUTIONS

THE DISTRIBUTION OF RAINDROPS WITH SIZE

By J. S. Marshall and W. McK. Palmer[1]

McGill University, Montreal

(Manuscript received 26 January 1948)

$$\boxed{Z_{[mm^6 m^{-3}]} = a \cdot R^b}$$

R = Rainfall rate [mm/h].

a and ***b*** depends on the precipitation type

(**Marshall and Palmer Equation or Z-R equation**, 1948)

EnviSens Technologies (EST) s.r.l.
C.so Ciro Menotti 4, 10138 Torino, Italy.
Ph. +39-011 0904200 - Fax. +39-011 0904200 - www.envisens.com

Z-R equation

The general model can be expressed as

$$Z = aR^b$$

Researchers have collected data from many sites around the world and under different atmospheric conditions in order to define the parameters "a" and "b"

Battan[1] list 69 different models

Stratiform rain:	$Z = 200\ R^{1.6}$
Orographic rain:	$Z = 31\ R^{1.71}$
Thunderstorm:	$Z = 486\ R^{1.37}$
Snow	$Z = 2000R^2$

1 Battan, Louis J., Radar Observation of the Atmosphere, revised edition, The University of Chicago Press, Chicago 1973.

EnviSens Technologies (EST) s.r.l.
C.so Ciro Menotti 4, 10138 Torino, Italy.
Ph. +39-011 0904200 - Fax. +39-011 0904200 - www.envisens.com

Z-R equation: some examples…

Reference	Precipitation type	a	b
Joss and Waldvogel (1990) [1]	Stratiform	300	1.6
Rosenfeld et. al. (1993) [2]	Tropical Rain	250	1.2
Marshal and Palmer (1948) [3]	Stratiform	200	1.6
Fujiwara (1965) [4]	Thunderstorm	486	1.37

1] J. Joss and A. Waldvogel (1990), *Precipitation measurement and hydrology*, In Radar in Meteorology, Ed. D. Atlas, Am. Met. Society, pp. 577-606.

[2] D. Rosenfeld, D. B. Wolff and D. Atlas, *General probability matched relations between radar reflectivity and rain rate*, Journal of Applied Meteorology, Vol. 32, No. 1, pp. 50 – 72, 1993

[3] Marshall, J. and W. Palmer, (1948), *The distribution of raindrops with size*, Journal of Meteorology, Vol. 5, pp. 165-166

[4] M. Fujiwara (1965), *Raindrop-size distribution from individual storms*, J. Atmos. Sci., 22, 585–59.

EnviSens Technologies (EST) s.r.l.
C.so Ciro Menotti 4, 10138 Torino, Italy.
Ph. +39-011 0904200 - Fax. +39-011 0904200 - www.envisens.com

Z-R equation: common reference Z levels

Level	Rain Fall Rate (mm/hr)	Reflectivity dBz	Category
1	0.49 to 2.7	18 to <30	Light Mist
2	2.7 to 13.3	30 to <41	Moderate
3	13.3 to 27.3	41 to < 46	Heavy
4	27.3 to 48.6	46 to < 50	Very Heavy
5	48.6 to 133.2	50 to < 57	Intense
6	133.2 and greater	57 and above	Extreme

EnviSens Technologies (EST) s.r.l.
C.so Ciro Menotti 4, 10138 Torino, Italy.
Ph. +39-011 0904200 - Fax. +39-011 0904200 - www.envisens.com

Z-R equation: comments

Single point estimates of rain rate using reflectivity (Z-R models)

- exhibit 50% to 100% error

Temporal and spatial averaging provides adequate rain fall estimates

- hydrology, flood forecasting, and agriculture

It is difficult to determine precipitant type from a single polarization reflectivity measurement

- in some cases, hail can be associated with large reflectivity measurements

Systems employing orthogonal polarizations have been shown to provide

- Differential reflectivity – ratio of return from horizontal and vertical polarizations
  - Used to identify hail & estimate hail size
- Differential phase change with range between horizontal and vertical polarizations
  - Provides better estimates of rainfall rates

EnviSens Technologies (EST) s.r.l.
C.so Ciro Menotti 4, 10138 Torino, Italy.
Ph. +39-011 0904200 - Fax. +39-011 0904200 - www.envisens.com

Sensitivity for weather radars

Usually expressed as:

- *SNR* [dB]
- *Z* [dBZ] at a certain distance *r* [km]

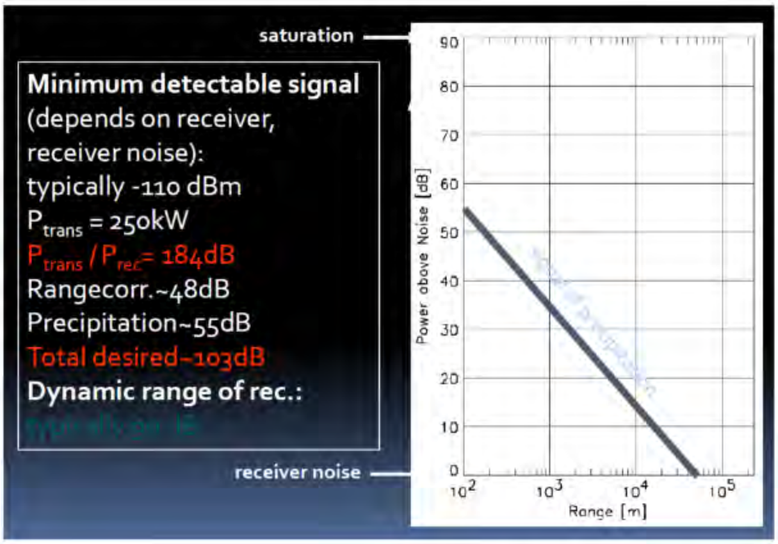

Example of operational C-band radar

EnviSens Technologies (EST) s.r.l.
C.so Ciro Menotti 4, 10138 Torino, Italy.
Ph. +39-011 0904200 - Fax. +39-011 0904200 - www.envisens.com

Radar Z maps: example 1

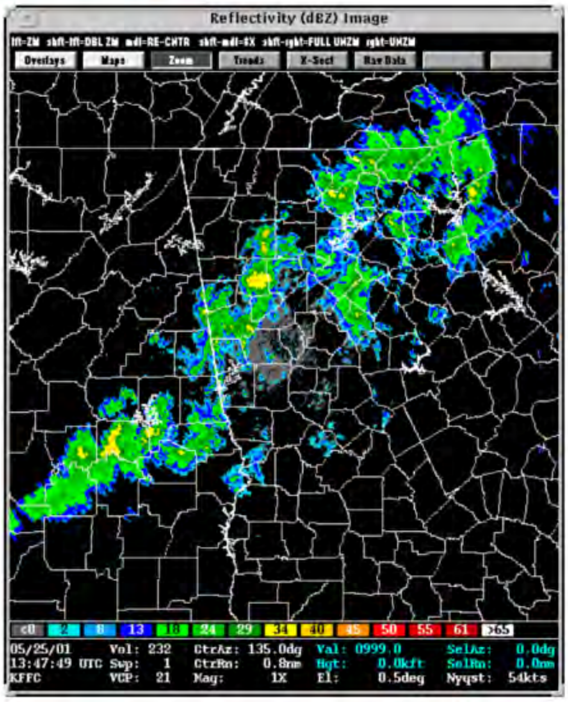

EnviSens Technologies (EST) s.r.l.
C.so Ciro Menotti 4, 10138 Torino, Italy.
Ph. +39-011 0904200 - Fax. +39-011 0904200 - www.envisens.com

Radar Z maps: example 2

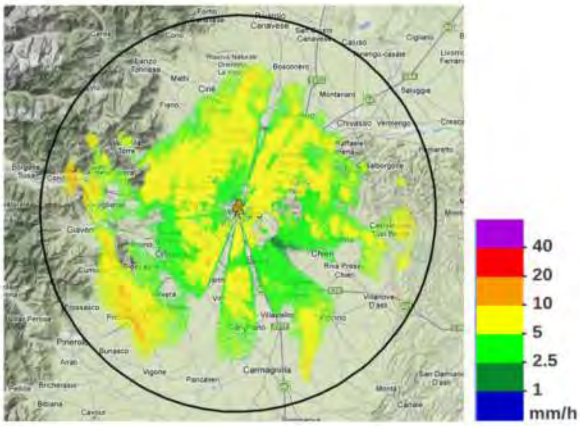

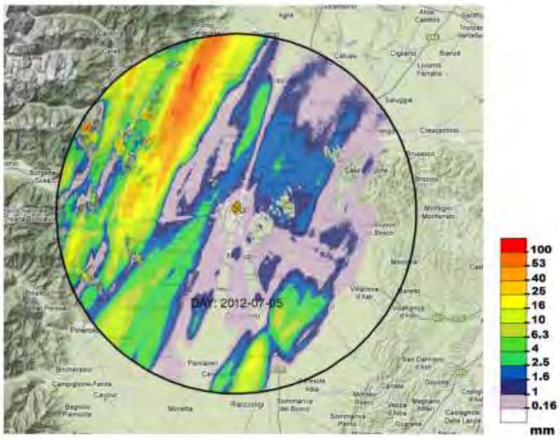

Envisens Technologies s.r.l. (EST)

Thank you!

Eng. Marco Allegretti
marco.allegretti@polito.it

Slides prepared by: Eng. M. Allegretti, Eng. S. Bertoldo, Prof. G. Perona

HORIZON 2020

COMPLETE

Bavarian Research Alliance

COMPLETE Summer School Day 6

EU Proposal Writing and Management of European Projects

Andreas Blume

Competent Support for Excellent Research in Bavaria, Europe and the World

---

Bavarian Research Alliance

Agenda

- European Funding Programmes for Research and Innovation
- Project Development and Proposal Writing
- Project Management and Dissemination

Introductory Round

European Funding Programmes for Research and Innovation

Bavarian Research Alliance

- **Horizon 2020**
- *(ERA-Nets)*
- *(Joint Programming Initiatives)*
- *(Eureka Eurostars)*

Bavarian Research Alliance

What do you imagine about an EU-R&I-Project?

SMARTER TOGETHER

Post bettervest bwsg Fraunhofer GOPA HESPUL kelag Wärme Algoé City of Vienna energycities GRANDLYON SECURITAS SIEMENS SYCUBE TUM TOSHIBA Leading Innovation University of St.Gallen WIENER STADTWERKE sunliquid® FP7

CLARIANT

IBB Netzwerk GmbH

ExportHungary We generate business

Bavarian Research Alliance

ENERGIE INSTITUT an der Johannes Kepler Universität Linz

© fotolia

Why EU projects?

© fotolia

© fotolia

Why EU projects?

Bavarian Research Alliance

EU Project: What are the benefits? (I)

- Realisation of your own project idea
- Acquiring third party funding and ongoing employment
- Positioning in international networks
- Access to third party knowledge and practices

Bavarian Research Alliance

EU Project: What are the benefits? (II)

- Insight in other fields of research
- Synergies with project partners
- EU-projects attract further co-operations and projects
- International visibility and image

© fotolia

EU / International

or

National / regional?

© fotolia

Requirements
and Challenges

© fotolia

Bavarian Research Alliance

Requirements (I)

- Inventive and novel idea that fits perfectly to the call requirements
- Explicit European added value
- Established partnership network
- Sufficient time and patience from the application to the project start

Bavarian Research Alliance

Requirements (II)

- Sound financial condition, i.e. companies
- Potential to pre-finance project activities to an certain extend
- Comply with programme provisions (e.g. reporting, review, audit etc)
- Compentency in international and interdisciplinary collaboration

Challenges, before and during projects (I)

- Work out an “interesting” proposal
- Time constraints → time management
- Find suitable and reliable project partners
- Accurate definition of work tasks (also between partners)
- Budgetary issues

Challenges, before and during projects (II)

- Formatting of the proposal
- Intellectual property (IPR)
- Understand Grant Agreement and Consortium Agreement
- Changes in the work plan (Amendment)

How has EU Research and Innovation funding evolved over recent years?

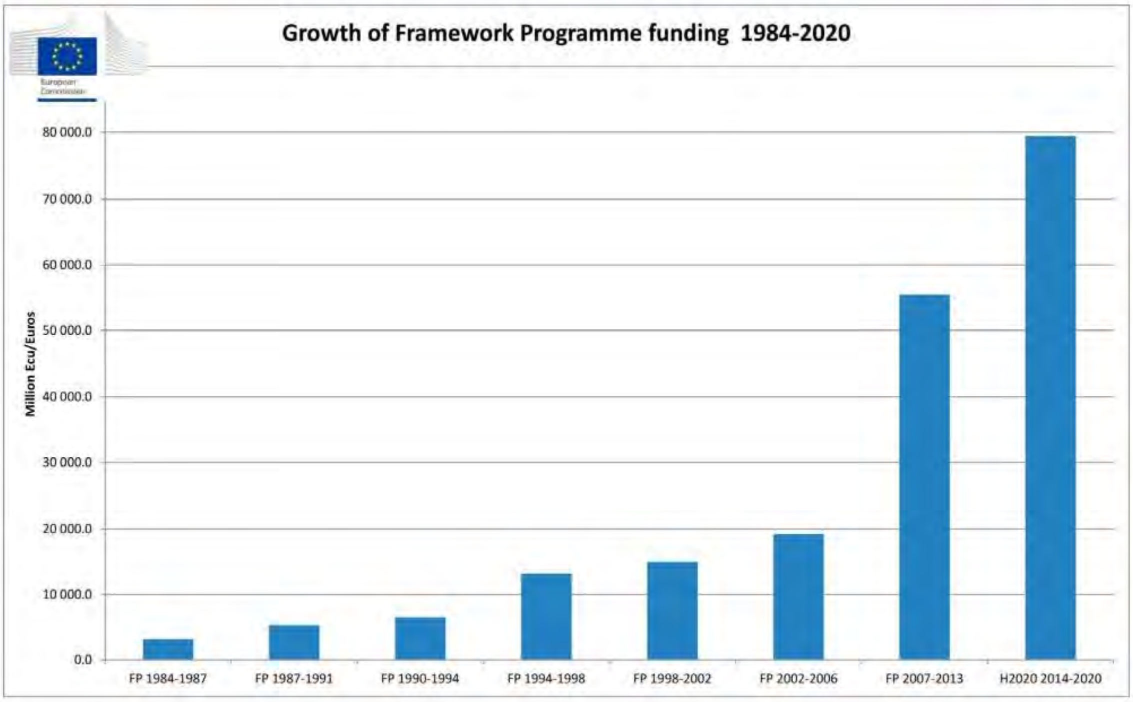

(c) European Union 2013

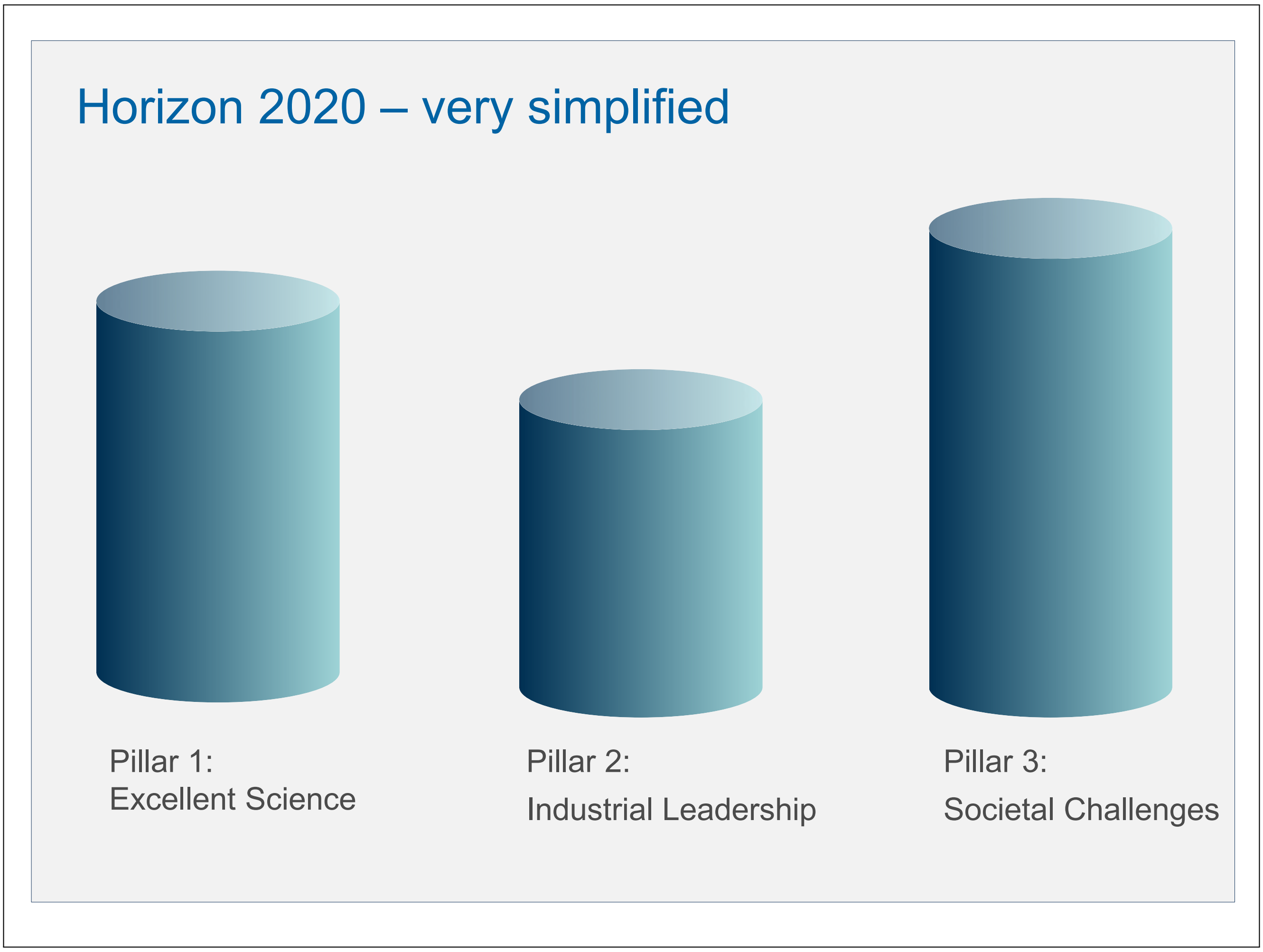
Horizon 2020 – very simplified
Pillar 1:
Excellent Science
Pillar 2:
Industrial Leadership
Pillar 3:
Societal Challenges

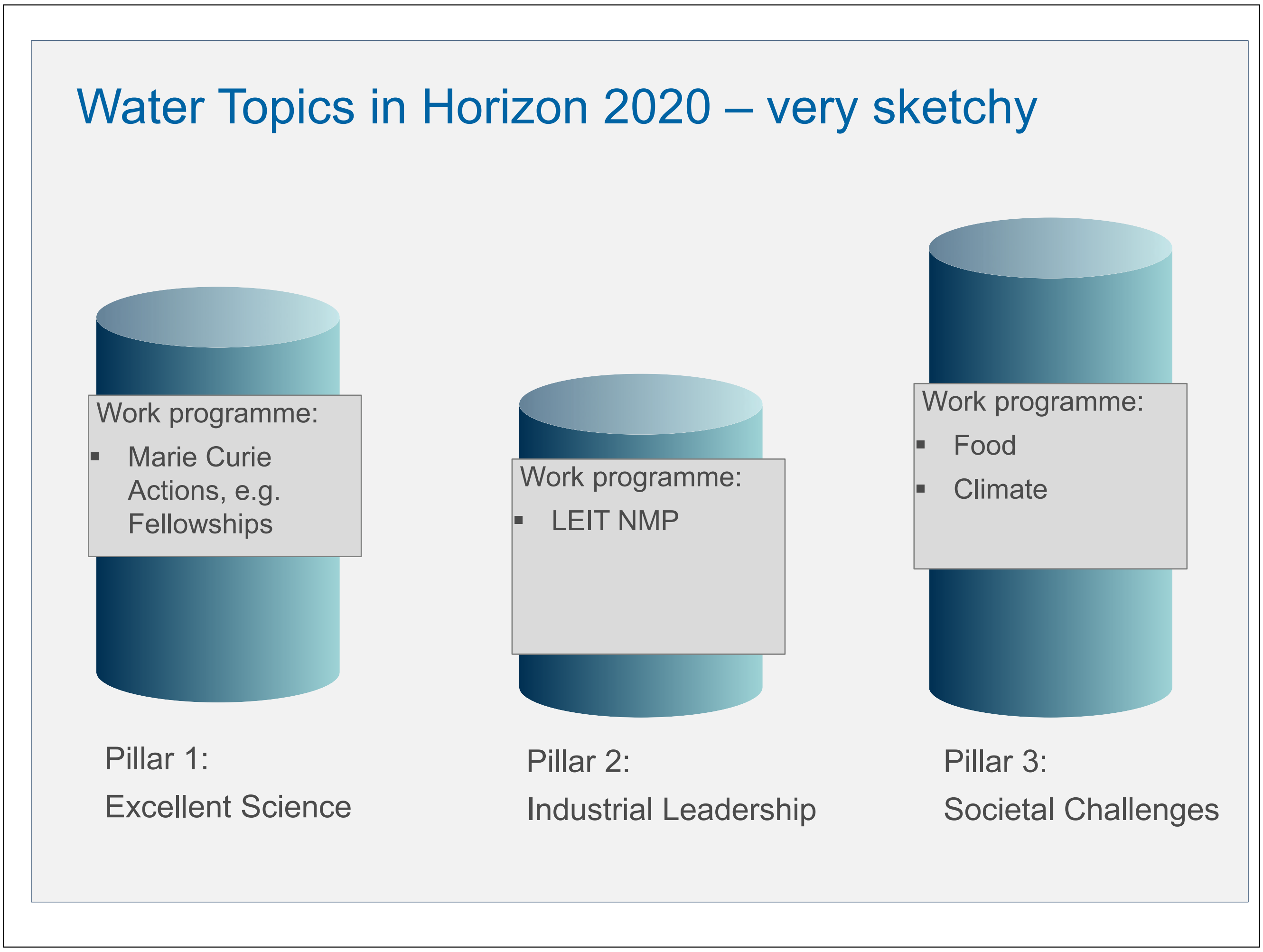
Water Topics in Horizon 2020 – very sketchy
Work programme:
Marie Curie Actions, e.g. Fellowships
Work programme:
LEIT NMP
Work programme:
Food
Climate
Pillar 1:
Excellent Science
Pillar 2:
Industrial Leadership
Pillar 3:
Societal Challenges

Excellent Science	Industrial Leadership	Societal Challenges	Cross Cutting Issues
European Research Council (ERC)	Leadership in Enabling and Industrial Technologies (LEIT) ▪ Information and Communication Technologies (ICT) ▪ Nanotechnologies ▪ Biotechnologies ▪ New Materials ▪ Innovative Manufacturing ▪ Space	Challenges: ▪ Health, Demographic Change and Wellbeing ▪ Food Security, Sustainable Agriculture, Forestry, marine & maritime research and Fishery, Bio-economy ▪ Secure, Clean and Efficient Energy ▪ Smart, Green and Integrated Transport ▪ Climate action, environment, resource efficiency and raw materials ▪ Inclusive, innovative and reflective societies ▪ Secure Societies	European Institute of Innovation and Technology (EIT)
Marie Skłodowska-Curie actions (researcher mobility)	Access to Risk Finance		Joint Research Centre (JRC)
Future & Emerging Technologies (FET)	Innovation in SMEs		Joint Technology Initiatives (JTI)
Research Infrastructures (RI)			Joint Progamme Planning (JPI)
			Science with and for Society

Bavarian Research Alliance

Types of Actions (collaborative projects)

- RIA – **R**esearch and **I**nnovation **A**ction
- IA – **I**nnovation **A**ction
- CSA – **C**oordination and **S**upport **A**ction

→At least 3 different Member States or Associated countries per project

Project Development and Proposal Writing

- Pathways to a successful proposal
- Proposal basics
- Organisation of development/writing
- How to find partners and consortium formation
- Budget, legal and financial rules

Pathways to a successful proposal

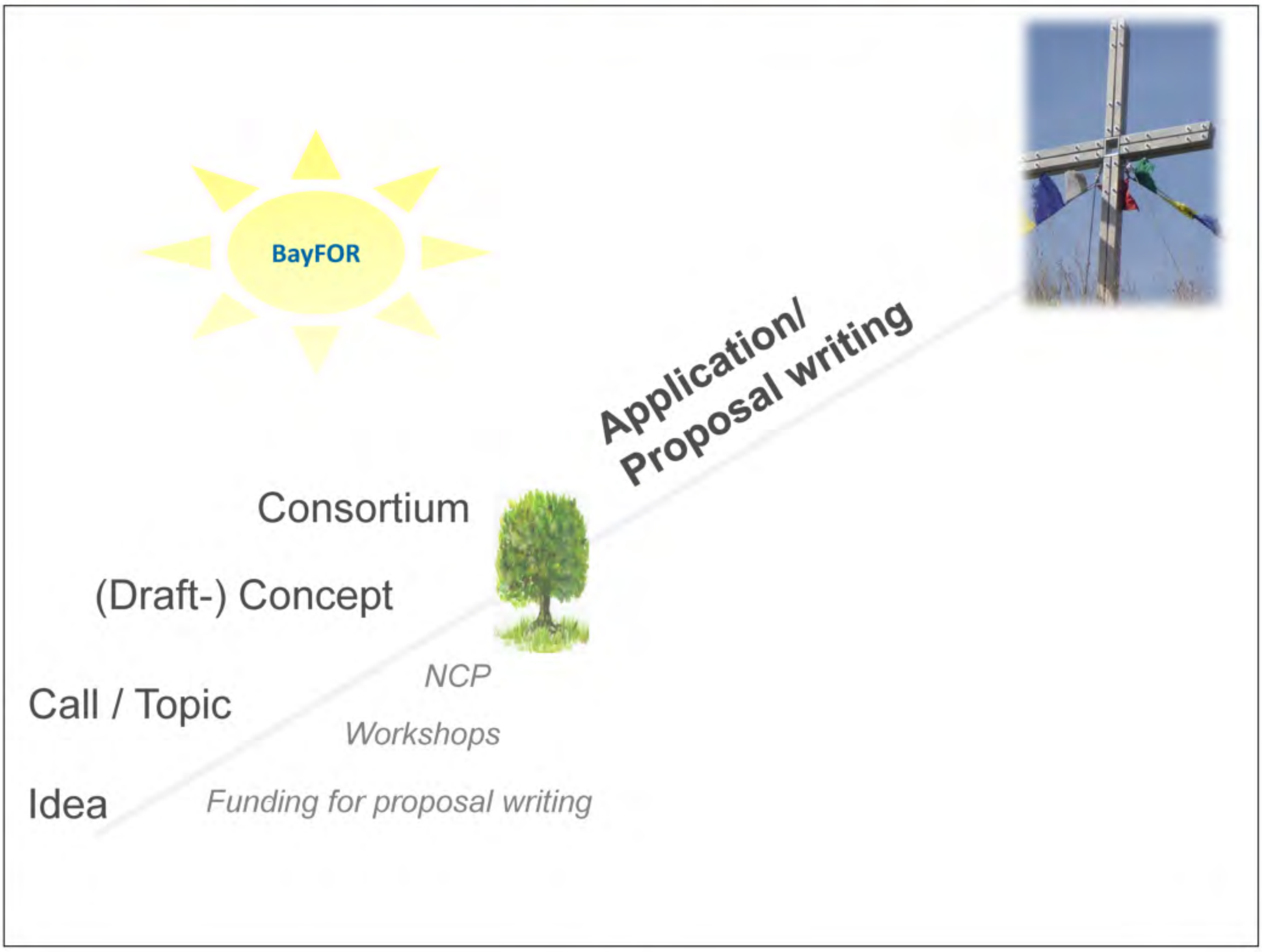
BayFOR
Application/
Proposal writing
Consortium
(Draft-) Concept
Call / Topic
NCP
Workshops
Idea
Funding for proposal writing

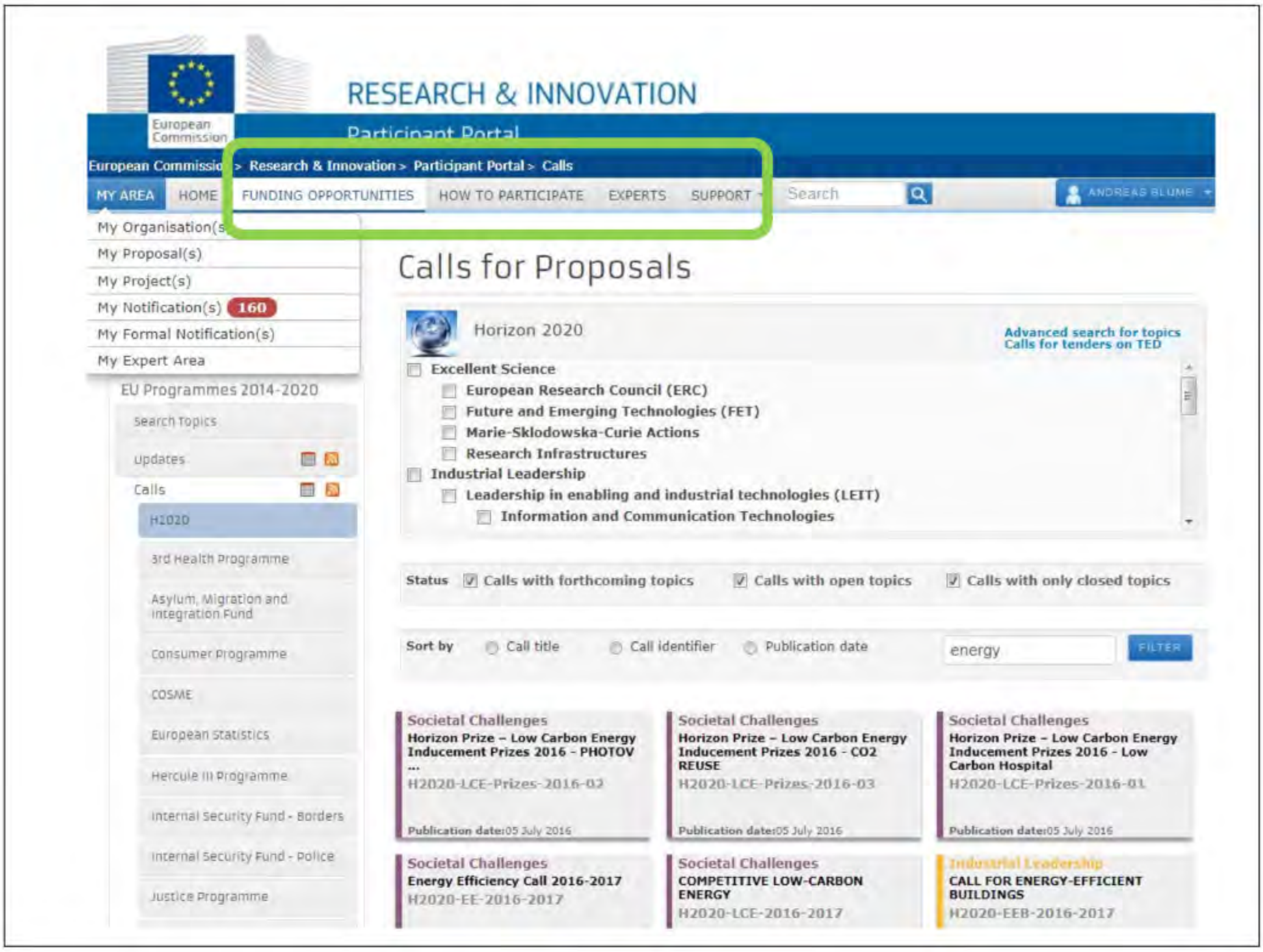

Bavarian Research Alliance

LC-SC3-EE-8-2018-2019:

Capacity building programmes to support implementation of energy audits

Bavarian Research Alliance

LC – SC3 – EE – 8 – 2019-2020 (= „Topic“)

LC	Call „Low Carbon“
SC3	Societal Challenge No. 3
EE	Energy Efficiency
8	Serial number
2018-2019	Years of publication (indicative)

COMPLETE | Andreas Blume | UFS Zugspitze 14.07.2018 | 32

Project consortium

© fotolia

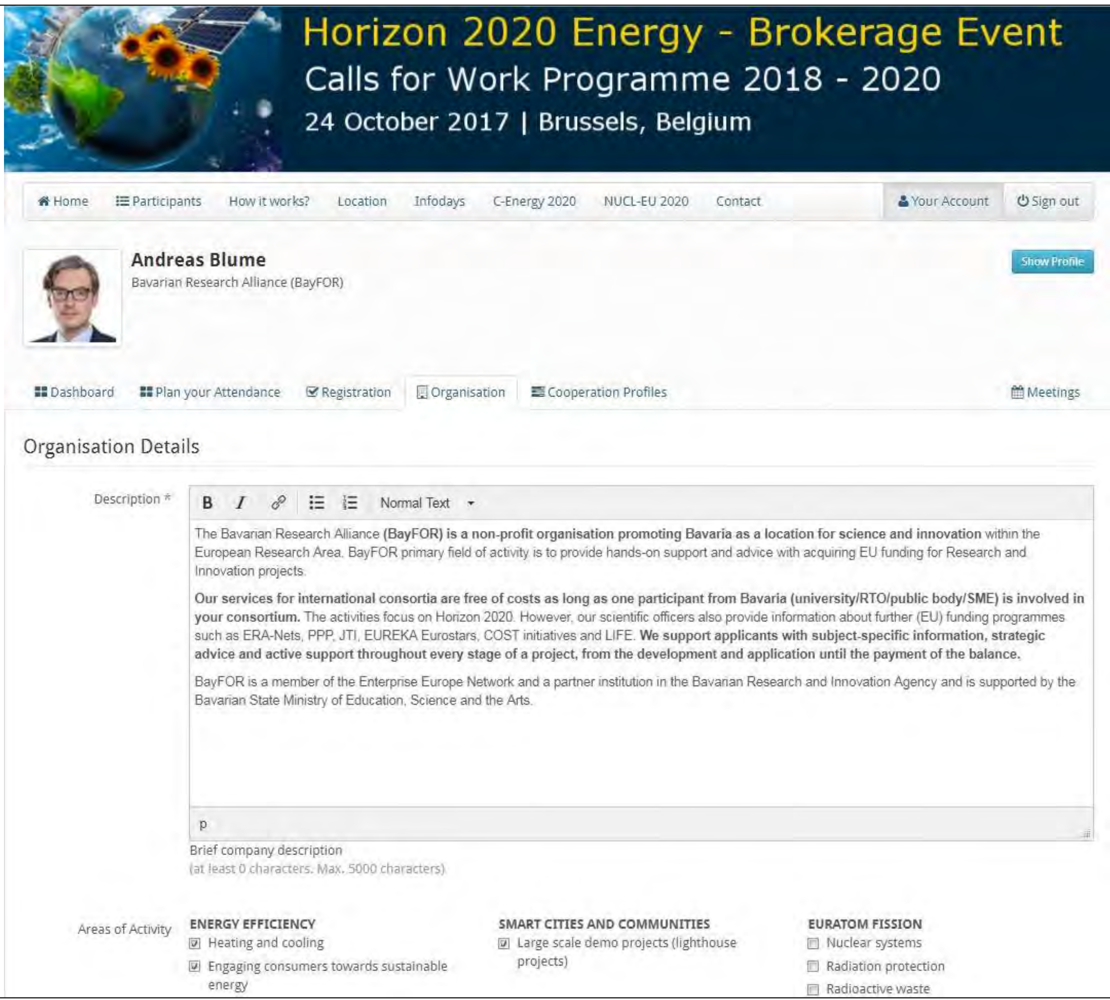

Coordinator or Partner ?

© fotolia

Bavarian Research Alliance

LC-CLA-06-2019: Inter-relations between climate change, biodiversity and ecosystem services

1. Please read the topic (10 minutes)

2. Let's discuss! Any ideas regarding:
    - Types of participants/organisations?
    - Size of consortium?
    - Which countries involved?

Bavarian Research Alliance

Advice and Support in EU funding (just some of them)

NKS Umwelt

enterprise europe network
Business Support at Your Doorstep

Life
Contact Point

NKS Energie

Bayerische Forschungsallianz

Alpine Space
Contact Point

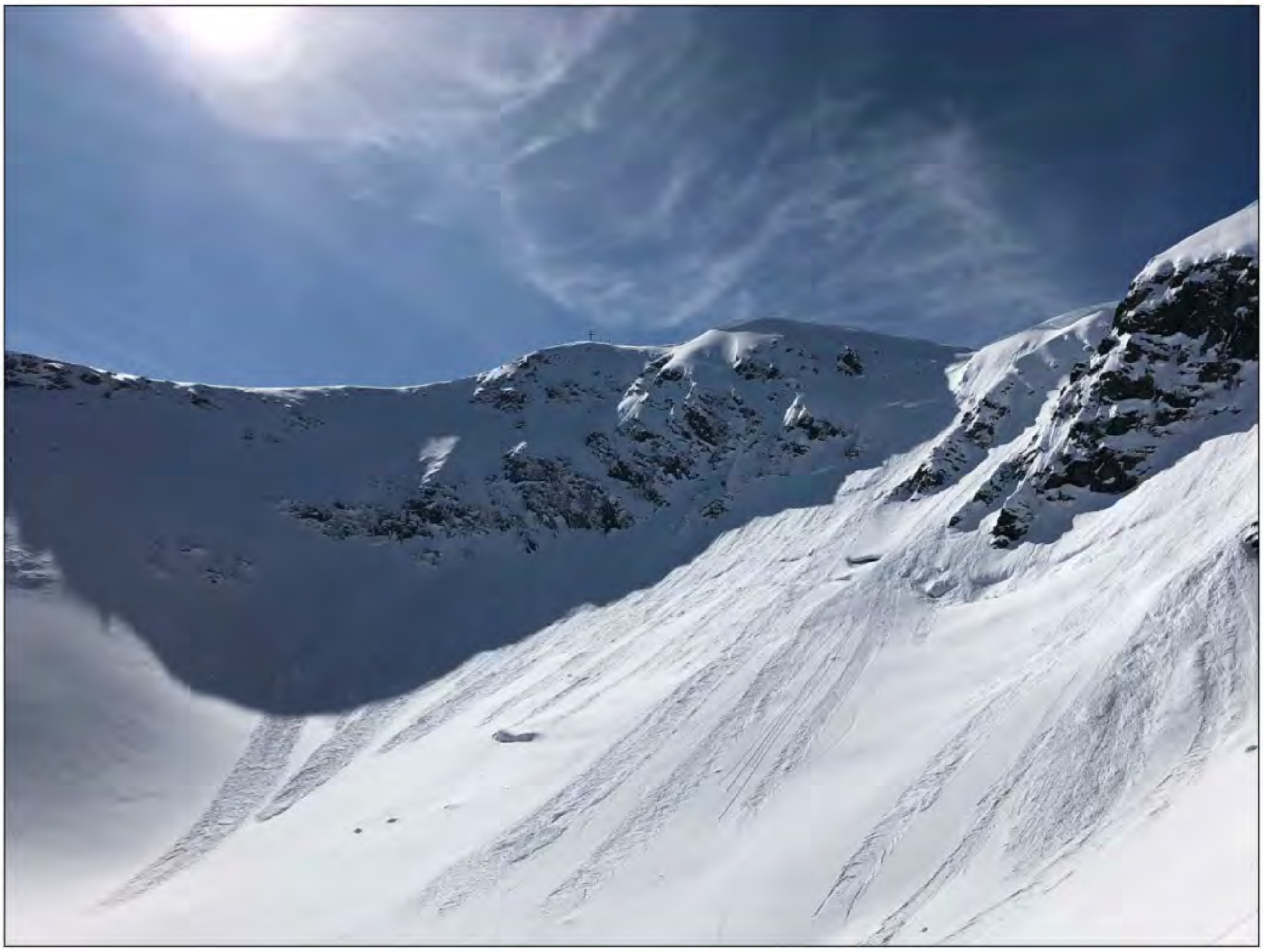

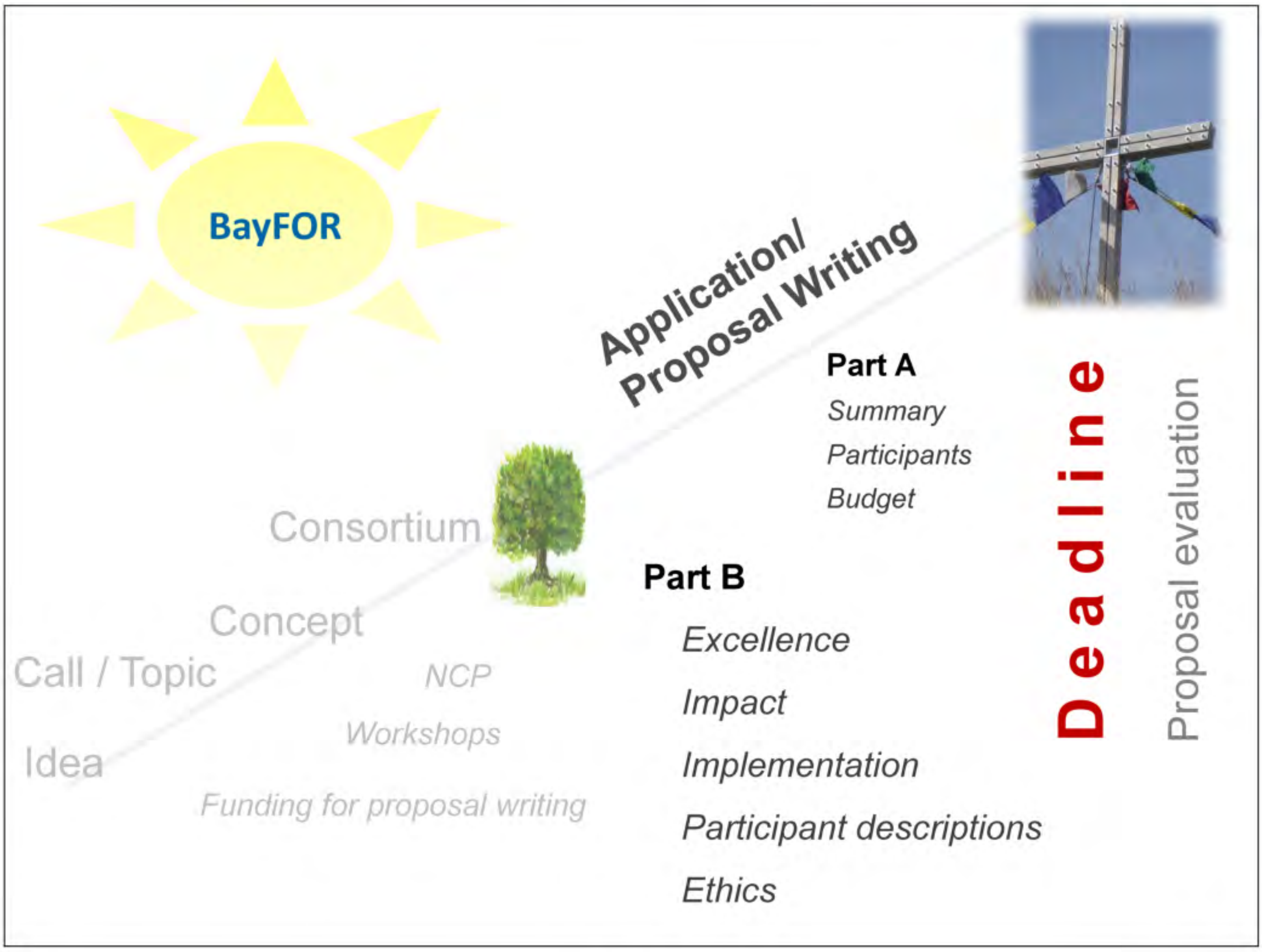

BayFOR
Application/
Proposal Writing
Part A
Summary
Participants
Budget
Consortium
Concept
Call / Topic
Idea
NCP
Workshops
Funding for proposal writing
Part B
Excellence
Impact
Implementation
Participant descriptions
Ethics
D e a d l i n e
Proposal evaluation

Bavarian Research Alliance

The basic outline

0. Cover Page (1 page)
1. Excellence (18 pages)
2. Impact (10 pages)
3. Implementation (26+ pages)
4. Members of Consortium
5. Ethics and Security

Max 70 Pages for Sections 1-3

Quantity of pages is meant only as a general guidance! No provision by the programme.

COMPLETE | Andreas Blume | UFS Zugspitze 14.07.2018 | 40

Bavarian Research Alliance

1. Excellence

1.1 Objectives (2 pages)

1.2 Relation to the work programme (2 pages)

1.3 Concept and methodology (8 pages)

1.4 Ambition (6 pages)

Quantity of pages is meant only as a general guidance! No provision by the programme.

COMPLETE | Andreas Blume | UFS Zugspitze 14.07.2018 | 41

Bavarian Research Alliance

2. Impact

2.1 Expected Impacts (5 pages)

2.2 Measures to maximise impact (5 pages)
- a) Dissemination and exploitation of results
- b) Communication activities

Quantity of pages is meant only as a general guidance! No provision by the programme.

Bavarian Research Alliance

3. Implementation

3.1 Work plan — Work packages, deliverables and milestones (14+ pages)
- *Table 3.1a – List of Work Packages (1 page)*
- *Table 3.1b – Work package (WP) description (1,5-2,5 pages for each WP)*
- *Table 3.1c – List of Deliverables (2 pages)*

3.2 Management structure and procedures (5 pages)
- *Table 3.2a – List of Milestones (1-2 pages)*
- *Table 3.2b – Critical risks of implementation (1-2 pages)*

3.3 Consortium as a whole (1-2 pages)

3.4 Resources to be committed (1 page)
- *Table 3.4a – Summary of staff effort (1 page)*
- *Table 3.4b – 'Other direct costs' items (1-2 pages)*

Quantity of pages is meant only as a general guidance! No provision by the programme.

How to organise proposal writing and proposal submission in the participant portal?

General Financial Rules of H2020 Projects

- Financing = on reimbursement basis: spend – then get refunded
  → **Saving does not make any sense!**
- All costs to be used for the sole purpose of **achieving the objectives of the project and its expected results**
- All costs to be spent in consistence with the **principles of economy, efficiency and effectiveness**
- **Depreciation of equipment:** The earlier the better!

Bavarian Research Alliance

H2020 Budget and financial provisions

Participant	Country	(A) Direct personnel costs/€	(B) Other direct costs/€	(C) Direct costs of sub-contracting/€	(D) Direct costs of providing financial support to third parties/€	(E) Costs of inkind contributions not used on the beneficiary's premises/€	(F) Indirect Costs / € (=0.25(A+B-E))	(G) Special unit costs covering direct & indirect costs / €	(H) Total estimat eligible c / € (=A+B+C+ +G)
		?	?	?	?	?	?	?	?
BAYERISCHE FORS	DE	0	0	0	0	0	0	0	
Total		0	0	0	0	0	0	0	

Bavarian Research Alliance

Cost Categories (I)

- **Direct costs** → directly linked to the project

Direct Costs	Article 6.2 GA
Personnel costs	Art. 6.2.A GA
Other direct costs	
- travel costs	Art. 6.2.D.1 GA
- equipment, infrastructure, other assets	Art. 6.2.D.2 GA
- other goods and services	Art. 6.2.D.3 GA
- Costs of internally invoiced goods and services	Art. 6.2.D.5 GA
Subcontracting	Art. 6.2.B GA

Overhead

No overheads on Subcontracting!

Bavarian Research Alliance

Cost Categories (II)

- **Indirect costs**, **Art. 6.2.E GA** (Overhead)
  - in RIA, IA and CSA grants
  - covering all costs of the action implementation that are not directly linked to it
  - declared as a **25 % fixed flat-rate** of the eligible direct costs
    (minus certain eligible direct costs as subcontracting etc
- Examples:
  Office supply, telephone and internet, maintenance

> Amount of indirect costs depends on reimbursement of direct costs.
> Be careful with budgeting indirect costs too early.

Bavarian Research Alliance

Project Management and Dissemination

- Grant preparation: Grant Agreement and Consortium Agreement
- Consortium management, Reporting and Deliverables
- Dissemination, Communication and Exploitation


SyGMa
Grant Agreement Data
Project 888823 (Project 888823)
HORIZON 2020
Call: H2020-INFRAIA-2014-2015 Action : CSA
Resp. Unit: RTD/B/07 Duration: 36
Beneficiaries
General Information
Reporting Periods
GA Information
GA Options
Financial Information
LF Overview
Work Packages
Deliverables
Milestones
Reviews
Critical Risks
DOCUMENTS
Beneficiaries
SAVE
Change Coordinator
Add New Beneficiary
Number | Short Name | Legal Name | Role | Country | PIC | PIC Status | Actions
1 | AST | AST ADVANCED SPACE TECHNOLOGIES GMBH | CO | DE | 973276467
2 | RHP | RHP-TECHNOLOGY GMBH & CO KG | BEN | AT | 973104001
3 | CNRS | CENTRE NATIONAL DE LA RECHERCHE SCIENTIFIQUE | BEN | FR | 999997930
4 | LANC UNIV | LANCASTER UNIVERSITY | BEN | UK | 999840984
Validate

The working group provides this model Consortium Agreement as draft without assuming any warranty or responsibility. The use of the text in total or in part takes place on the users own risk and does not release users from legal examination to cover their interests and protect their rights.

DESCA

Horizon 2020 Model
Consortium Agreement
www.DESCA-2020.eu

Version 1.2,
March 2016

Bavarian Research Alliance

Implementation of the project

Establishment and execution of an efficient project management

- Administrative project management (Project Manager)
- Scientific/technical project coordination (Coordinator)

Main tasks, usually described in the concerned work package in detail

- Coordination and daily management of project and consortium
- Scientific and overall coordination of the work packages
- Management and communication between stakeholders
- Tracking of project progress and risk

Reporting (Grant Agreement Article 19 & 20)

- Continuous Reporting (e.g. deliverables, milestones, publications)
- Periodic Reporting (technical report, financial statements)

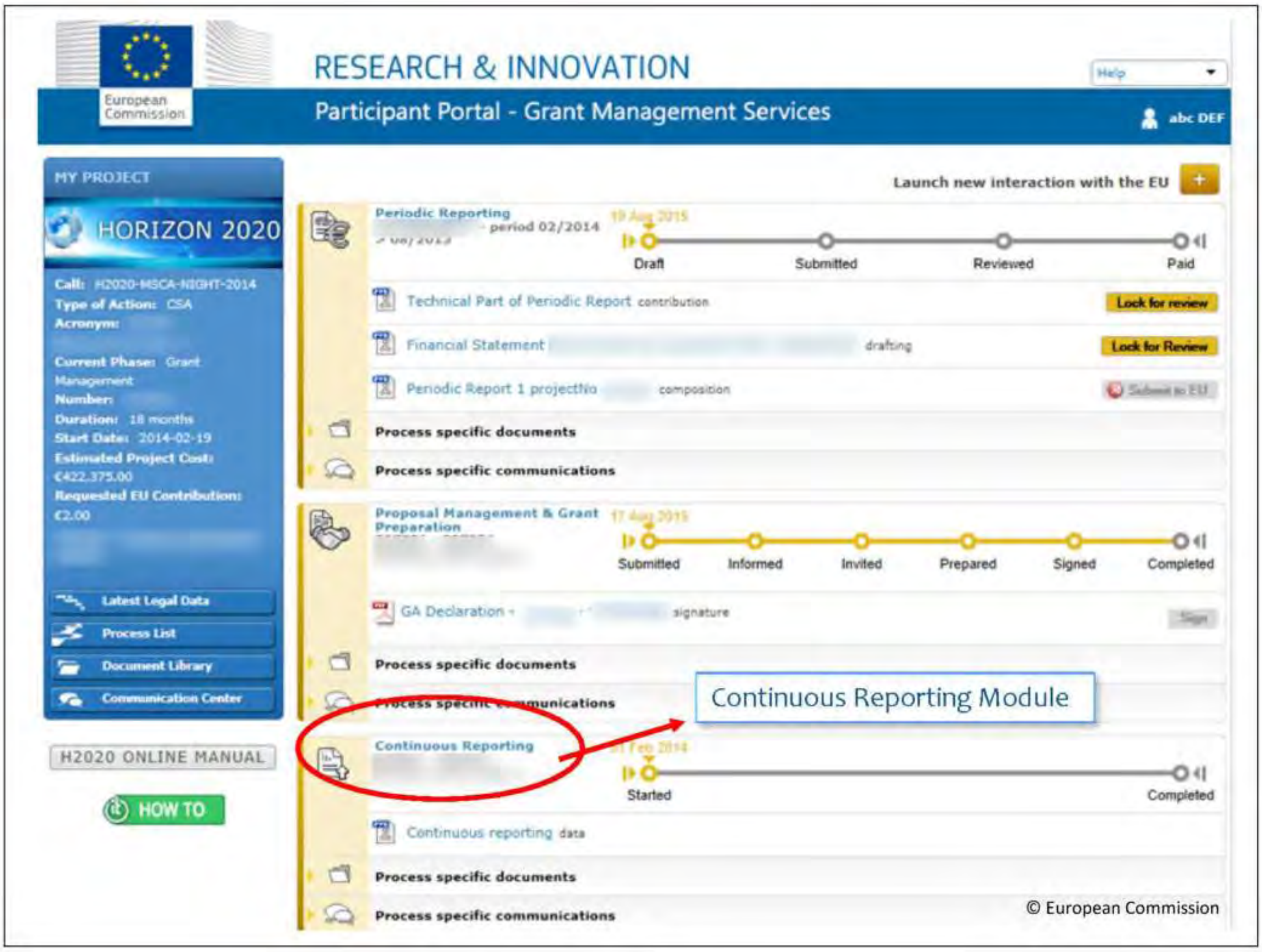

Reporting Timeline

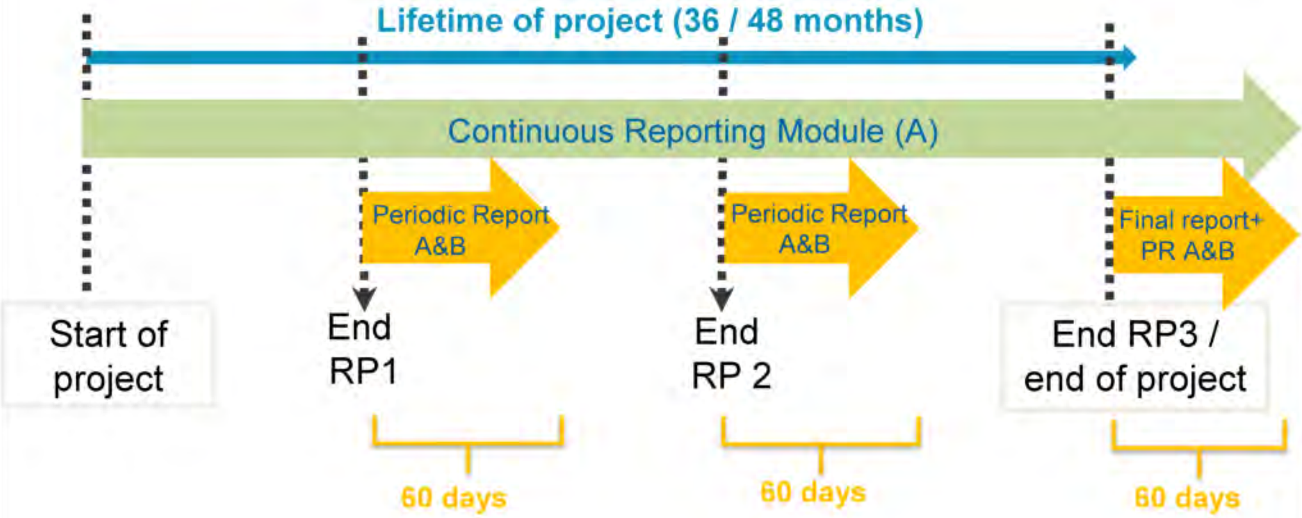

RP = Reporting Period

In Horizion 2020…

… Dissemination ≠ Exploitation ≠ Communication

Dissemination vs. Communication in your proposal

2.2 Measures to maximize IMPACT

Dissemination and exploitation of project results

Communication

Measures to maximise impact

- Dissemination
  - *Making available results*
- Exploitation
  - *Making use of results*
- Communication
  - *Information and outreach of the project*

Horizon 2020: Open Access and Open Data

Open Access = **scientific literature** (peer-reviewed) that was written within a EU-funded project has to be made available online, completely free of charge, so that it can be reused (taking into account the author‘ rights)

Open Data = scientific **raw data** that were gained during a EU-funded project have to be made available online, completely free of charge, so that they can be reused (taking into account the author‘ rights)

COMPLETE Summer School Day 6

EU Proposal Writing and Management of European Projects

Andreas Blume

Breakout session: Hardware group

A meeting about sharing

Sharing problems

Started with a quick summary of what people were doing, and pressing problems

- Guus: Particle detection and camera calibration.
  - Particle detection
  - Camera calibration
  - Building a simple "cloud detector"
- Tessa
  - Testing different materials for the balloon project
  - Needs a light (but dense) biodegradable material, must keep He in.
- Miryam
  - Transmission between radio probes and ground station
  - Developing the code, hardware is done
  - Data transfer might be disrupted by simultaneous signals or wind fluctuations

Sharing problems

- Moein
  - Shadowgraphy of droplets in-situ
  - Interested in size/velocity distribution
  - Looking for a cloud chamber larger than 1.25m x 1.25m x 0.2 m
- Tung
  - Currently working on the positioning system of the balloons
  - Needs large (> 100 samples/sec) amount of data from the system
  - Need a light, temperature resistant, high capacity battery
- Antonio
  - Developing a high spatial/temporal resolution hotwire
  - Design based around 3D-printing combined with either metal coating or electroplating.
- Johannes
  - Droplet Generator: Piezoelectric cables are not properly isolated from water
  - Settling particles : Particles are hard to manipulate, as they stick to most surfaces.

Sharing knowledge

- Healthy discussion about the projects gave birth to new ideas
- Johannes sent an overview of different batteries to Tung.
- Tessa suggested some film-preparation techniques to Antonio and a possible way to solve Johannes watery problems.

Sharing facilities (maybe)

- Moein needs a bigger cloud chamber for testing his setup: Might be available at Goettingen.
- Turin balloon electronics might be tested on the tether of MPI-DS CloudKite (depending on the campaign's dates)
- Measurement campaigns on Mt. Zugspitze at least 2 weeks per month for the period July-October. People can join and do experiments if interested.

Thank you ☺

Numerical Resources Discussions

UFS Summer School

Available Codes (DNS, LES etc)

- Incompact3d (Tai)
  - Sixth-order compact finite difference NS solver (spatial)
  - https://github.com/xcompact3d/Incompact3d
- Sparkle (Vishnu, Marco)
  - Fourth-order central difference NS solver (temporal/spatial)
  - Not open (Ask Maarten)
- System for Atmospheric Modeling (Sara)
  - evolved from the Large-Eddy Simulation (LES) model
  - http://rossby.msrc.sunysb.edu/~marat/SAM.html

Available Codes (DNS, LES etc)

- Eulag (Emmanuel)
  - Fractal SGS model, fractal model
  - https://www.swmath.org/software/14823
- Turbulencia (Juan Pedro, MPI)
  - Compact finite difference NS solver (temporal/spatial)
  - https://github.com/turbulencia/tlab
- Geophysical High-Order Suite for Turbulence (Alain, Dhawal)
  - highly scalable pseudospectral code that solves a variety of PDEs
  - https://wp.df.uba.ar/mininni/ghost/

Available Codes (DNS, LES etc)

- TurIsMis (Tara and Mina, Politecnico di Torino)
  - HIT solving Boussinesq approximation, scalars and Lagrangian particles.
  - https://areeweb.polito.it/ricerca/philofluid/

Available tools?

- Professors (Alain, Paolo, Juan Pedro)
  - If you find interesting techniques in their paper, they might be able to share small tools!

Problems

- Tara
  - 2048^3 simulation (attached two HIT box)
  - NS solver is fine. Droplets code is slow.
  - What scale (or nondimensional number) is needed? – Case Design Problem
  - Starting from working state or smaller DNS could be the key?
  - (Still open question)
- Mina
  - Nucleation modeling
  - (Still open question)

Collaboration

- People working on particle tracking in their code can share their experiences? (Or possibly working together?)
  - Most effective MPI implementation
  - Particle/Droplets Seeding etc….

A Changelog

Version	Date	Changes
a	12 Oct 2018	Initial version
b	15 Oct 2018	Added Prof. Allegretti's contribution. Added changelog.